

Western Kentucky University

TopSCHOLAR®

---

Masters Theses & Specialist Projects

Graduate School

---

Summer 2017

## Measuring Inorganic Carbon Fluxes from Carbonate Mineral Weathering from Large River Basins: The Ohio River Basin

Autumn B. Singer

Western Kentucky University, autumnbturner@gmail.com

Follow this and additional works at: <https://digitalcommons.wku.edu/theses>



Part of the [Climate Commons](#), [Geochemistry Commons](#), [Geology Commons](#), and the [Water Resource Management Commons](#)

---

### Recommended Citation

Singer, Autumn B., "Measuring Inorganic Carbon Fluxes from Carbonate Mineral Weathering from Large River Basins: The Ohio River Basin" (2017). *Masters Theses & Specialist Projects*. Paper 2044.  
<https://digitalcommons.wku.edu/theses/2044>

This Thesis is brought to you for free and open access by TopSCHOLAR®. It has been accepted for inclusion in Masters Theses & Specialist Projects by an authorized administrator of TopSCHOLAR®. For more information, please contact [topscholar@wku.edu](mailto:topscholar@wku.edu).

MEASURING INORGANIC CARBON FLUXES FROM CARBONATE MINERAL  
WEATHERING FROM LARGE RIVER BASINS: THE OHIO RIVER BASIN

A Thesis  
Presented to  
The Faculty of the Department of Geography and Geology  
Western Kentucky University  
Bowling Green, Kentucky


In Partial Fulfillment  
of the Requirements for the Degree  
Master of Science

By  
Autumn B. Turner


August 2017

MEASURING INORGANIC CARBON FLUXES FROM CARBONATE MINERAL WEATHERING FROM LARGE RIVER BASINS: THE OHIO RIVER BASIN

Date Recommended 3/31/17

  
Chris Groves, Director of Thesis

  
Michael May

  
Jun Yan

  
Albert Meier

  
Dean, Graduate School

8/8/17  
Date

## ACKNOWLEDGMENTS

Several people were instrumental in the success of this work. To my advisor and committee chair, Dr. Chris Groves: thank you for your excellent advice and guidance throughout this process, for your unfailing optimism, your friendship, and the many opportunities that you have facilitated during my time as your graduate student. It has been my privilege to work with someone of your caliber. To my committee members, Dr. Mike May, Dr. Albert Meier, and Dr. Jun Yan: thank you for sharing your expertise, lending your time, and your willingness to entertain my questions. I feel quite fortunate to have had a committee composed of such diverse backgrounds, which enabled me to view my research from geologic, biologic, and GIS perspectives. Your contributions and ideas have added great strength to this work. To my supervisor at the Crawford Hydrology Laboratory, Lee Anne Bledsoe: I'm so pleased we've had the opportunity to work together. My experiences as a research assistant in the lab have resulted in immense professional growth and a profound sense that the work that we are doing is of great importance to human and environmental well-being. That is all I have ever wanted out of a career, and I'm incredibly blessed to have begun my journey in such an amazing working environment. To my family: Christian Turner, I could not have done this without you. Thank you for supporting my goals, for keeping everything on track, listening to thesis conundrums, and for understanding the priority that an undertaking of this nature requires. Mom and Dad, you have encouraged and supported me all along. I was so lucky to have been born the daughter of adventurers and old souls. Thank you for raising me to be a child of the woods and rivers, to know and appreciate the natural world, and for instilling in me a passion to preserve and protect the environment.

## TABLE OF CONTENTS

Chapter 1. Introduction .....	1
Chapter 2. Literature Review .....	7
2.1 Introduction.....	7
2.2 The Carbon Cycle .....	8
2.3 The “Missing Sink” and Changes in Storage.....	9
2.4 Overview of Carbon Reservoirs.....	11
2.4.1 Atmospheric Carbon Storage.....	11
2.4.2 Carbon Storage in the Ocean .....	13
2.4.3 The Terrestrial Carbon Sink.....	14
2.5 Carbon Sink from Carbonate Rock Dissolution .....	17
2.6 Controls on Carbonate Mineral Dissolution and DIC Flux .....	22
2.6.1 Thermodynamic Controls .....	23
2.6.2 Kinetic Controls .....	24
Surface and Transport Reactions .....	26
Variation in Carbonate Mineral Type and Purity .....	27
2.6.3 Proposed Major Controls .....	28
Area of Carbonate Outcrop.....	28
Duration of Water-Rock Contact.....	29
Amount of Water Available for Dissolution.....	30
2.6.4 Proposed Lesser Controls .....	31
A. Carbonate Minerals Not Mapped as Surface Deposits .....	32
Subsurface Carbonate Minerals .....	34
Loess Deposits .....	36
Lacustrine Facies .....	39

	Thin Surface Carbonate Deposits .....	40
	Calcite Replacement of Non-Carbonate Grains.....	41
	Bedload Carbonate Minerals and CO <sub>2</sub> Outgassing....	42
	Climate-Driven Feedback in Geologic Processes.....	44
	B. Biological Activity .....	45
	Vegetation .....	45
	Organic Acids .....	46
	Climate-Driven Feedback in Biological Processes....	48
	C. Soil and Land Use .....	49
	2.8 Previous Estimates of the Sink by Carbonate Dissolution.....	50
	2.9 Summary .....	52
Chapter 3. Study Area.....		54
3.1 Introduction to the Ohio River basin .....		54
3.2 Geologic Setting.....		54
3.3 Climate.....		60
3.4 Hydrologic and Geochemical Setting .....		62
Chapter 4. Methods.....		64
4.1 Introduction.....		64
4.2 Water Chemistry and Discharge Data.....		67
4.3 Precipitation and Temperature Data .....		71
4.4 GIS Data.....		73
4.5 Data Processing.....		74
4.6 Drainage Basin Delineation .....		74
4.7 Calculation of Volume Available for Carbonate Dissolution.....		76
4.8 Calculation of Dissolved Inorganic Carbon (DIC) .....		77

4.9 Calculation of Atmospheric Carbon Sink .....	78
4.10 DIC Flux Normalization Procedure .....	79
Chapter 5. Results .....	80
5.1 Basin Delineation and Geologic Mapping.....	80
5.2 Precipitation (P), Evapotranspiration (ET), and (P-ET) Kriging .....	83
5.3 Hydrophysical Data .....	86
5.4 Hydrochemical Data .....	91
5.5 Annual DIC Flux.....	99
5.6 Agreement Comparisons of Normalized DIC Flux .....	106
5.7 Statistical Correlation by Regression Analysis.....	112
5.8 Magnitude of Atmospheric Carbon Sink by Carbonate Dissolution .....	114
5.9 Influence of Hydrochemical Data Resolution on Flux Estimates.....	114
Chapter 6. Discussion and Conclusions.....	116
6.1 Review of Research Objectives .....	116
6.2 Discussion .....	121
6.3 Future Work.....	131
6.4 Conclusions.....	133
References.....	136

## LIST OF FIGURES

Figure 1.1. Atmospheric CO <sub>2</sub> concentration over the past 420,000 years .....	1
Figure 1.2. Historical record of changes in atmospheric carbon dioxide levels .....	2
Figure 1.3. Components of the carbon cycle .....	3
Figure 1.4. Carbon reservoirs and fluxes .....	4
Figure 2.1. Activity of carbonic acid, bicarbonate, and carbonate species.....	21
Figure 2.2. Relative distribution of exposed and buried carbonate rocks.....	35
Figure 2.3. Peoria Loess deposits in North America .....	36
Figure 2.4. Calcite concretions found in the loess deposits of south central Indiana .....	37
Figure 2.5. Near-surface carbonate lens in the Big Clifty Sandstone in Kentucky .....	41
Figure 2.6. Calcite replacement of quartz crystals.....	42
Figure 3.1. Geographic extent of the Ohio River Drainage Basin.....	55
Figure 3.2. Physiographic provinces of the Ohio River Basin .....	57
Figure 3.3. Bedrock geology of the Ohio River Basin and nested sub-basins.....	58
Figure 3.4. Carbonate karst of the conterminous United States .....	59
Figure 3.5. Köppen climate classification map of the United States .....	61
Figure 4.1. Location of hydrochemical monitoring points .....	70
Figure 4.2. Location of NOAA COOP weather stations .....	72
Figure 5.1. Corrected sub-basins reflecting drainage upstream.....	81
Figure 5.2. Geographic distribution of exposed carbonate rock surface .....	82
Figure 5.3. Monthly average water balance available for dissolution .....	84



Figure 5.4. P-ET surface for depth of water available for carbonate rock dissolution .....	85
Figure 5.5. Discharge for the Ohio, Tennessee, and Cumberland rivers .....	87
Figure 5.6. Discharge for the Green, Licking, and Kentucky rivers.....	88
Figure 5.7. Discharge for the Kanawha, Monongahela, and Allegheny rivers.....	89
Figure 5.8. Discharge for the Scioto, Great Miami, and Wabash rivers.....	90
Figure 5.9. Water Temperature for the Ohio River .....	93
Figure 5.10. Mean water temperature for the major sub-basins .....	94
Figure 5.11. Recorded pH values for the Ohio River .....	95
Figure 5.12. Mean pH values for the major tributaries to the Ohio River .....	96
Figure 5.13. Recorded alkalinity values for the Ohio River .....	97
Figure 5.14. Mean bicarbonate alkalinity values for the major tributaries.....	98
Figure 5.15. Sum DIC for the Ohio River .....	100
Figure 5.16. DIC for the major sub-basins of the Ohio River .....	101
Figure 5.17. DIC flux for the Ohio, Tennessee, and Cumberland rivers .....	102
Figure 5.18. DIC flux for the Green, Kentucky, and Licking rivers.....	103
Figure 5.19. DIC flux for the Kanawha, Monongahela, and Allegheny rivers.....	104
Figure 5.20. DIC flux for the Scioto, Great Miami, and Wabash rivers.....	105
Figure 5.21. Regression analysis of DIC flux vs. time-volume for sub-basins .....	113
Figure 6.1 Physiographic provinces of the Ohio River basin .....	129
Figure 6.2. Groups represented by the geologic units of West Virginia.....	130

## LIST OF TABLES

Table 2.1. Carbon storage within the major reservoirs on Earth .....	18
Table 2.2. Summary of lesser factors that may influence DIC flux in a drainage Basin..	33
Table 5.1. Minimum, maximum, and average discharge for the Ohio River .....	86
Table 5.2. Summary table for the Ohio River and major sub-basins.....	111

MEASURING INORGANIC CARBON FLUXES FROM CARBONATE MINERAL  
WEATHERING FROM LARGE RIVER BASINS: THE OHIO RIVER BASIN

Autumn Turner

August 2017

152 Pages

Directed by: Chris Groves, Jun Yan, Albert Meier, and Michael May

Department of Geography and Geology

Western Kentucky University

Rising atmospheric CO<sub>2</sub> concentrations have motivated efforts to better quantify reservoirs and fluxes of Earth's carbon. Of these fluxes from the atmosphere, one that has received relatively little attention is the atmospheric carbon sink associated with carbonate mineral dissolution. Osterhoudt (2014) and Salley (2016) explored new normalization techniques to improve and standardize a process for measuring this flux over large river basins. The present research extends this work to the 490,600 km<sup>2</sup> Ohio River drainage basin and 11 subbasins. The study estimated the DIC flux leaving these basins between October 1, 2013, and September 30, 2014, based on secondary hydro-geochemical, geologic, and climatic data. The total annual DIC flux for the Ohio River basin was estimated to be  $7.54 \times 10^{12}$  g carbon (C). The time-volume normalized value of DIC flux for the Ohio basin was  $3.36 \times 10^8$  g C/km<sup>3</sup> day, where the km<sup>3</sup> refers to the amount of water available during the year. This was within 71.4% agreement with the Barren River data (Salley, 2016) and within 63.9% agreement with the Green River data (Osterhoudt, 2014). In general, normalized DIC flux values of sub-basins containing at least modest amounts (more than 8%) of exposed carbonates (Tennessee, Cumberland, Green, Kentucky, Licking, Monongahela, and Allegheny) were in strong agreement with the normalized DIC flux of the Ohio River basin, whereas inclusion of basins with little or no near surface carbonates (Wabash, Great Miami, Scioto and Kanawha) yielded poor agreement. Regression analysis yielded strong agreement between DIC flux and the

normalization parameters for the carbonate-bearing sub-basins ( $R^2 = 0.97$ ,  $p = <0.001$ ). Therefore, the normalization procedure appears to be an effective means of estimating DIC flux where surface carbonates serve as the primary source of alkalinity, even though these can constitute even a relatively small percentage of rock outcrop area. However, the normalization technique does not appear to be as effective among basins that do not receive alkalinity from interactions with surface carbonates. Additional study is required to refine this technique to become more broadly applicable in generating estimates of atmospheric C flux from carbonate mineral weathering processes.

## Chapter 1. Introduction

Atmospheric carbon dioxide (CO<sub>2</sub>) has steadily increased in association with human activities since the mid-seventeenth century (Figure 1.1). Concentrations currently exceed 400 ppm (Tans and Keeling, 2017) (Figure 1.2) and are expected to continue rising (Cox et al., 2000). CO<sub>2</sub> is a known greenhouse gas (GHG), shown to trap heat within the atmosphere leading to increasing global temperatures (Solomon et al., 2009). Concerns over the effects of these increases with regard to mitigating and predicting climate change have led to much investigation into the factors that control atmospheric concentrations of CO<sub>2</sub>. Some have suggested that atmospheric CO<sub>2</sub> must be balanced among other C stores to control the effects of climate change (Le Quéré et al., 2009).

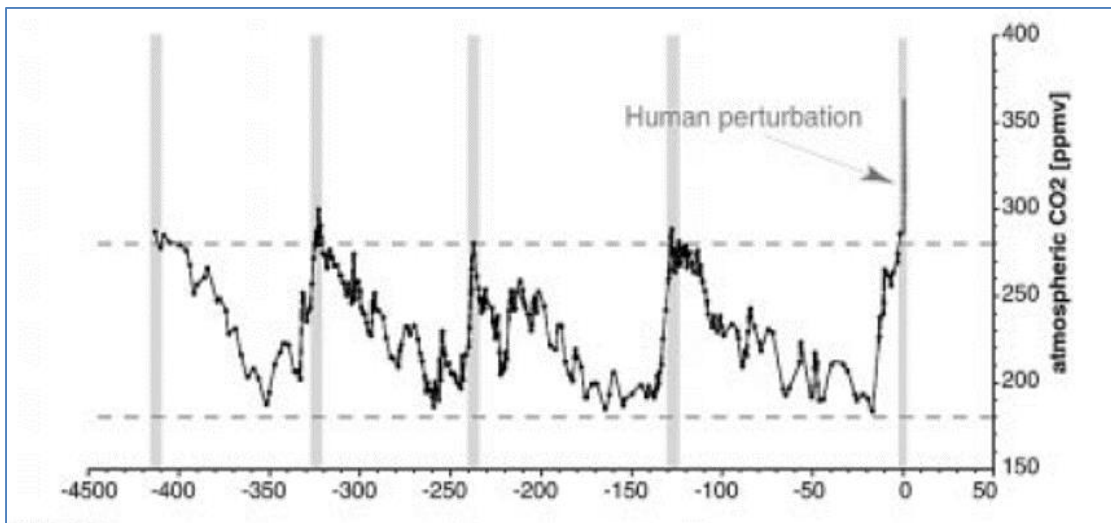


Figure 1.1. Atmospheric CO<sub>2</sub> concentration over the past 420,000 years.  
Source: Modified from Falkowski et al. (2000).

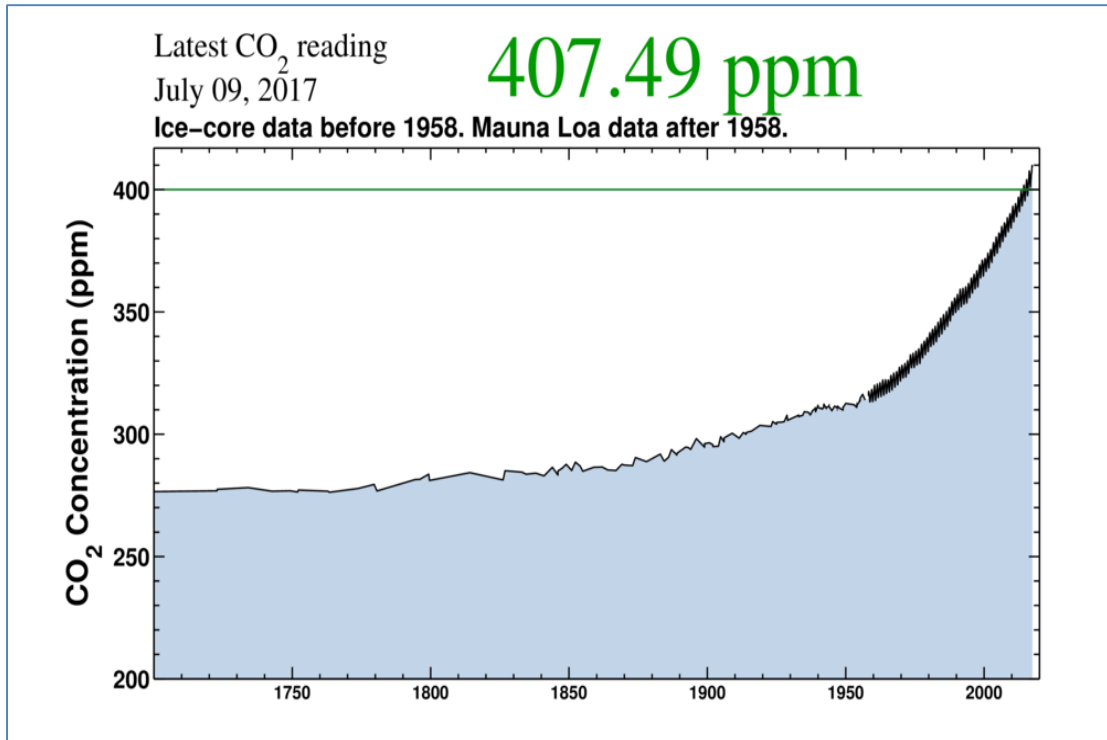


Figure 1.2. Historical record of changes in atmospheric carbon dioxide levels since the early eighteenth century.

Source: Tans and Keeling (2017).

Carbon budgeting is an appropriate method for tracking fluctuations of C as it cycles through the major reservoirs. The C cycle circulates C among various reservoirs, including the atmosphere, hydrosphere, lithosphere, and biosphere (Figure 1.3). Recent studies estimate that approximately half of the billions of tons of C produced annually remains in the atmosphere, while the remaining C is unaccounted for, leading to the so-called “missing sink” (Sabine et al., 2004). The remaining C is assumed to be stored in the ocean and terrestrial reservoirs. However, the comparative roles of ocean and terrestrial storage are not fully understood, and conflicting reports of the magnitude of C uptake by the oceans present a challenge to the goal of understanding where and how C is exchanged among Earth’s reservoirs (Siegenthaler and Sarmiento, 1993).

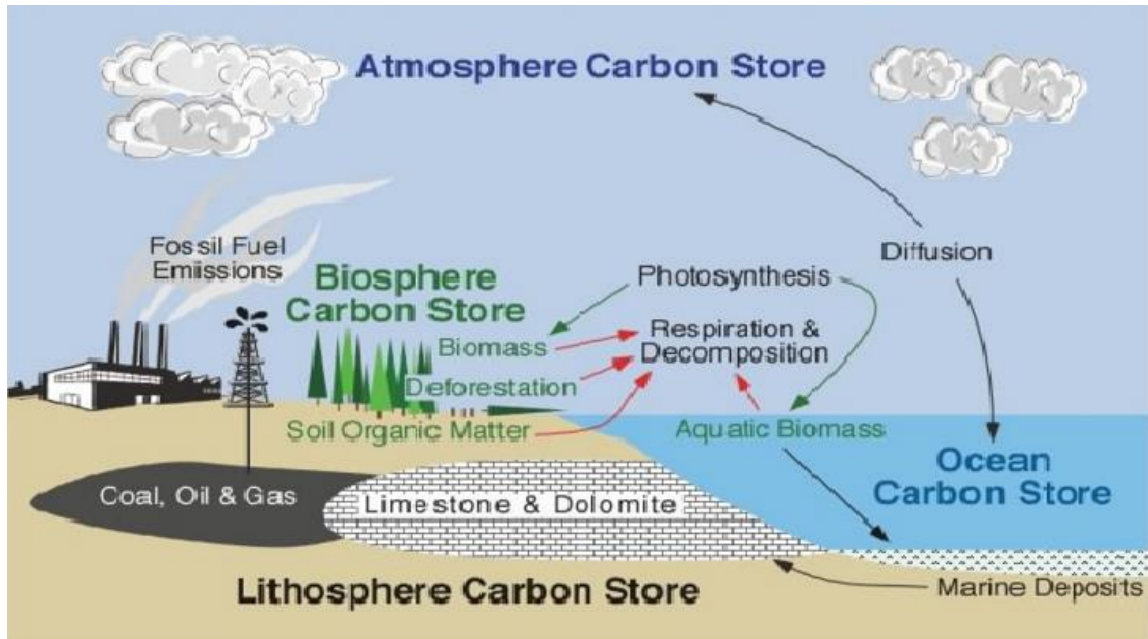


Figure 1.3. Components of the carbon cycle  
 Source: Pidwirny (2006).

Among the terrestrial reservoirs, the lithosphere is thought to have substantial sink capacity. Through the process of carbonate rock dissolution,  $\text{CO}_2$  is removed from the atmosphere. Here, waters that have been acidified through interactions with  $\text{CO}_2$  in the air and soil react with calcium carbonate ( $\text{CaCO}_3$ ) found in carbonate rocks. Carbonate rocks are considered an atmospheric sink because they contribute alkalinity and consume  $\text{CO}_2$  from the atmosphere via dissolution of carbonate minerals. The resulting solutions contain various inorganic C species that are dominated by carbonic acid ( $\text{H}_2\text{CO}_3$ ) at low pH, and bicarbonate ( $\text{HCO}_3^-$ ) and carbonate ( $\text{CO}_3^{2-}$ ) ions under neutral and basic conditions, respectively. This process of chemical weathering can result in the burial of carbon-bearing sediments among inland waters, or the transport of dissolved aqueous species to the oceans where they are eventually precipitated. It is believed that the North American continent is particularly well-suited to act as a terrestrial sink with relatively

widespread carbonate rock outcrops (Figure 1.4), but uncertainty exists as to the actual magnitude of the potential sink. Estimates of the North American sink have yielded values ranging from 0.1 to 2.0 Pg C yr<sup>-1</sup> (King et al., 2007). This broad range is most likely a consequence of the fact that a variety of methods has been used to measure the carbonate dissolution sink and a lack of a uniform approach to conducting such measurements. Standardized methods for measurement are required to assess more accurately the capacity of carbonate rock to sequester atmospheric carbon.

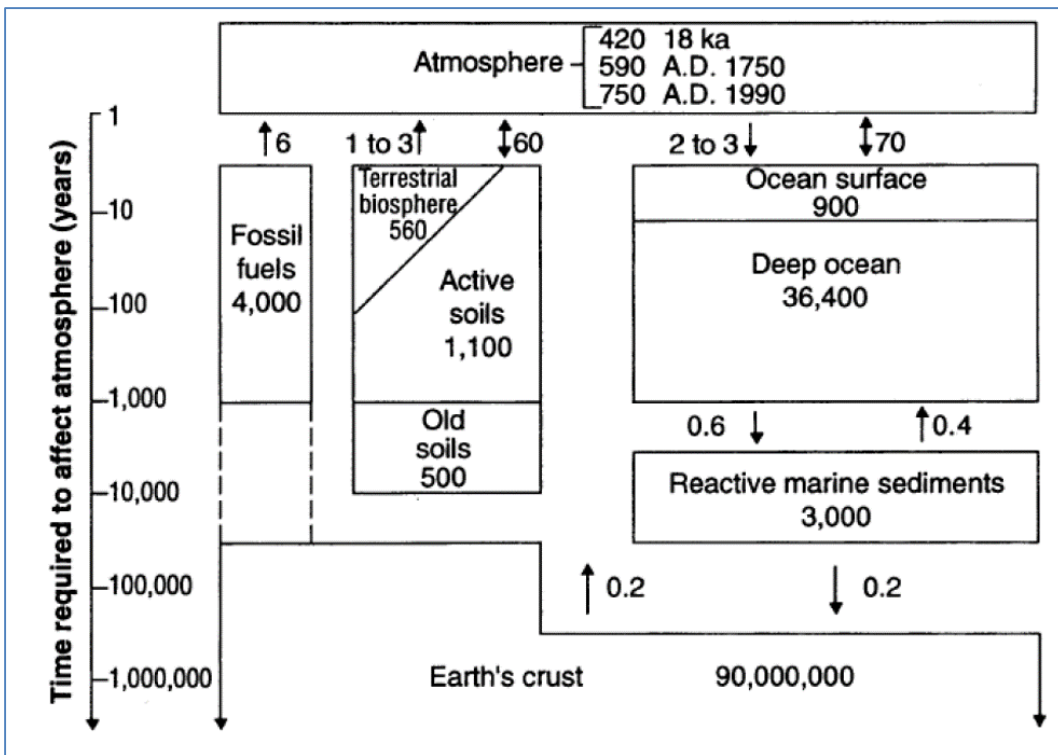


Figure 1.4 Carbon reservoirs and fluxes.  
Source: Sundquist (1993).

This research has sought to evaluate a method for calculating the atmospheric C sink via a better understanding of carbonate dissolution processes. Available secondary data as provided by geospatial and other publicly available databases were used to determine total C flux leaving the Ohio River basin. In doing so, this research evaluated



the validity of the proposed calibration for the carbon flux of Salley (2016), to test its applicability over a broad range of basin areas, geological conditions, study periods, and climate types. The study evaluated previous work that suggested by normalizing calculations of inorganic C flux according to area of carbonate-rock outcrop, length of exposure, and the volume of water available for dissolution, the major variables affecting C flux have been determined. If the primary factors that influence DIC flux are captured within the model, it would indicate that other factors, such as land-use practices and carbon-soil interactions, do not significantly impact the inorganic C flux for a given basin and, thus, are negligible in terms of calculating flux. Prior investigations suggest that such a calibration exists that would enable researchers to arrive at a value for the inorganic C flux leaving a drainage basin, using only the known area of the carbonate rock outcrop and the total amount of water available (rainfall-evapotranspiration) over a given time interval. Studies employing this technique over smaller regional basins have yielded results in very close agreement. Regression analysis of these data points reveals a linear correlation ( $R^2 = 0.97$ ,  $p = <0.001$ ) (see Osterhoudt, 2014; Salley, 2016) for the inorganic C flux (grams of C) as a function of the flux of water in contact with carbonate rock areas of each basin ( $\text{km}^3 \text{H}_2\text{O day}^{-1}$ ). Prior to this investigation, the approach had not been tested at much larger scales. Furthermore, the data collected previously by Osterhoudt (2014) were acquired through a labor-intensive process requiring direct measurements of water chemistry. These methods are not practical for application in many locations and are not feasible for implementation at the continental or global scale. This project aimed to determine whether the methods used by Osterhoudt (2014) in the Green River basin, and by Salley (2016) in the Barren River basin, could be applied to

substantially larger drainages by inclusion of additional data points to that linear relationship, such that the probability of a chance linear relationship among these points became less as the number of data points increased. The project also sought to determine whether the use of secondary data provided similarly accurate flux estimates for the Ohio, Tennessee, Cumberland, Green, Kentucky, Licking, Kanawha, Monongahela, Allegheny, Scioto, Great Miami, and Wabash drainages as did the high-resolution data used in prior studies.

The Ohio River drainage basin was used as the study area as part of an ongoing series of investigations intended to improve the methods by which the inorganic carbon flux from the associated carbonate rock weathering could be applied to drainage basins of various sizes, time intervals, and volumes of water available for dissolution. The total inorganic carbon sink from the atmosphere by carbonate rock weathering may be estimated as one half of the total DIC flux leaving a river basin influenced by carbonate rock interactions (Jiang and Yuan, 1999; Liu and Zhao, 2000; Groves and Meiman, 2001; Groves et al., 2002; Amiotte Suchet et al., 2003; He et al., 2013). The following research questions are addressed by this study:

1. What are the inorganic carbon flux rates for the Ohio River basin and its major subbasins?
2. Are the variables of carbonate rock outcrop area, volume of water available (precipitation – evapotranspiration), and time of exposure suitable considerations in the normalization of carbon flux for a large drainage basin?
3. If so, does the use of secondary water chemistry data appear to be as effective in determining carbon flux as similar methods employing high-resolution measurements?

## Chapter 2. Literature Review

### 2.1 Introduction

Revelle and Suess (1957: 19) described a natural experiment taking place at the global scale wherein humans were "... returning to the atmosphere and oceans the concentrated organic C ( $C_{org}$ ) stored in sedimentary rocks over hundreds of millions of years." Although the experiment had no deliberate design, it brought valuable awareness to the impacts of human activities on carbon cycling. Contemporary concerns over climate change have subsequently motivated a more precise understanding of what factors contribute to the observed changes in climate patterns and how these variables may be managed to minimize risk to human and environmental well-being (Fan et al., 1998; Cox et al., 2000; Falkowski et al., 2000). Atmospheric  $CO_2$  concentrations have been an important governing factor in determining global climate, which has been significantly impacted by human activity. Studies of the impacts of atmospheric  $CO_2$  have demonstrated an increase in temperature associated with the heat-trapping GHGs (Solomon et al., 2009). Scientists expect that, without interventions, both atmospheric  $CO_2$  concentrations and temperature should experience a steady increase over the coming century (Hoffert et al., 1998; Cox et al., 2000). Research has suggested that, to counteract the effects of climate change, atmospheric  $CO_2$  concentrations must be stabilized (Le Quéré et al., 2009). One way to accomplish this is to reduce anthropogenic  $CO_2$  emissions, yet the potential impacts on national economies and soaring human populations make implementation of these goals politically difficult. Because the level of atmospheric C is controlled by various fluxes that either add or remove C from the atmosphere, many are now looking in the direction of C sinks to regulate naturally the excess C contributed by human activities. Atmospheric  $CO_2$  budgeting has become an

area of great interest in contributing to a better understanding of climate change through developing an understanding of CO<sub>2</sub> exchange among various reservoirs by identifying and quantifying the C flux from each. This review aims to establish a context for evaluating the extent of the C sink created by carbonate rock dissolution on the continents.

## 2.2 The Carbon Cycle

Carbon is the fundamental unit of all living organisms and is important in many of the chemical processes occurring on Earth. Carbon circulates on a global scale through various reservoirs via a series of transfers between those reservoirs (fluxes) in chemical composition in a process known as the carbon cycle. The three major C reservoirs include the atmosphere, ocean, and terrestrial systems (Post et al., 1990). The Earth's crust represents the largest global carbon reservoir (Sundquist, 1993), within which most carbon is stored in carbonate rocks (Liu and Zhao, 2000). Other sources of carbon storage (in order of decreasing magnitude) include the intermediate and deep ocean, terrestrial soils and detritus, the surface ocean, the atmosphere, and land biota (Figure 1.4) (Siegenthaler and Sarmiento, 1993; Sundquist, 1993). Carbon is cycled between the atmosphere and ocean by gas transfers, while biota exchange C with the atmosphere and terrestrial environment via photosynthesis and respiration (Siegenthaler and Sarmiento, 1993). The amount of C interchanged between these stores is known as the overall carbon cycle and is dependent on the amount of C in each reservoir, in addition to turnover rates that fluctuate according to several environmental variables (Post et al., 1990). Humans influence the C budget in numerous ways, including emissions produced from burning fossil fuels. Fossil fuel combustion mobilizes carbon previously sequestered in the

preserved products of photosynthesis in the distant geologic past, resulting in carbon exchange between terrestrial features and the atmosphere. Other anthropogenic practices, such as deforestation, decrease the capacity of vegetation to store C via uptake for photosynthetic processes (Post et al., 1990). Attempts to quantify the net fluxes have yielded an imbalance of C storage within the three major reservoirs relative to known magnitudes of CO<sub>2</sub> introduced into the atmosphere by human activities since the Industrial Revolution. An understanding of the magnitude and location of atmospheric C sources and sinks is crucial for predicting how changes in atmospheric C are likely to influence climate.

### 2.3 The “Missing Sink” and Changes in Storage

The atmospheric concentration of CO<sub>2</sub> for the remote, unpolluted atmosphere is accurately known from a record of continuous measurements at Mauna Loa, Hawaii Observatory, since 1958, and is currently over 400 ppm. Estimates of the C uptake and storage by the oceans compared to the measured atmospheric C sink reveal that less C has been sequestered between these reservoirs than what has been contributed to the atmosphere by anthropogenic C emissions. Thus, a large balance of C is unaccounted for and is assumed to be held within terrestrial reservoirs. The term ‘missing sink’ has been used to describe this disparity and the existence of inaccuracy in attempts to quantify a global C flux (Tans et al. 1990; Sarmiento and Sundquist, 1992; Siegenthaler and Sarmiento, 1993; Sundquist, 1993). During the 1980s alone, CO<sub>2</sub> emissions from fossil-fuel combustion and the deficit in CO<sub>2</sub> uptake from deforestation totaled about 7 Gt C yr<sup>-1</sup> (gigatons C per year) (1 Gt = 10<sup>9</sup> tons). Increases in atmospheric CO<sub>2</sub> accounted for approximately half the amount of C emissions released during this time (Siegenthaler and

Sarmiento, 1993). Tans et al. (1990) examined C budgets for the period 1980-1989 and found that, of the  $7 \pm 1 \text{ Gt C yr}^{-1}$  total C emissions, only  $\sim 4.5 \text{ Gt C yr}^{-1}$  were accounted for between the  $3.5 \text{ Gt C yr}^{-1}$  stored in the atmosphere and  $<1 \text{ Gt C yr}^{-1}$  from ocean uptake. Siegenthaler and Sarmiento (1993) reexamined this same period using surface water  $\text{pCO}_2$  data and determined that  $\sim 5.5 \text{ Gt C yr}^{-1}$  were accounted for between the atmospheric and oceanic reservoirs, with atmospheric storage remaining equal to previous estimates, but considered  $\sim 2 \text{ Gt C yr}^{-1}$  as coming from ocean uptake. More recent studies by Sabine et al. (2004) suggested approximately 3.4 Gt of the total 7 Gt C produced annually are contained within the atmosphere, while 3.6 Gt remains unaccounted for. The residual  $\text{CO}_2$  must, therefore, be taken up by the oceans, terrestrial biosphere, or a combination of the two (Sabine et al., 2004). The so-called missing sink has led to detailed exploration into development of an overall C budget that could explain the discrepancy (Liu and Zhao, 2000; Liu et al., 2008).

Further obscuring our knowledge of C sinks are changes in the storage capacities of the various sinks themselves. A study of observed trends in C sources and sinks found that, between 1959 and 2008, an average of 43% of all emissions produced remained within the atmosphere, with the other 57% absorbed by combined terrestrial and oceanic sinks. Over the past several decades, the amount of C remaining in the atmosphere has increased to 45% and models suggest that this trend is highly influenced by decreased  $\text{CO}_2$  uptake by C sinks, which is thought to be a result of positive feedback cycles contributing to climate change and variability. At present, the magnitude of the change in C uptake among various sinks in response to climate change is highly uncertain but may significantly impact atmospheric  $\text{CO}_2$  concentrations into the future. Therefore, a clearer

understanding of the available C sources and sinks, particularly the less-explored terrestrial sinks, and fluctuations in the amount of C being removed from the atmosphere by each, is crucial for managing future climate change (Le Quéré et al., 2009).

## 2.4 Overview of Carbon Reservoirs

### *2.4.1 Atmospheric Carbon Storage*

The burning of fossil fuels has been identified as a major agent responsible for the observed increase in atmospheric CO<sub>2</sub> concentrations (Sabine et al., 2004; Tans and Keeling, 2017). Atmospheric CO<sub>2</sub> concentrations before the Industrial Revolution averaged about 6 Pg C (1 Pg = 10<sup>15</sup> g) (Sigman and Boyle, 2000), but this average increased considerably around the mid eighteenth century. Approximately 337 Gt of C have been introduced into the atmosphere from fossil fuel burning and production of cement from 1751 to the present. Particularly alarming is the fact that over of half that amount has been released by human activities since 1970 (Boden et al., 2010). The Scripps Institute of Oceanography observatory in Mauna Loa, Hawaii, has a record of atmospheric CO<sub>2</sub> concentrations dating from 1958 to the present. The well-known Keeling Curve generated from these data shows a continuous increase in CO<sub>2</sub> concentrations in Earth's atmosphere over the entire span of the record. Currently, the remote atmospheric CO<sub>2</sub> concentration is over 400 ppm throughout the year, though this level fluctuates seasonally with the timing of deciduous forest activities (i.e., growth and photosynthesis) in the northern hemisphere (Keeling et al., 2005).

Some have questioned whether recent increases in atmospheric C concentrations could be the result of the natural cyclic fluctuations in the C cycle. These arguments suggest that natural fluxes between C reservoirs may outweigh those resulting from

anthropogenic perturbations. Several lines of opposition refute this, including a multitude of evidence that indicates a relatively stable balance of the sum fluxes into and out of all reservoirs prior to industrialization. Estimates of CO<sub>2</sub> fluxes into and out of the atmosphere prior to the industrial period reveal that C emissions to the atmosphere were roughly equal to the C stored within the atmosphere and ocean (see Siegenthaler and Sarmiento, 1993; Falkowski et al., 2000; Sabine et al., 2004). Data from ice cores taken from the Antarctic, and dated between 1000 and 1800 CE, demonstrate that atmospheric CO<sub>2</sub> levels varied with a range of only ~10 parts per million (ppm) over the past 1,000 years (Siegenthaler and Sarmiento, 1993). Falkowski et al. (2000) reported that, over the past 420,000 years, atmospheric CO<sub>2</sub> oscillated in approximately 100,000-year cycles between about 180 and 280 ppm (Figure 1.1). Sabine et al. (2004) offered a slightly more concise estimate of 200-280 ppm. The current rate of increase in atmospheric carbon is equal to at least 10 and perhaps as much as 100 times greater than during any period within the past 420,000 years (Falkowski et al., 2000). Evidence of the annual mean CO<sub>2</sub> concentration measurements in the Northern Hemisphere, where about 95% of fossil fuel emissions originate, has consistently exceeded the levels in the Southern Hemisphere since the onset of atmospheric monitoring (Siegenthaler and Sarmiento, 1993). The Intergovernmental Panel on Climate Change (IPCC, 2014) provided a summary of the observed changes and causes of climate change, prediction of future climate change, risks and impacts, and the development and implementation of adaptive and mitigation strategies including best management practices. With regard to the existence and causes of climate change, the IPCC (2014: 1) wrote:

“Anthropogenic greenhouse gas emissions have increased since the pre-industrial era, driven largely by economic and population



growth, and are now higher than ever. This has led to atmospheric concentrations of carbon dioxide, methane and nitrous oxide that are unprecedented in at least the last 800,000 years. Their effects, together with those of other anthropogenic drivers, have been detected throughout the climate system and are *extremely likely* to have been the dominant cause of the observed warming since the mid-20<sup>th</sup> century.”

#### 2.4.2 Carbon Storage in the Ocean

A large portion of the remaining CO<sub>2</sub> contributed by human activity is absorbed by the ocean. Although it is known that the oceans function as impressive C reservoirs, many of the details remain unknown. Conflicting estimates of the actual amount of C uptake have been noted in reviews (Siegenthaler and Sarmiento, 1993), and the comparative roles of terrestrial and ocean CO<sub>2</sub> uptake are not well known. The current estimates are derived from simulations and do not fully consider the actual DIC measurements from the ocean (Sabine et al., 2004). Sabine et al. (2004) developed an estimate of the global oceanic CO<sub>2</sub> sink between 1800 to 1994 equal to  $118 \pm 19$  Pg C, which accounts for approximately 48% of all C emission products of fossil fuel and cement manufacturing during that time. Tracer-calibrated models used by Sarmiento and Sundquist (1992) estimated the total oceanic uptake of anthropogenic CO<sub>2</sub> at  $\sim 2$  Gt C yr<sup>-1</sup>.

Carbon is present in the ocean in several forms. Dissolved inorganic carbon (DIC) is essentially equal to the sum of the carbon stored as dissolved CO<sub>2</sub>, carbonic acid (H<sub>2</sub>CO<sub>3</sub>), or the carbonate (CO<sub>3</sub><sup>2-</sup>) and bicarbonate (HCO<sub>3</sub><sup>-</sup>) ions. Dissolved organic carbon (DOC) composed of C<sub>org</sub> molecules represents the second most prevalent form of C stored in the ocean. The smallest proportion of C storage in the ocean is in the form of particulate organic C (POC) represented as living organisms and detritus. Measurements

of ocean C concentrations during the 1990s determined that approximately 37,000 Gt C were present as DIC, ~1000 Gt C as DOC and ~30 Gt C as POC (Post et al., 1990).

#### 2.4.3 *The Terrestrial Carbon Sink*

The balance of C not stored in the atmosphere or ocean must be stored within the terrestrial biosphere. Terrestrial C sinks include biological, lithological, and pedological components. Recent studies suggest that the North American continent has become a large sink of atmospheric CO<sub>2</sub> (Fan et al., 1998; Myneni et al., 2001; Butler et al., 2010). Analysis of the global C budget has suggested that the North American sink may represent up to one-third of the combined global land and ocean CO<sub>2</sub> sink (Pacala et al., 2007). The *State of the Carbon Cycle Report (SOCCR)* was developed as an anthology of late-20<sup>th</sup> century research on the C budget in North American terrestrial ecosystems (King et al., 2007). The report revealed the level of uncertainty associated with quantifying the atmospheric C sink in terrestrial systems with sink estimate values ranging from 0.1 to 2.0 PgC yr<sup>-1</sup>. The large variation in land flux estimates is primarily the result of inconsistent methodologies employed to evaluate flux between C sources and sinks (Hayes et al., 2012).

Inland waters are also considered part of the terrestrial C reservoir. However, because these bodies occupy a minimal fraction of the Earth's surface area relative to the oceans and continents, they often have been overlooked in attempts to describe the C cycle quantitatively at both global and regional scales. Conservative estimates indicate that inland waters receive an annual C load about 1.9 Pg C yr<sup>-1</sup> from natural background and anthropogenic C sources associated with the terrestrial landscape. Of this total load, it is estimated that about 0.2 Pg C yr<sup>-1</sup> is diverted to the lithosphere by burial in the

sediments,  $0.9 \text{ Pg C yr}^{-1}$  is deposited in the oceans, and the other  $0.8 \text{ Pg C yr}^{-1}$  is returned to the atmosphere by  $\text{CO}_2$  out-gassing. Thus, only about half of the C load entering inland waters is transported to the ocean (Cole et al., 2007). A portion of the C that enters inland bodies of water is prevented from entering the ocean because the C is trapped in lakes and reservoirs. Investigation of the C source-sink ratio of a eutrophic lake revealed that the ratio of C emissions to C sediment burial was equal to 0.8, suggesting that the lake behaved as an effective sink (Yang et al., 2008). Another study found that, although the area of lake basins represents only 2% of the land surface area or only 0.8% of the area of the ocean surface, a significant amount of atmospheric-source C was contained within the lake sediments, equal to  $0.07 \text{ Pg C yr}^{-1}$  and equivalent to more than 25% of C sedimentation in the oceans (Einsele et al., 2001). The high productivity associated with lacustrine systems leads to increased sedimentation rates, which likely accounts for the increased turnover rate among these inland water bodies compared to those observed in the ocean.

The terrestrial C sink exhibits numerous facets aside from the sink associated with dissolution of carbonate minerals. Factors such as storage of  $\text{CO}_2$  in the soil, and the weathering of silicates and island basalts, may have substantial influence on the drawdown of atmospheric  $\text{CO}_2$ . For example, soils are estimated to store approximately 80% (2,500 Gt) of the total carbon in the terrestrial biosphere. The carbon pool that is stored in the soil is about 4.5 times greater than carbon stored in the biotic reservoir (560 Gt). The potential capacity of the soil sink is estimated at 55-78 Gt C; however, the actual soil-carbon sink capacity is between 50-66% of the potential (Lal, 2004). Silicate weathering due to tectonic uplift is also proposed as a mechanism for enhancing the sink

of atmospheric CO<sub>2</sub>. Silicate weathering is a component of the ‘uplift driven climate change’ hypothesis that contends the sequestration of atmospheric CO<sub>2</sub> by silicate weathering is a strong function of continental relief and a pCO<sub>2</sub>-weathering feedback system (Li and Elderfield, 2013). Silicate weathering is occurring on massive scales in the Himalayan and Tibetan Plateaus as a result of climate-change-driven tectonic uplift (Garzzone, 2008; Li and Elderfield, 2013). Two of the most accepted potential feedback mechanisms for global cooling through decreases in atmospheric CO<sub>2</sub> involve increasing precipitation of silicates in the deep sea or decreasing the weathering of island basalts due to elevated pH of seawater. Models of tectonic-climatic feedback systems associated with weathering of the Himalayas and Tibetan Plateau suggests that silicate weathering and organic C burial may be responsible for the decrease in atmospheric CO<sub>2</sub> necessary to foster a global cooling phase (Garzzone, 2008). Weathering of island basalts may have an important contribution in the atmospheric CO<sub>2</sub> sink, as most oceanic islands are in areas of high tectonic activity and typically have strong relief leading to increased rates of physical erosion (Li and Elderfield, 2013).

While other forms of atmospheric CO<sub>2</sub> sinks are accepted as present in the terrestrial reservoir, the significantly greater solubilities and dissolution rates of carbonate rocks relative to silicates suggest that the associated sink capacity is immense and worthy of consideration, at least over longer timescales. The remainder of the discussion on terrestrial C sinks builds on this information to focus on the significance of the terrestrial C sink as it arises from water-rock interactions and the process of carbonate dissolution.

## 2.5 Carbon Sink from Carbonate Rock Dissolution

Morse and Arvidson (2002: 51) stated “Among the most important set of chemical reactions occurring under near Earth surface conditions are those involved in the dissolution of sedimentary carbonate minerals.” In terms of lithology, C sequestration by carbonate minerals estimated at  $6 \times 10^7$  Pg C is about four orders of magnitude greater than storage in the biosphere or buried fossil fuels and about five orders of magnitude greater than atmospheric C storage (Falkowski et al., 2000) (Table 2.1). Geologically, carbonic acid is the most abundant acid on the planet, whereas bicarbonate and carbonate ions are the major contributors of alkalinity (England et al., 2011). Increases in atmospheric CO<sub>2</sub> have contributed to decreases in surface water pH, thus affecting mineral stability in carbonate rocks. It has been proposed, and generally accepted, that rivers in carbonate karst terrains have a more significant impact than non-carbonate rivers in regulating regional and global carbon cycling via dissolution and precipitation reactions among carbonate minerals. These dissolution and precipitation reactions are related to primary production. The C<sub>org</sub> in vegetation is fixed from the atmosphere via photosynthesis, but as plants decay the carbon once stored in their tissues becomes part of the soil, eventually remineralizing in watersheds to form dissolved CO<sub>2</sub>, and then gradually returned to the atmosphere (Martin et al., 2013). Interactions between infiltrating precipitation and CO<sub>2</sub> contained in the soil from microbial respiration processes are also closely associated with carbonate-mineral weathering. Carbonate-rock weathering on the continents represents a carbon sink, as carbonate minerals undergo dissolution in response to increasing acidity of ground and surface waters resulting from interactions of atmospheric and soil CO<sub>2</sub>, thereby removing carbon that once was held in

the atmosphere and preventing release of CO<sub>2</sub> from the soil (Yuan, 1997; Ludwig et al., 1998; Liu and Zhao, 2000).

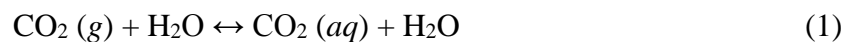
Table 2.1. Carbon storage within the major reservoirs on Earth.

<b>Reservoir</b>	<b>Quantity (Gt)</b>
Atmosphere	720
Oceans	75,800
Total inorganic	37,400
Surface layer	670
Deep layer	36,730
Total organic	1,000
Lithosphere	
Sedimentary carbonates	>60,000,000
Kerogens	15,000,000
Terrestrial biosphere (total)	2,000
Living biomass	600-1000
Dead biomass	1,200
Aquatic biosphere	1-2
Fossil fuels	4,130
Coal	3,510
Oil	230
Gas	140
Other (peat)	250

Source: From Falkowski et al. (2000).

Relative to the span of geologic history, sink growth by carbonate dissolution is applicable on relatively short time scales. The close association between carbonate mineral weathering and the hydrologic cycle allows for an estimated average turnover time for terrestrial carbon leaving a watershed to be akin to that of the ocean-water cycle, equal to approximately 2,000 years. By comparison, the atmospheric CO<sub>2</sub> turnover rate is 3-5 years, approximately 50 years for vegetation, and soil release may range from decades to millennia (Cao et al., 2012). Because CO<sub>2</sub> sequestration by carbonate dissolution process may affect the carbon cycle on time scales relevant to human activity, a precise understanding of the extent of this sink is necessary to support global source/sink estimates of carbon. Understanding the role of carbonate mineral dissolution sinks on the continents could contribute to better short-term models of the carbon cycle over comparatively small time spans coincident with human impact.

The specific processes by which carbonate mineral weathering acts as a carbon sink requires an understanding of the chemical interactions taking place in the system. The buffering capacity of carbonate systems represents the primary mechanism for acid neutralization among aquatic systems via contribution of bicarbonate ions (Yadav, et al., 2008). Hydrolysis of CO<sub>2</sub> produces carbonic acid (H<sub>2</sub>CO<sub>3</sub>) that contributes hydrogen ions to the solution, resulting in lowered pH (Orr et al., 2005). The hydrolysis of CO<sub>2</sub> to form H<sub>2</sub>CO<sub>3</sub> and subsequent formation of bicarbonate (HCO<sub>3</sub><sup>-</sup>) and carbonate (CO<sub>3</sub><sup>2-</sup>) ions is an extensively studied process. The chemical reactions for CO<sub>2</sub> dissolution, hydrolysis and equilibrium in water are as follows:





and



Carbonate-rock weathering in natural waters can in turn be described by the following set of chemical equations for limestone and dolomite respectively:



and



The inorganic C flux leaving a given basin is the product of the concentration of DIC and the discharge of the river. The total dissolved inorganic carbon present in solution is found by summing the concentration of each species ( $\text{H}_2\text{CO}_3$ ,  $\text{HCO}_3^-$ , and  $\text{CO}_3^{2-}$ ) present in solution. The proportion of each species in solution is controlled by pH, such that for a pH of 7 to 9 most of the DIC in ground and ocean water is in the form of bicarbonate, while at higher pH values (>9) carbonate dominates ionic concentrations (Figure 2.1) (Drever, 1988; Dreybrodt, 1988). In waters of most naturally occurring pHs, DIC can be obtained from measurements of  $\text{HCO}_3^-$ , pH and temperature in combination with calculations of relevant species activities and equilibrium constants (Stumm and Morgan, 1981).



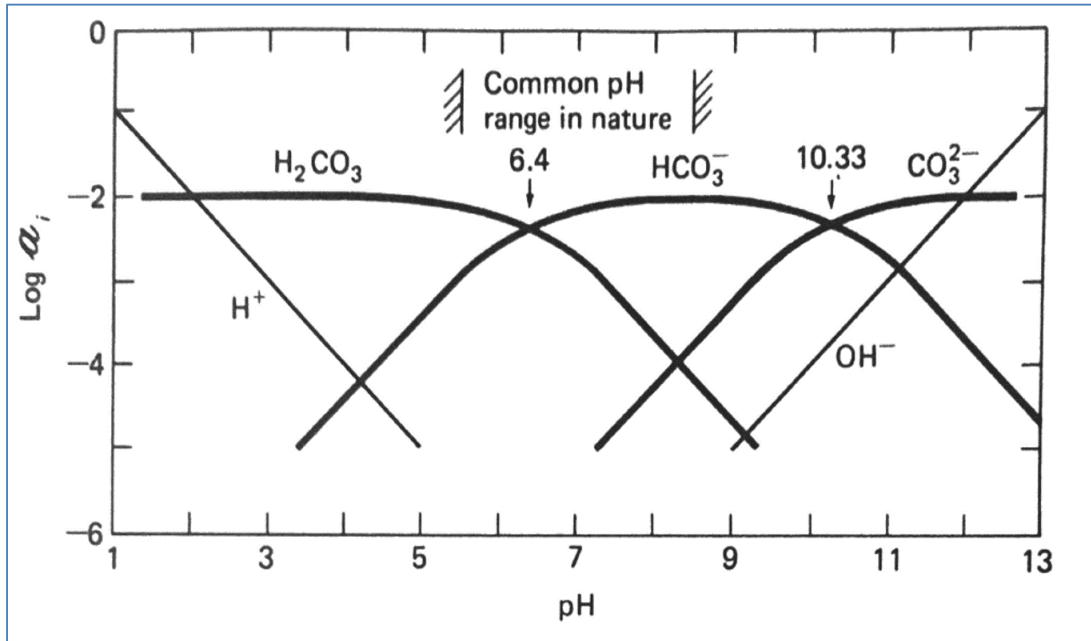


Figure 2.1. Activity of carbonic acid, bicarbonate, and carbonate species in solution versus pH.  
Source: Drever (1988).

The molar ratios of reactants and products shown in Equations 5 demonstrate a fundamental assumption that is related directly to the partitioning of DIC sources. The basis of this assumption relies on the stoichiometry of Equations 5 and 6, showing a 1:1 molar ratio of C between atmospheric and carbonate rock sources. Equation 5 shows that for every two moles of C produced as bicarbonate ion ( $\text{HCO}_3^-$ ) that results from the reaction, one is considered to have originated from the atmosphere in the form of  $\text{CO}_2$  and one mole is derived from the limestone. In the case of dolomite, the atmospheric to carbonate rock ratio for C is also 1:1, but four moles of  $\text{HCO}_3^-$  are produced by the reaction, with two moles derived from the atmosphere and two moles from the dolomite rock. Using the stoichiometric approach, an estimate of inorganic carbon flux from the atmosphere by carbonate rock weathering can be considered as one-half of the total DIC

leaving a river basin influenced by carbonate rock interactions (Jiang and Yuan, 1999; Liu and Zhao, 2000; Groves and Meiman, 2001; Groves et al., 2002; Amiotte Suchet et al., 2003; He et al., 2013). Numerous other factors are proposed to complicate the partitioning of DIC observed in natural systems, such that the actual proportion of flux contributed by carbonate-mineral weathering is difficult to separate from myriad other potential sources of DIC in a drainage basin. However, since the flux of DIC in natural systems is primarily associated with weathering of terrestrial carbonates (Falkowski et al., 2000) (see Table 1), factors such as  $\text{DCO}_2$  contributed to waters by decomposition of OM and bacterial respiration are responsible for only a small portion of the DIC in freshwater systems. Hereafter, numerous major and minor controls on carbonate-mineral weathering are discussed with respect to how these processes contribute to DIC flux.

## 2.6 Controls on Carbonate Mineral Dissolution and DIC Flux

Several factors control carbonate mineral dissolution, thereby directly influencing the magnitude of the atmospheric carbon sink associated with carbonate rock dissolution. Carbonate minerals are highly susceptible to dissolution by weak carbonic acid solutions that form within surface and ground waters. At the molecular level, thermodynamic and kinetic principles are barriers that govern the solubility properties of minerals and the rates of dissolution or precipitation reactions. These topics are discussed first to establish a fundamental basis for the macroscale processes (area of carbonate rocks in contact with water, amount of water available for dissolution, and time) that serve as constraints for the microscale thermodynamic and kinetic processes.

### 2.6.1 Thermodynamic Controls

The dissolution of calcite in acidic surface waters is a product of chemical thermodynamics that dictate the direction of reactions occurring in solutions near equilibrium. The use of mass-balance calculations is the classic approach to making predictions of chemical systems using thermodynamic principles. The mass-balance approach is useful in interpreting mineral weathering, as it accounts for the sources of dissolved mineral constituents found in solution using concentration or activity data for products and reactants in solution, and the solubility product constant associated with the dissolution of a mineral. The mass-balance calculations for the reaction shown in Equation 5 are shown in Equations 7, 8, and 9.

$$[H_2CO_3] = \frac{[H^+][HCO_3^-]}{K_1} \quad (7)$$

$$[HCO_3^-] = \frac{[K_1][H_2CO_3]}{H^+} \quad (8)$$

$$[CO_3^{2-}] = \frac{[K_2][HCO_3^-]}{H^+} \quad (9)$$

In non-ideal solutions, activity coefficients must be assigned to determine the degree to which individual species participate in a reaction where ionic concentrations do not equal species activities. Species activities can be calculated using the Debye-Hückel expression (Stumm and Morgan, 1981; Drever, 1988; White, 1988) (Equation 10).

$$-\log \gamma_i = \frac{Az_i^2\sqrt{I}}{1+\alpha_i B\sqrt{I}} \quad (10)$$

The relative concentrations of dissolved ions in solution dictate the weather a given mineral will be ionized in solution, or if a solid precipitate will form. The saturation state of a fluid with respect to calcium carbonate is a major factor in determining the potential for carbonate-mineral dissolution. A value for the saturation index (SI) can be used to predict the behavior of carbonate minerals based upon saturation state. Stumm and Morgan (1981) provided an elegant and functional method for calculation of saturation index as follows:

$$SI_{cal} = \log \left( \frac{[Ca^{2+}][CO_3^{2-}]}{k_{cal}} \right) \quad (11)$$

where brackets denote species activities and  $k_{cal}$  is the temperature dependent equilibrium constant (or solubility product) for calcite dissolution. When applied to carbonate hydrochemistry, saturation indices predict the direction the reaction will proceed based on the chemistry and temperature of the water. In general,  $SI_{cal}$  values  $>0$  represent oversaturated solutions, where dissolved ions are in abundance and precipitation of solids is predicted (though there may be kinetic barriers). Values equal to zero represent systems at equilibrium with  $CaCO_3$  neither dissolving or precipitating, and values  $<0$  indicate states of undersaturation wherein soluble minerals would be expected to undergo dissolution (Langelier, 1936; Stumm and Morgan 1981).

### 2.6.2 Kinetic Controls

The DIC flux from carbonate mineral weathering cannot be fully defined from a purely thermodynamic approach of calculating sum concentration of carbonate species present in solution. In natural systems, reactions are controlled by factors other than species activities. Kinetic considerations must be made in evaluating the rate in which a

reaction will occur, or if there are barriers that will prohibit a reaction from occurring.

Three types of kinetic processes govern mineral dissolution/precipitation rates, including 1) physical detachment of grains from a mineral surface, 2) transport (diffusion) of ions in solution to or from the mineral surface, and 3) mixed kinetics (both reaction and diffusion controlled) (Drever, 1988). Numerous physical, chemical and biological aspects control kinetics of carbonate mineral weathering.

Kinetics determines the rates at which reactions occur. Most rate processes can be described by the Arrhenius equation:

$$Rate = A \exp\left(\frac{-\Delta E}{RT}\right) \quad (12)$$

Where R is the ideal gas constant, T is the Kelvin temperature, A is an empirical constant, and  $\Delta E$  is the activation energy required to convert the initial reactant to the transition state, regarded as the energy difference between the initial state and the maximum energy of the intermediate state (Drever, 1988). From Equation 12, temperature is clearly an important control on reaction rates, such that an increase in temperature results in rate increase. Temperature also affects the saturation state of  $\text{CaCO}_3$  via its influence on kinetic rates that determine the amount of mineral weathering that takes place over time, therefore influencing the abundance and behavior of solutes in solution and whether these are expected to undergo dissolution or precipitation (Larson and Buswell, 1942). Studies of dynamic epikarst regions in China, for example, have demonstrated that under dry climatic conditions pH and electrical conductivity exhibited diurnal fluctuations and rose in association with increases in water temperature during the

day. The increase in conductivity reveals an increase in dissolved ions present in solution resultant of increased dissolution under increased temperatures (Cheng et al., 2005).

Plummer et al. (1978) developed a rate law for predicting the rate of calcite dissolution as a function of water chemistry:

$$r = k_1[\text{H}^+] + k_2[\text{H}_2\text{CO}_3^*] + k_3[\text{H}_2\text{O}] - k_4[\text{Ca}^{2+}][\text{HCO}_3^-] \quad (13)$$

where  $r$  is dissolution rate in mass dissolved per surface area of mineral/water contact per time, the  $k$  values are temperature dependent kinetic rate constants (Plummer et al., 1978) and bracketed terms denote activities of ion species activities in aqueous solution. Reedy et al. (1981) used calcite precipitation from  $\text{Ca-HCO}_3^-$  solutions to test the reverse reaction of the calcite dissolution rate law model and found that measured crystallization rates were in close agreement with those predicted by Plummer (Reedy et al., 1981).

#### *Surface and Transport Reaction*

Specific surface area (SSA) is a type of reaction control that has a significant impact on dissolution/precipitation rates. Rates of dissolution/nucleation are much higher for mineral surfaces with more than one plane of exposure (Drever, 1988). Since chemical weathering occurs along mineral surfaces, the water and acids that control chemical weathering require access to the surface. Weathering processes begin on the exterior of a mineral, and rates are limited by the area of mineral exposed to solution. Physical weathering processes break up rocks to increase the surface area that can be exposed to weathering and create pathways for the water to enter rock. The presence of bedding planes, joints, and fracture networks in bedrock contributes to the rate of mineral weathering by enabling acidic water to penetrate to the interior and allow for weathering in a 3-dimensional sense, rather than on the exterior surface only. In bedrock where the

number of fractures per unit area is high, the rates of mineral weathering can be increased by several-fold relative to massive rocks that contain no bedding planes, joints, or fractures (Gabet et al., 2006). As discussed below, biological inputs also affect the kinetics of mineral weathering, particularly through root wedging and production of humic and fulvic organic acids, which infiltrate fractures to create solution-enhanced conduits. Therefore, extensive fracture networks may have a great impact on the amount of DIC export from basins due to enhanced weathering rates in the sub-surface. Weathering rates are also a function of grain size, which is related to SSA, with fine grains entering solution more rapidly. This association may offer insight to the comparatively large DIC flux export among the sub-basins where calcium-rich, fine-grained, unconsolidated sediments constitute surface geology.

#### *Variation in Carbonate Mineral Type and Purity*

Additionally, inherent differences exist in the behavior of carbonate minerals as they interact with water. The properties of minerals undergoing weathering processes dictate the extent to which these influence DIC in aqueous systems. This can be observed from the difference in solubility products among various carbonate minerals. For example, calcite solubility under neutral pH at standard temperature and pressure (STP) is reported to be 100 mg/L. The solubility of dolomite is lower under neutral pH and STP (90 mg/L). In systems where pH is not neutral the difference in solubility between calcite and dolomite increases (Freeze and Cherry, 1979). Drever (1988) noted that these differences are due not only to the constituents of the minerals themselves, but also to the ratio of these in relation to other constituents that make up the mineral and crystallographic orientation of minerals. Large differences exist in mineral stability among calcite,

dolomite, calcite concretions, and in rock units where carbonates are interbedded in other rock types (Drever, 1988). Such differences translate to variation in dissolution rates and affect the chemical signature of water as it interacts with these minerals. Basins with less carbonate area may still produce a large DIC flux if the type of carbonate present is very pure, soluble or has a high weathering rate. Alternatively, basins with a large area of carbonate rocks may produce a small flux if the carbonates are impure, have lower solubility or the conditions within the basin dictate low weathering rates. Carbonate rocks were not distinguished on the basis of solubility or the rate at which these minerals contribute alkalinity to aqueous systems in this pursuit, but future studies may wish to evaluate the comparative roles of different types of carbonate rocks in contributing carbonate alkalinity to streams.

### *2.6.3 Proposed Major Controls*

Although the thermodynamic and kinetic processes described in the previous section exert considerable influence upon the carbonate dissolution process, at the landscape scale these microscale processes ultimately depend on macroscale events. This study investigated the hypothesis that the primary macroscale controls that influence carbonate dissolution and the amount of carbon removed from the atmosphere include: 1) the surface area of carbonate rock exposed, 2) the duration of the study period, and 3) the volume of water available for mineral dissolution.

#### *Area of Carbonate Outcrop*

Carbonate-mineral dissolution and the magnitude of the associated DIC flux is certainly a function of the surface area of rock in contact with water. Geometric surface areas have been used successfully in estimating weathering rates in situ (White and



Peterson, 1990). A large area of carbonate rock outcrop will yield more carbonate dissolution as greater surface areas are exposed to chemically undersaturated waters. Since calcite dissolution consumes CO<sub>2</sub> from the fluid solution, as increased carbonate dissolution occurs the amount of carbon being sequestered from the atmosphere as a result of these dissolution processes also increases. Several other studies have suggested it is appropriate to normalize flux calculations by the area of the carbonate rock present in the drainage basin for the purposes of calculating global carbon fluxes and the sink due to carbonate dissolution (Lüttge, 2005; Osterhoudt, 2014; Salley, 2016). Accordingly, the model used in this project to estimate DIC flux from carbonate mineral weathering normalizes flux by area of carbonate outcrop exposed within the basin. Carbonate outcrop area represents the geologic component of the normalization of calculated DIC flux values for the Ohio River Basin and major nested sub-basins.

#### *Duration of Water-Rock Contact*

The duration of the water-rock interaction must also be quantified in estimates of the carbon sink from dissolution. For example, a mineral sample left in a solution to dissolve for twice as much time will experience a two-fold reduction in mass. Increases in contact time between chemically active water and minerals promotes weathering of base cations, resulting in increases in weathering products (Finlay, 2003). The U.S. Geological Survey uses a 12-month period known as a water year to report on matters associated with surface-water supply; defined as the period between October 1 of a given year and September 30 of the following year, and is designated as the calendar year in which it ends. The water year 2014 was used in this research. The period of interaction between potentially understaturated water and carbonate minerals represents the temporal

component of the parameters used to normalize DIC flux from the Ohio River Basin and major sub-basins.

#### *Amount of Water Available for Dissolution*

Probably the most significant control on the sink from carbonate-mineral weathering is the volume of water available for dissolution. This value can be estimated as precipitation minus evapotranspiration (P-ET) over the area of the carbonate rock outcrop within a drainage basin (Cao et al., 2011; Haryono, 2011) or as the discharge coming out of the drainage area (Groves and Meiman, 2001; White, 2013). DIC dynamics have been shown to vary greatly with stream size and channel flow. Finlay (2003) demonstrated that aqueous  $\text{CO}_2$  is positively related to discharge for large, open-canopied rivers, where the expanse of the channel prevents canopy formation, with larger/wider channels indicative of greater discharge. Additionally,  $\text{HCO}_3^-$  and  $\text{Ca}^{2+}$  were found to be inversely related to discharge, a pattern consistent with expected results for large contributions from carbonate weathering during periods of high discharge and control of  $\text{HCO}_3^-$  via the duration of contact between groundwater and carbonate-mineral surfaces. Finlay (2003) also determined that aqueous  $\text{CO}_2$  was correlated to  $\text{Ca}^{2+}$  and  $\text{HCO}_3^-$  only among small streams, indicating that relationships between  $\text{CO}_2$  (aq) and  $\text{HCO}_3^-$  are increasingly decoupled as stream size increases. In contrast, Groves and Meiman (2005) found the inorganic carbon flux to be almost linearly correlated to discharge from a study of carbonate weathering in an underground river in south-central Kentucky. It was determined that although the highest discharge stage in the conduit was observed only <5% of the time, this stage resulted in the largest amount of carbonate dissolution, or 38% of the total dissolution for all stages. A study by White (2013) in a

karst landscape found that carbon flux corresponded to discharge. Liu et al. (2008) found that the atmospheric CO<sub>2</sub> sink factor doubled during rainstorms due to increased stage height. He et al. (2013) used monitoring data from the Banzhai subterranean stream located in the Guizhou province of China to support the conclusion that the amount of karst carbon sequestration depends on the discharge of karst catchment in addition to the inorganic carbon concentration of the water. They determined that about 353 t C yr<sup>-1</sup> are removed from the atmosphere via carbonate dissolution processes in this basin and that a good linear relationship existed between the carbon flux leaving the basin and the stream discharge across various time scales. The amount of water available for dissolution is controlled by climate patterns for a given location. As such, the balance of P-ET represents the climatic component and the final proposed parameter used to normalize DIC flux observed in the Ohio River Basin and the major tributary sub-basins.

#### *2.6.4 Proposed Lesser Controls*

Aside from the temporal, geologic, and climatic variables discussed above, numerous “lesser” factors are capable of influencing carbonate weathering and thus the capacity of the C sink from those processes. Collectively, these processes may have a substantial influence on the drawdown of atmospheric C. The emphasis of this work is to evaluate the relative contribution of the proposed major controls (time, area of carbonate rock, and water available for dissolution) relative to a host of other events occurring over broad scales. Time, geology, and climate-regulated water availability were accounted for in the normalization procedure applied in this study. While the time- and climate-based controls on carbonate dissolution are definitive, the geologic aspects of the normalization procedure create complexity in evaluating the success of the model described herein.

Challenges exist in geologic characterizations of drainage basins that may affect the reliability of flux estimates generated by the model as currently described. The following discussion includes several considerations that may complicate the direct interpretation of DIC flux patterns that are not included within the scope of this work. A summary of myriad additional variables that may contribute to the observed DIC flux issuing from a river basin is presented in Table 2.2.

#### *A. Carbonate Minerals Not Mapped as Surface Deposits*

The research design of this project relies on maps of surface geology. The existence of calcium and carbonate sources of DIC beyond the mapped carbonate bedrock (see Weary and Doctor (2014) U.S. karst map) is an important consideration when estimating DIC flux over very large areas, such as the Ohio River Basin. The DIC observed in a water sample may include C contributed from a variety of additional sources including: 1) carbonate minerals in the subsurface, 2) calcium-rich loess deposits, 3) calcium- and magnesium-rich lacustrine facies, 4) thin surface carbonates and interbedded carbonate lenses, 5) grain replacement of non-carbonate rocks by carbonate minerals found in calcite cements, 6) bedload carbonate grains in streams, and 7) DIC flux contributed from non-carbonate rocks associated with climate-driven feedback mechanisms. These additional factors become more important considerations among drainages where carbonate rock outcrops are less prevalent and observed DIC must be contributed from other sources. A basic discussion of the auxiliary processes that may influence DIC in surface streams within the Ohio River Basin, aside from exposed carbonate rocks related to the project objective of defining the magnitude of the DIC flux from carbonate mineral weathering, is presented in the following sections.

<b>Variable</b>	<b>Control Type</b>	<b>Action</b>	<b>Reference(s)</b>
Carbonate Mineral Type	Thermodynamic	$K_{sp} \text{ limestone} \neq K_{sp} \text{ dolomite} \neq K_{sp} \text{ Loess} \neq K_{sp} \text{ calcite concretions}$	Drever (1988)
Specific Surface Area	Kinetic	Affects surface reaction rates	Drever (1988)
Buried Carbonates	Geochemical	Contribute DIC from areas unaccounted for by surface geology maps	Ray (1965; 1974); Thompson et al. (2016)
Ca <sup>2+</sup> /Mg <sup>2+</sup> -Rich Quaternary Deposits	Geochemical	Same as above	Cook and Montgomery (1914); Thornbury (1940); Ray (1965)
Thin Surface Carbonates	Geochemical	Same as above	Shrock and Malott (1929); Bodine (2016)
Impure/Interbedded Carbonates	-Thermodynamic -Kinetic	-Solubility products $\neq$ -Weathering rates $\neq$	Bodine (2016)
Calcite Replacement	-Thermodynamic -Kinetic	Same as above	Butler (2016)
Carbonate Precipitation and CO <sub>2</sub> Outgassing	-Thermodynamic -Geochemical	Portions of C load that are not captured by chemical signature (DIC) of stream	Jiang and Yuan (1999); Richey (2003); White (2013); Khadka et al. (2014)
Vegetation	Biological	-Physical and chemical weathering -Increase C storage beyond saturation thresholds	Li et al. (2005); Thorley et al. (2015); Lambers et al. (2015); Silva (2017)
Organic Acids	-Kinetic -Biological	Chiefly by affecting pH	Huang and Keller (1970); Tan (1986); Drever (1988); Drever and Stillings (1997)
Microorganisms	Biological	-Bacterial respiration affects pH of soil solutions -Microbial production of carbonic anhydrase (CA)	Li et al. (2005); Taylor et al. (2012); Thorley et al. (2015); Lambers et al. (2015)
Climate Feedback Systems	-Geochemical -Biological -Kinetic	-Increased uplift of silicates in Tibetan Plateau -Increased soil microbial activity produces more CO <sub>2</sub> under increased temperatures -Weathering rates are function of temperature	Drever (1988); Walter et al. (2006); Garziona (2008); Li and Elderfield (2013)

Table 2.2. Summary of lesser factors that may influence DIC flux in a drainage basin. Source: Compiled by the author.

### *Subsurface Carbonate Minerals*

Much of the Wabash, Great Miami, and Scioto river basins were impacted by Wisconsin and Illinoian glaciations. Here, glacial sediments form a thick covering over extensive deposits of carbonate bedrocks (Ray, 1965; 1974; Thompson et al., 2016). The glacial till overlying limestone units is of variable thickness, reaching 300 feet in some places (Veni et al., 2001; Weary and Doctor, 2014). These areas of carbonate bedrock beneath mapped surface deposits may supply alkalinity to rivers through baseflow. The DIC contribution from sub-surface carbonates is undoubtedly reflected in the chemical signature of the water, yet the area representing these deposits is not included in the carbonate area used in flux normalization as a part of this investigation. The use of mapped surface or near surface carbonates was chosen for a first approximation and based on the assumption that acidified waters are gradually neutralized through interactions with carbonate minerals beginning with the first interactions with rocks exposed to the surface, and waters tend to approach equilibrium with respect to carbonate rocks as a result. As such, vadose and phreatic water are at or near equilibrium, and minimal alkalinity is contributed from interactions with the subsurface carbonates. The example drawn from the formerly glaciated basins presents the complexity that incorporation of subsurface carbonate area may be necessary among river systems where alkalinity is high but surface carbonate deposits are not well-represented.

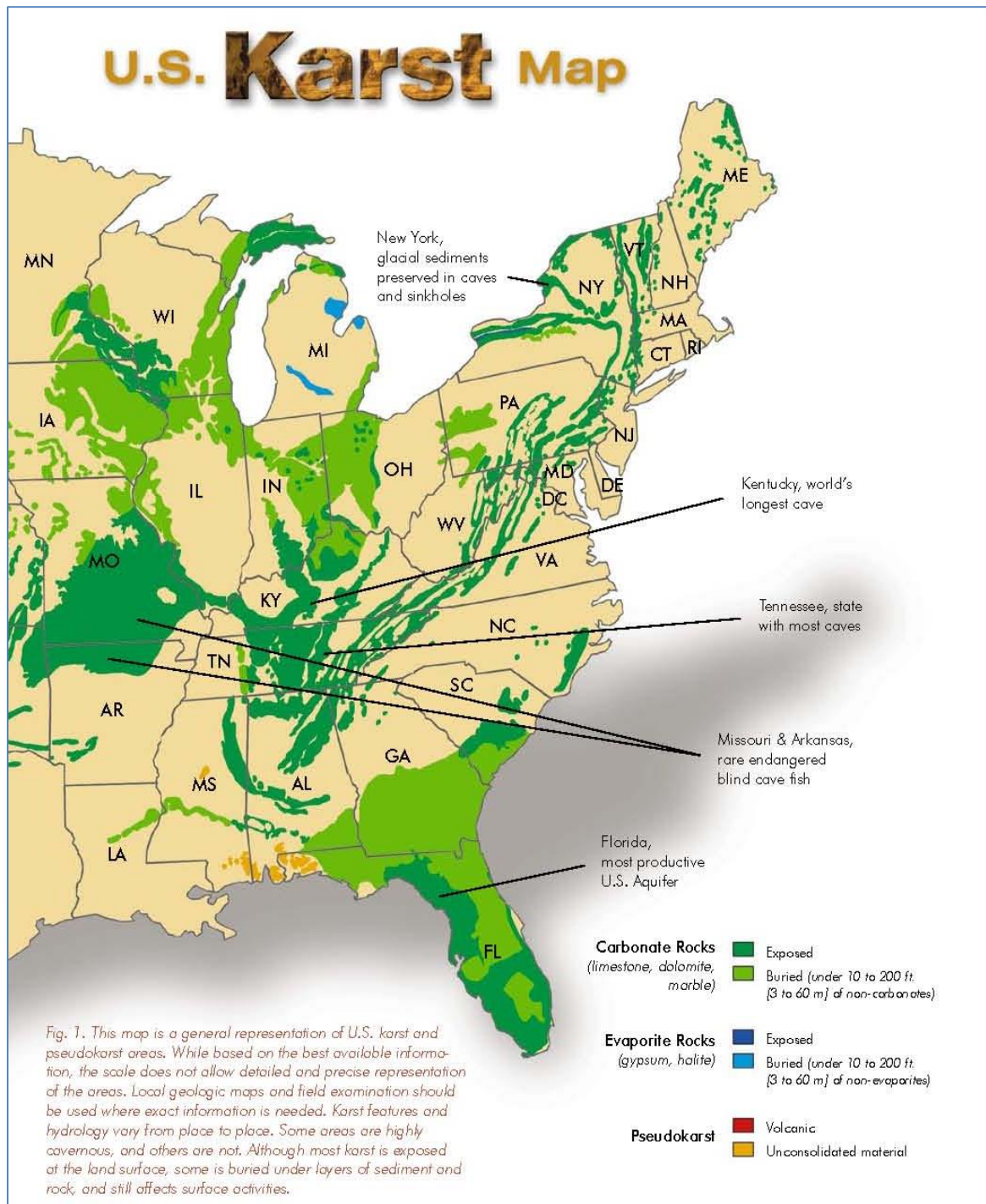


Figure 2.2. Relative distribution of exposed and buried carbonate rocks in the eastern portion of North America.

Source: Veni et al. (2001).

## Loess Deposits

The presence of calcium-rich loess deposits may act as a source of alkalinity among the Wabash, Great Miami, and Scioto rivers. Extensive Quaternary deposits comprise much of the surface geology of southern Indiana and southwest Ohio, including widely distributed loess deposits. Most of the loess in the Wabash and Ohio basins is of Illinoian or Wisconsin age. Loess deposits from the Wisconsin glaciation are consistent with the Peorian Loess described in Iowa and Illinois by Kay and Leighton (1933).

Figure 2.3 displays the distribution of Peoria Loess in North America.

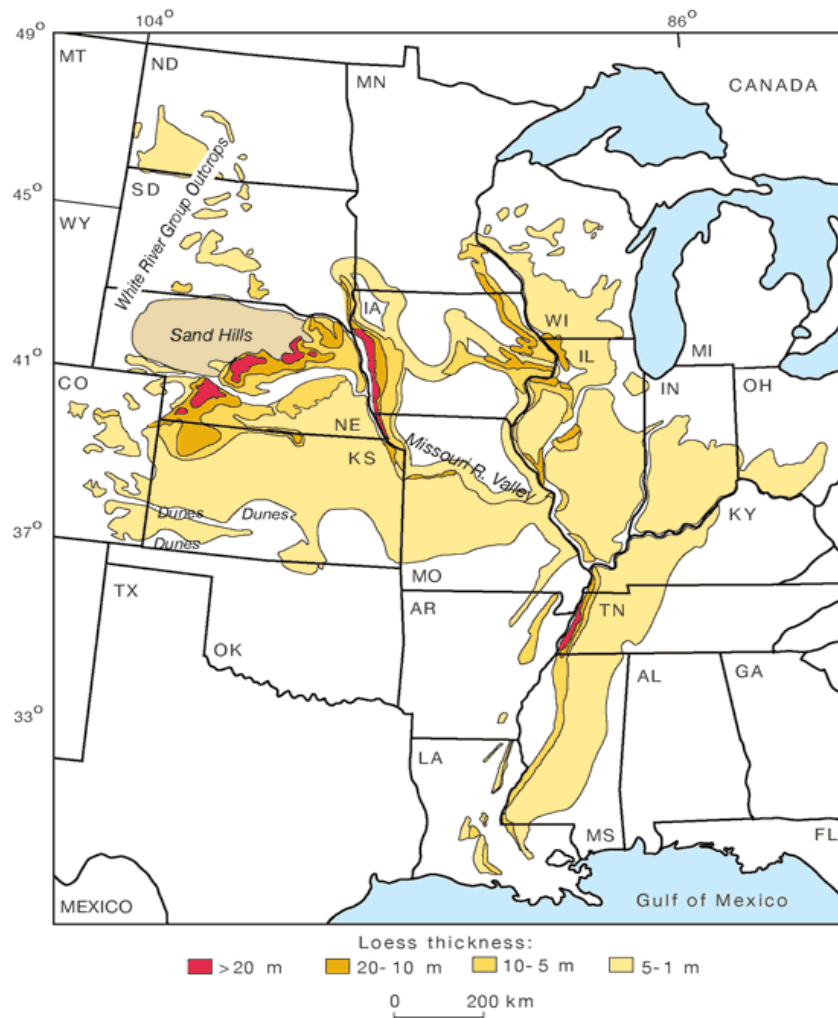


Figure 2.3. Peoria Loess deposits in North America.  
Source: Mason et al. (2006).



Loess is physically characterized as fine grained, silicious material that is ashy in color with a slight yellow hue and often highly calcareous. Calcareous concretions are hallmark features of loess and occur in belts at various depths throughout the deposits and assume various physical forms that are generally spherical or oblong and studded with rough projections (Figure 2.4).



Figure 2.4. Calcite concretions found in the loess deposits of south central Indiana  
Source: Ray (1965).

Call (1882) examined over 2,800 calcareous concretions taken from loess units. The specimens were found to be hollow, and exhibited a deeply fissured interior associated with evaporation of water and contraction of the calcium nodules. The portion interior to the calcareous envelope is composed of over one-half calcium carbonate, a third is silica, and a small percentage of aluminum. The composition of the calcium

concretions is roughly the same as the loess proper. From this, Call (1882) concluded the concretions to be decidedly hydraulic, formed as soil-zone precipitates, based on their composition. Whitney (1877: 709) described the mode of formation of the concretions, stating that they "... have been formed in the loess by infiltration along the lines of cleavage and resultant chemical action on calcareous matter occurring in large quantity along certain planes..." Substantial loess deposits are present in south-central Indiana (Cook and Montgomery, 1914). Loess and lake silts are well known to the lower Wabash Valley and were described in New Harmony, IN, as early as 1862 (Thornbury, 1940). In the southwest portion of Indiana, loess deposits have been reported with thicknesses of 12 to 15 meters (Thornbury, 1950). Ray (1965) described the hilly uplands near the Ohio valley as blanketed in a dense layer of loess that is thickest on the uplands adjacent to the alluviated valley, growing progressively thinner with distance. Within the Owensboro quadrangle in southcentral Indiana, loess deposits average about one-meter thickness, but depths up to three meters are reported. The mantle of loess deposits is so extensive that bedrock is only exposed at bluffs, roadcuts, and in excavated areas. Here, at least three distinct units of loess deposits are present and have considerable regional distribution. These units are not regarded as formations because, although they are distinct, they are not able to be individually mapped (Ray, 1965). The surface geology of southwestern Ohio also exhibits extensive loess deposits, with an average thickness of 1.5 meters covering the uplands in this region (Cook and Montgomery, 1914). Considering the well-documented and widely distributed presence of calcium-rich loess soils and the presence of calcareous concretions containing up to 50 percent calcium carbonate within the Wabash, Great Miami, and Scioto basins, it is likely that such factors contribute alkalinity

to the water. However, the area covered by these loess deposits is not accounted for in the current model because they are not classified as karst features or exposed bedrock.

### *Lacustrine Facies*

Lacustrine facies developed within the tributaries draining glacial meltwaters, as sediment deposition along glacial sluiceways blocked rivers causing pooling at the former outlets. Carbonate-rich layers of silts and clays known as marls have formed by the precipitation of calcite in the bottom of former lakes and swamps in Indiana. Along the lower Wabash River, lake sediments comprise more of the surficial deposits than do the true wind-blown loess sediments. Ray (1965) described the calcium and carbonate composition of the near-surface lacustrine deposits in the Owensboro quadrangle of southwestern Indiana. Where least weathered, the lacustrine deposits were reported as calcareous clayey silts. The outcrop transitions were marked by numerous calcareous nodules weathered from lacustrine deposits directly above. Within the upper meter of soil the transition between the superficial deposits and calcareous clayey silts can be identified by a dense concentration of small (typically <1.25 cm) calcareous nodules termed “popcorn” for their physical appearance. The clayey zone at 1.5 meters contained films of calcite and occasionally horizontal blocks of limestone up to 0.63 cm thick and 20 to 25 cm long. Below the calcium-rich clay zone are compact calcareous silts with abundant nodules, some of which flattened. The differences in the shape of nodules at varying depths have been cited as evidence that these features are secondary, formed from redeposition of carbonates leached from surficial zones (Ray, 1965). Thornbury (1950) noted that, although the percentage of calcium carbonate within lacustrine deposits tends to decrease moving upvalley, highly calcareous sands may extend several

kilometers beyond the main valley sluiceway that supplied the sediments. In general, the lacustrine deposits are more calcareous than the loess and are likewise prolific in distribution. Thus, it is probable that lacustrine sediments contribute to the alkaline chemical signature of the rivers in the glaciated basins to the north. As with the loess sediments, lacustrine facies are unconsolidated surficial features that are not represented in the carbonate bedrock geology maps used in the model. Although these sediments surely act as sources of alkalinity, no area is designated to the deposits in the normalization process for DIC flux. The use of Quaternary soil maps may be of use to this end in future studies.

#### *Thin Surface Carbonate Deposits*

Thin surface carbonates that are not regarded as karst environments may also influence the alkalinity observed in the rivers flowing through terrain shaped by recent glaciations in the Ohio Valley. The West Franklin Limestone member of the Shelburn Formation in southern Indiana and its equivalent member in northwest Kentucky, the Somerville Limestone, represent examples of thin surface carbonates that may contribute to the observed DIC flux issuing from the Wabash Basin, despite the absence of these units in the U.S. karst map (Weary and Doctor, 2014). The West Franklin consists of a lower, brecciated limestone member with an average thickness of about 1.5 m, below a shale layer of varying thickness over which lies the upper, dense crystalline limestone member with an average thickness of about 1 m (Shrock and Malott, 1929). In southwestern Ohio, abundant outcrops of upper Ordovician shale and limestone units comprise the hills of Cincinnati and surrounding areas. In central Ohio, the Columbus and Delaware limestones are exposed. Surface rocks in eastern Ohio are Pennsylvanian and

Permian in age and are composed of interbedded sandstones, shales, coals, and thin limestones. Nearly outcropping limestones interbedded in the Big Clifty Sandstone have been described in Logan County, Kentucky (Figure 2.5) (Bodine, 2016). The existence of these thin surface carbonate deposits may act as a source of alkalinity for the river basins in question. However, as has been noted for the loess and lacustrine deposits, any area occupied by these deposits was not used in the normalization calculation.

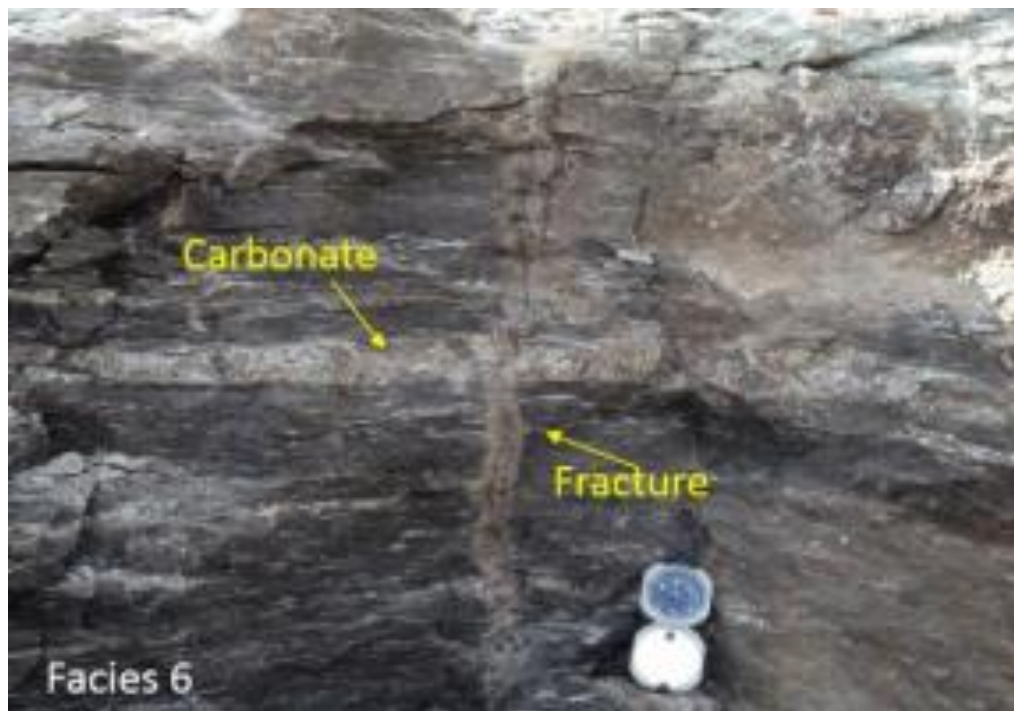


Figure 2.5. Near-surface carbonate lens in the Big Clifty Sandstone in Kentucky  
Source: Bodine (2016).

#### *Calcite Replacement of Non-Carbonate Grains*

Other sources of alkalinity not captured by mapped surface carbonates may include diagenetic changes in clastic rocks involving replacement of framework grains by calcite minerals. This event has been reported in the Chester Series sandstone formations of southcentral Kentucky (Butler, 2016) (Figure 2.6). Here, the aggressiveness of calcite

replacement of silicate minerals is so great that the phenomenon has been described as a “metastasis” of framework minerals by calcite. Calcite cements in sandstones of Indiana and Ohio may be replacing quartz crystals, thereby contributing alkalinity observed in the Wabash, Great Miami, and Scioto rivers through water-rock interaction. Interactions of infiltrating precipitation with the carbonates found within rocks described as non-carbonate in geologic maps may contribute significant carbonate alkalinity to streams in the drainage via baseflow and springs.

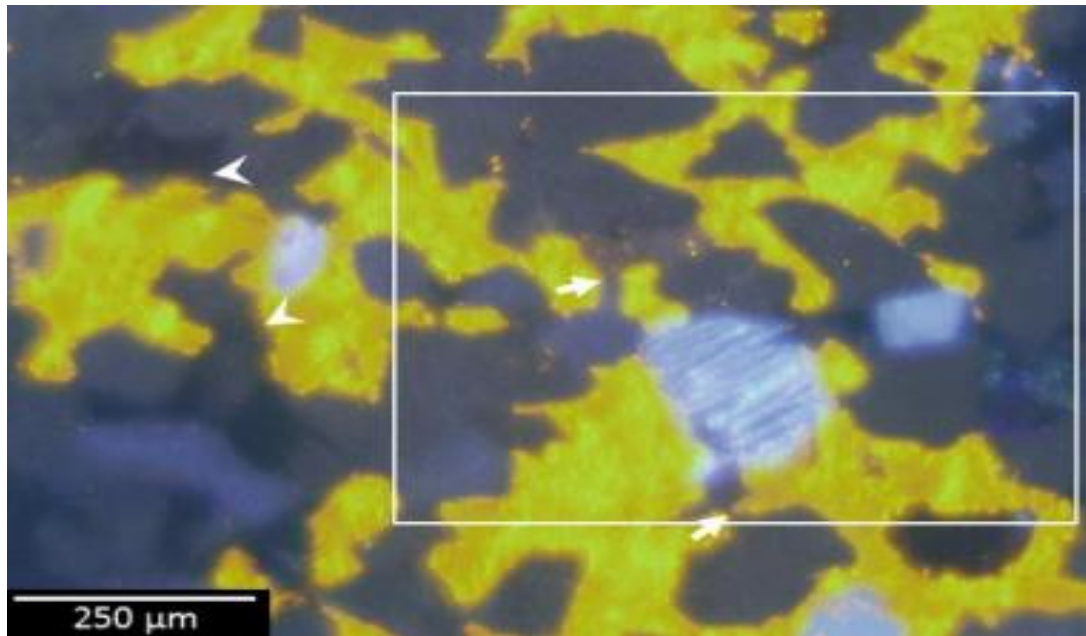


Figure 2.6. Calcite replacement of quartz crystals, in a sample taken from the Big Clifty Sandstone in Kentucky. Replace calcite (yellow) has embayed earlier cements and framework grains (white arrowheads) creating several contacts between framework grains (white arrows).  
Source: Butler (2016).

#### *Bedload Carbonate Minerals and CO<sub>2</sub> Outgassing*

Precipitation of carbonate minerals within the basin also influences DIC flux. This has been observed as bedload carbonate minerals, mineral deposits of speleothems, and as tufa-carbonate minerals formed near springs and waterfalls. White (2013) found

that speleothem precipitation is not a significant loss in terms of carbon flux because such a minor fraction of the total carbon load is precipitated in this way and because air-filled conduits intercept only a fraction of all water descending from the epikarst or infiltrating from the surface. Jiang and Yuan (1999) examined a carbonate rock-dominated basin in China and found that the distribution area over which tufa deposition takes place was much smaller than that for carbonate mineral dissolution. This study suggested that the carbon sink to dissolution was greater than the carbon source from precipitation.

Transfer of CO<sub>2</sub> from basin waters to the atmosphere by degassing can also potentially impact the carbon flux from dissolution. The partial pressure of aqueous carbon dioxide ( $p\text{CO}_2$ ) determines the behavior of gas exchange along the air-water interface and is indicative of whether rivers act as a sink or source of atmospheric CO<sub>2</sub> (Richey, 2003). When  $p\text{CO}_2$  is high, water is approaching a state of supersaturation that favors CO<sub>2</sub> out-gassing to the atmosphere, such that these conditions among inland waterways result in an atmospheric carbon source. White (2013) found that, for some spring-runs, degassing translates to a 5-10% loss of total carbon load to the atmosphere. Khadka et al. (2014) examined the effects of degassing among two unique hydrogeologic environments of a carbonate karst dominated region of the Santa Fe River located in north-central Florida. The upper river catchment flows over portions of the Floridian aquifer that are confined by clastic silicates, while the lower river catchment flows over the unconfined carbonate karst Floridian aquifer. The study found that the upper catchment degassed more CO<sub>2</sub> to the atmosphere ( $1156 \text{ g C m}^{-2} \text{ yr}^{-1}$ ) than the lower catchment ( $402 \text{ g C m}^{-2} \text{ yr}^{-1}$ ), due to an increase in carbon from soil respiration processes and higher organic matter decomposition that increased dissolved CO<sub>2</sub> concentrations.

However, increases in dissolved CO<sub>2</sub> are consumed during carbonate dissolution processes in the lower basin regions where the Santa Fe River flows over carbonate rocks not confined by silicates. The study illustrated that, while degassing occurs to a lesser degree among basin regions that exhibit relatively pure carbonate rocks, regions upstream or downstream may exhibit different hydrogeologic environments that favor CO<sub>2</sub> degassing and, thus, influence whether a given drainage acts as a carbon sink or source.

#### *Climate-Driven Feedback in Geologic Processes*

There is strong evidence to suggest climate change has affected weathering of silicates and island basalts, and that these processes may enhance the terrestrial sink of the atmospheric CO<sub>2</sub> (e.g., Garziona, 2008; Li and Elderfield, 2013). This process has been referred to as uplift driven climate change (Li and Fang, 1999; Li and Elderfield, 2013). Records of Strontium (Sr) isotopes in seawater suggest an increase in continental weathering since approximately 40 million years ago (mya) (Garziona, 2008). Reduction of CO<sub>2</sub> degassing has been proposed as the primary driver for the decrease in  $p\text{CO}_2$  in the atmosphere through negative feedbacks between  $p\text{CO}_2$  and silicate weathering (Berner et al., 1983). According to such models, weathering reactions are largely controlled by climatic factors that are sensitive to fluctuations in  $p\text{CO}_2$ , such as temperature and runoff. These findings have led researchers to hypothesize that tectonic uplift and erosion of the Himalayan-Tibetan Plateau during the past 40 million years have acted as a sink for atmospheric CO<sub>2</sub>, resulting in the glacial climate that persists today (e.g., Taymo and Ruddiman, 1992; Edmond, 1992).



## *B. Biological Activity*

The flux estimates generated by this study do not account for biological controls on mineral weathering. The objective of the investigation was to evaluate whether or not the major controls on carbonate weathering (and the associated sink of atmospheric CO<sub>2</sub>) could be described sufficiently absent a host of other processes. However, it bears acknowledging that biological factors may have substantial influence with respect to rates of carbonate mineral weathering. The following examples illustrate how vast networks of seemingly weak interactions between soil, plants, and the atmosphere may result in strong fluctuations among terrestrial C stocks.

### *Vegetation*

Ecosystem productivity and C storage depend on interactions of relatively fast processes (e.g., photosynthesis and respiration) and slower processes that occur over broad spatial scales (e.g., bedrock weathering and soil production). Recent studies suggest that the influence of plants on mineral weathering may substantially increase C storage beyond lithological saturation thresholds (Silva, 2017). Terrestrial plants influence weathering process through chemical and physical action. The root systems of large trees may break up rock, creating fracture networks within which chemically aggressive waters can enter and begin to weather rock. Plants also secrete acids and contribute to the accumulation of high CO<sub>2</sub> levels in the soils, which interacts with infiltrating precipitation to enhance rates of carbonate mineral weathering (Berner, 1992). Trees and associated microbial flora of the soil act as major drivers for continental weathering (Thorley et al., 2015). In particular, the effect of symbiotic root-mycorrhizal associations (Taylor et al., 2012) and carboxylate-releasing root clusters (Lambers et al.,

2015) on mineral weathering is several times greater than the influence of climate. Increased soil acidification linked to symbiotic partnerships between tree roots and ectomycorrhizal (EM) fungi was shown to significantly enhance weathering among calcite-containing grains. The process is so effective that contemporary studies have theorized that planting of fast-growing EM angiosperm taxa in carbonate-rich terrains may accelerate the sink of atmospheric CO<sub>2</sub> (Thorley et al., 2015). The mechanism by which soil microorganisms influence carbonate diagenesis is via production of carbonic anhydrase (CA). CA is an enzyme that converts soil CO<sub>2</sub> to carbonic acid and bicarbonate ions and is also involved in the reverse reaction wherein bicarbonate is converted to CO<sub>2</sub>. Investigations of soil science have demonstrated that mean activity of CA is strongly correlated to the amount of Ca<sup>2+</sup> found in leachates ( $R^2 = 0.86$ ,  $p < 0.01$ ). Therefore, microbial CA may be highly influential in the control of Ca<sup>2+</sup> release and leaching in karst systems (Li et al., 2005). As vegetation decays, the C that was stored as cellulose in the plant during photosynthesis is released as CO<sub>2</sub>. Decomposition of plant material in the epikarst regions supplies that primary source of C that enters karst systems, and a great deal of the karst denudation process takes place as rainwater infiltrates through the epikarst, which has been acidified by the breakdown of OM.

### *Organic Acids*

Organic acids may alter rates of weathering by affecting both surface reaction- and transport-controlled mechanisms. Surface reaction-controlled processes (i.e., adsorption, surface complexing, and pH) alter mineral dissolution rates by affecting mineral-solution systems far from equilibrium through lowering of activation energy, mobilization of metallic central atoms from complexes, increasing the rates of

decomposition for transition state compounds, and formation of polydentate ligands that produce mononuclear complexes that affect stability of mineral surfaces. The distinction between these mechanisms is difficult to parse out since the effects of complexing and adsorption are closely linked to changes in pH. Experimental data suggest that the effect of pH is relevant only when values are below about 4.8. OA may accelerate or dampen dissolution rates by adsorption to mineral surfaces to form surface complexes or mobilization of central metal ions from existing complexes. OA influence transport-controlled processes by affecting saturation state near the solid-fluid interface, and by speciation of Al and other ions. Naturally occurring levels of OA in soil solutions do not appear to be concentrated enough to produce a significant increase in dissolution rates, and in general concentrations of 1 mM or greater are required to observe enhanced dissolution. However, in the microenvironments associated with plant roots, fungal hyphae, and in areas of high microbial activity, OA concentrations are capable of significantly accelerating dissolution rates. Saturation state inherently limits the dissolution of carbonates and oxyhydroxides of iron and aluminum (Drever and Stillings, 1997). Soil and surface waters are often near saturation with respect to K-feldspar, such that OA may accelerate the dissolution of the mineral. In contrast, plagioclase feldspars and other silicates are typically highly undersaturated in the soil; however, solutions in microenvironments are closer to saturation than the bulk solution. Mineral dissolution may be inhibited through chemical affinity effects, a process that may be unaffected by presence of OA. A lack of well-controlled experimental data representative of conditions in natural environments regarding the effects of chemical affinity on dissolution rates obscures a clear understanding of the influence this process has on mineral weathering.

The influence of OA on inorganic Al speciation appears to be insignificant since concentrations of Al species are controlled by solubility of aluminum hydroxide phases irrespective of the present of OA. Secondary processes such as transport of metal ions may increase permeability on macro- and microscopic scales, indirectly influencing dissolution rates. Overall, the influence of OA in natural systems is apparently minimal (Huang and Keller, 1970; Tan, 1986; Drever, 1988; Drever and Vance, 1994; Drever and Stillings, 1997; Jones, 1998).

#### *Climate-Driven Feedback in Biological Processes*

The influence of biological interactions on mineral weathering, and the carbon cycle in general, is further complicated by positive feedback mechanisms associated with increased production of CO<sub>2</sub> and methane (CH<sub>4</sub>) from microorganisms proliferating in areas where permafrost is thawing. These processes release vast amounts of previously sequestered C as greenhouse gases, which then trap heat in the atmosphere (Walter et al., 2006). At the same time, the respiration by-products of these microorganisms contributes acidity to the soil, and the increase in atmospheric carbon yields more aggressive rainwater, both contributing to increased weathering of carbonate minerals. Land-use practices such as whole tree removal extract base cations from the system leading to soil acidification. Nitrification processes result in short-term release of acidity in the form of nitrate. Furthermore, the decomposition of organic matter from forested areas contributes protons (acidity) to the soil solution, thus affecting the acid-alkaline balance and promoting the weathering of base minerals (Drever, 1988).

### *C. Soil and Land Use*

The amount of CO<sub>2</sub> present in the soil is one such driving force among carbonate rock dissolution processes. The uptake of atmospheric and soil CO<sub>2</sub> by carbonate rock dissolution significantly impacts the global carbon cycle and is one of the most important sinks (Cao et al., 2012). Soil CO<sub>2</sub> concentrations range from fractions of a percent to as much as ten percent due to OA and CA produced in association with plant roots, microbial activity, and from decomposition of organic matter (OM) (White, 2013). A study by Zhang (2011) demonstrated that carbonate-rock dissolution is much greater beneath soil than for exposed rocks. Cao et al. (2011) substantiated this, reporting soil CO<sub>2</sub> concentrations that far exceed those of the air (Zhang, 2011). It has been argued that the contributions of CO<sub>2</sub> to aqueous solutions are much greater than the amount sourced from the atmosphere (Cao et al., 2011; Zhang, 2011; White, 2013). Thus, processes that affect soil acidity, including plant and tree root excretion, decay of vegetation, microbial activity in the soil, and land-use practices, may have strong influence on carbonate mineral weathering processes.

Land-use practices and land cover may also influence the magnitude of the carbonate dissolution sink. Zhang (2011) found that carbonate dissolution increased with land cover from (in increasing order) tilled land, to shrub land, secondary forest, grassland and, lastly, primary forest. Thus, it was concluded that regeneration of vegetation can significantly augment rates of carbonate dissolution (Liu et al., 2008). Calculated dissolution rates of limestone tablets in association with various land-use practices were found to be higher for some land uses than others. However, when the average rate for all land-use types was compared against the total rate for the basin as

determined from hydrochemical data, the two values were found to be in close agreement. It has been suggested that dissolution rates for a basin should consider the different land-use types represented therein, rather than applying a blanket land-use type (Zhang, 2011). This study sought to determine whether factors such as soil type, land cover, and land-use practices significantly influence DIC flux, or if the hypothesized normalization factors capture sufficient detail to improve large-scale flux estimates without consideration of the aforementioned processes.

## 2.8 Previous Estimates of the Sink by Carbonate Dissolution

The carbon sink effect from carbonate dissolution has been evaluated using a range of approaches mainly determined as a function of spatial scale and data availability (Amiotte Suchet and Probst, 1995; Liu and Zhao, 2000; Groves and Meiman, 2001; Amiotte Suchet et al., 2003; Cao et al., 2011; He et al., 2013; Osterhoudt, 2014; Salley, 2016). However, there may be special challenges associated with “scaling up” the results of these efforts to a basin the size of the Ohio River Basin. Several approaches have been used to estimate the sink from carbonate-mineral dissolution, some of which are described below.

A formula for calculating the denudation rate of carbonate rocks was derived by Sweeting (1972) as:

$$D_r = 0.0043P^{1.26} \quad (9)$$

where  $D_r$  is dissolution rate and  $P$  is precipitation. Amiotte Suchet and Probst (1995) successfully correlated runoff and weathering coefficients for the major rock types from

statistical data taken from 232 small, monolithic basins in France using the Global Erosion Model for CO<sub>2</sub> fluxes (GEM-CO<sub>2</sub>) model to give the carbon flux as:

$$F_{CO_2} = a * Q \quad (10)$$

where  $F_{CO_2}$  represents CO<sub>2</sub> consumption rate,  $a$  is a weathering coefficient assigned to different rock types and  $Q$  is the runoff discharge. Liu and Dreybrodt (1997) developed a linear rate law that calculated carbonate dissolution in turbulent CO<sub>2</sub>-H<sub>2</sub>O solutions by:

$$R = \alpha(C_{eq} - C) \quad (11)$$

where  $R$  is the dissolution rate,  $C$  is the Ca<sup>2+</sup> concentration, and  $C_{eq}$  is the equilibrium concentration of Ca<sup>2+</sup>, and  $\alpha$  is a rate constant dependent on temperature, P<sub>CO<sub>2</sub></sub>, thickness of the diffusion boundary layer adjacent to the mineral and the thickness of the sheet of water flowing over the mineral. Marble and limestone disks 3 cm in diameter were cored from marble slabs 5 mm in thickness, with 7 cm<sup>2</sup> of the disk surface area in contact with a solution of bovine carbonic anhydrase (BCA). It is important to note that the rate law developed from this study reflects laboratory conditions, and these may not be realistic for describing carbonate-mineral weathering in situ. Liu and Zhao (2000) resolved a linear correlation between runoff and carbonate rock denudation from secondary data sources using:

$$D_r = 0.0544 (P - E) - 0.0215 \quad (12)$$

where  $D_r$  is dissolution rate,  $P$  is precipitation and  $E$  is evapotranspiration. Regression analysis (a statistical measure for how well two parameters correlate, where  $R^2 = 1.0$  indicates total correlation) of this relationship yielded strong agreement of 0.98.

## 2.9 Summary

Mounting concerns over global climate change have motivated an understanding and quantification of the capacity for terrestrial carbon sequestration. It is clear that the amount of carbon removed from the atmosphere by the ocean, in addition to the amount still contained within the atmosphere, is less than known contributions from anthropogenic emissions. Several approaches have been employed in efforts to quantify the extent of the terrestrial carbon sink, with mixed results. The carbon sink by carbonate rock dissolution on the continents is an area of particular interest in this search for understanding. Previous studies have yielded estimates of the global carbon sink from carbonate weathering spanning a broad range, from 0.088 Pg C/a (Hartmann et al., 2009) to 0.6433 Pg C/a (Liu et al., 2008). While variation is expected among regional basins due to inherent differences in basin area, precipitation, lithology, and other factors, such variation is not useful in making accurate assessments of predictions based on global CO<sub>2</sub> sequestration. The disparity of these results reveals the inadequacy of the current level of research in estimating this component of the terrestrial carbon sink. A more comprehensive method for evaluating the sink from carbonate dissolution that can be applied equally well over a wide range of carbonate rock-bearing drainage basins is critical to enhancing our understanding of carbon cycle processes and how these might be managed to ameliorate long-term repercussions for human and environmental health. This research thus seeks to develop further the methods used by Osterhoudt (2014) and Salley (2016) to arrive at a value for carbon sink due to carbonate mineral dissolution, normalized by area, time, and rainfall minus ET over a large and ecologically significant drainage basin. In doing so, the methods will be appraised for their range of



applicability. The aim of this research is to determine whether these methods do prove valid in large-scale settings and that existing data could be used to significantly increase the efficiency and accuracy associated with making global carbon sink estimates.

## Chapter 3. Study Area

### 3.1 Introduction to the Ohio River Basin

White et al. (2005) described the Ohio River drainage system, including the hydrology, geology, ecology, climate, landscape, and land-use patterns of the Ohio River and its major tributaries. The Ohio River basin has the third largest discharge (average 8,733 m<sup>3</sup>/s) in the United States. The basin spans an area between 34°N and 41°N latitude and 77°W and 89°W longitude that drains major portions of eight states and parts of six more, totaling 490,601 km<sup>2</sup> (Figure 3.1). The basin extends from New York in the northeast to Georgia and Alabama in the south to Illinois in the west, and slopes generally from east to west (White et al., 2005).

### 3.2 Geologic Setting

The Ohio River basin spans six physiographic provinces (Hunt, 1967). The eastern region of the basin originates in the Blue Ridge, Valley and Ridge, and Appalachian Plateaus within the Appalachian Highlands province. The north and central portions of the basin drain the Interior Low Plateaus and glaciated Central Lowland provinces. The western end extends to the Gulf Coastal Plains (White et al., 2005; Weary and Doctor, 2014) (Figure 3.2). Numerous stratigraphic units are present among the provinces encompassed within the Ohio River basin (Figure 3.3). Within the Blue Ridge province are some of the highest peaks in the eastern United States, formed of metamorphic Precambrian granites, gneiss, sandstone, and conglomerate units. The Valley and Ridge province contains mostly Paleozoic limestones, shale, and sandstones, as well as anthracite coal deposits.

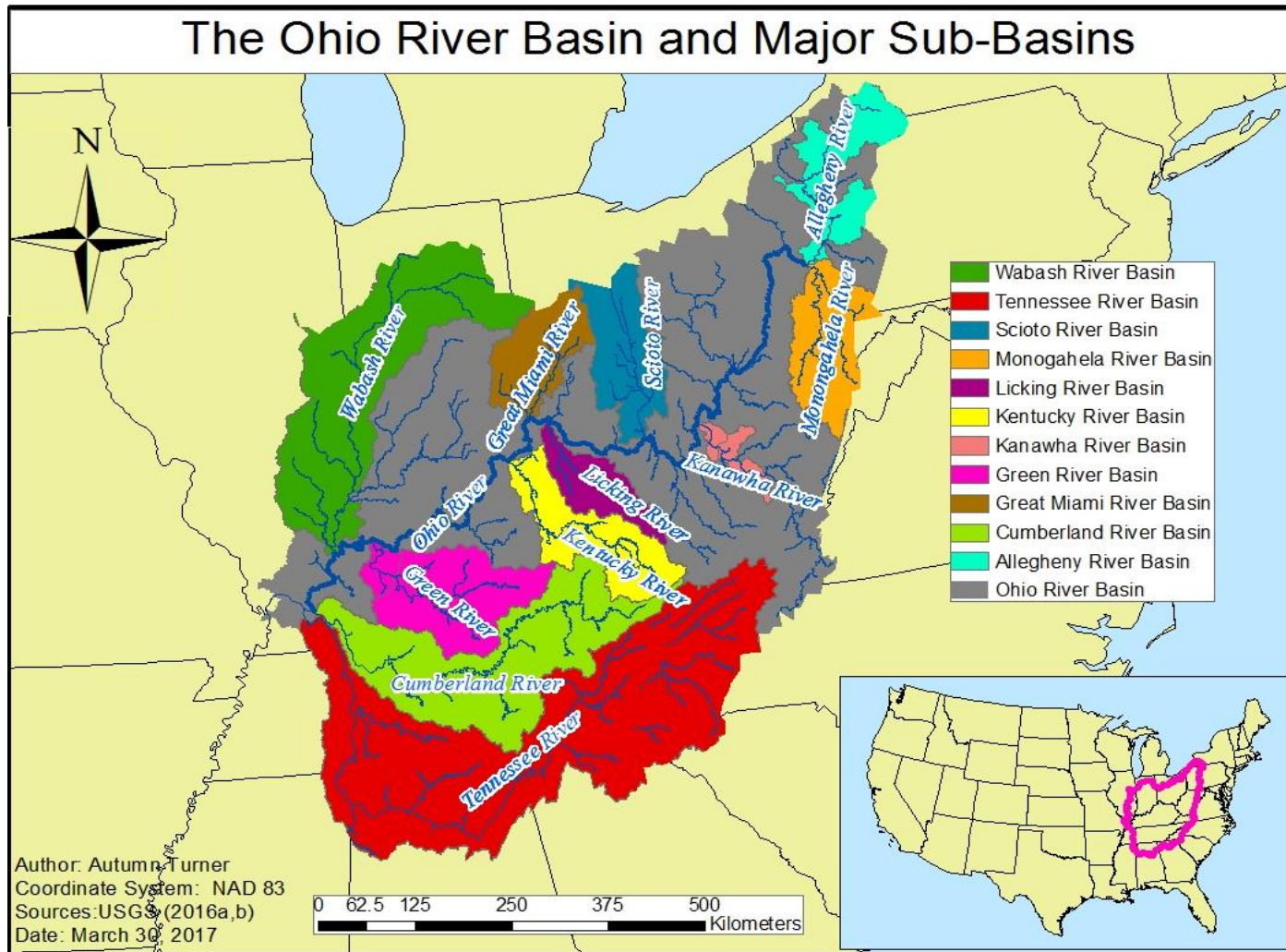


Figure 3.1. Geographic extent of the Ohio River drainage basin.  
 Source: Created by author from USGS (2016a,b) data.

The larger Appalachian Plateaus province exhibits younger Ordovician, Silurian, and Devonian limestone, sandstone, shale, and bituminous coal in the east. The western region of the Appalachian Plateau covers eastern Tennessee, Kentucky, and Ohio and contains Mississippian and Pennsylvanian limestones. The Mississippian rocks within the Appalachian Plateau demonstrate extensive karst development. This karst topography stretches from southcentral Indiana through northern Alabama, and includes the world's most extensive cave system, Mammoth Cave, in Kentucky. Relatively few surface streams are found in this area, with most water flowing in subsurface conduits. Finally, the portion of the basin from Ohio to central Illinois represents the Central Lowland province. Here the landscape has been influenced by Pleistocene glaciation, which persisted as recently as 15,000 years ago. The topography varies in this physiographic province, including rolling and flat plains and deeply incised rivers with intermittent Pennsylvanian limestone outcrops (White et al., 2005). Surface geology to the north of the Ohio River is distinct from other parts of the basin, where Illinoian and Wisconsin glaciation has formed a buried landscape (Thornbury, 1940). Here, thick deposits of unconsolidated Quaternary materials include glacial till, loess, and lacustrine deposits that overlie carbonate bedrock, resulting in a sparse presence of exposed carbonates in the region (Thornbury, 1940; Ray, 1965; Weary and Doctor, 2014) (Figure 3.4). This is particularly evident among the Wabash, Great Miami and Scioto drainages.

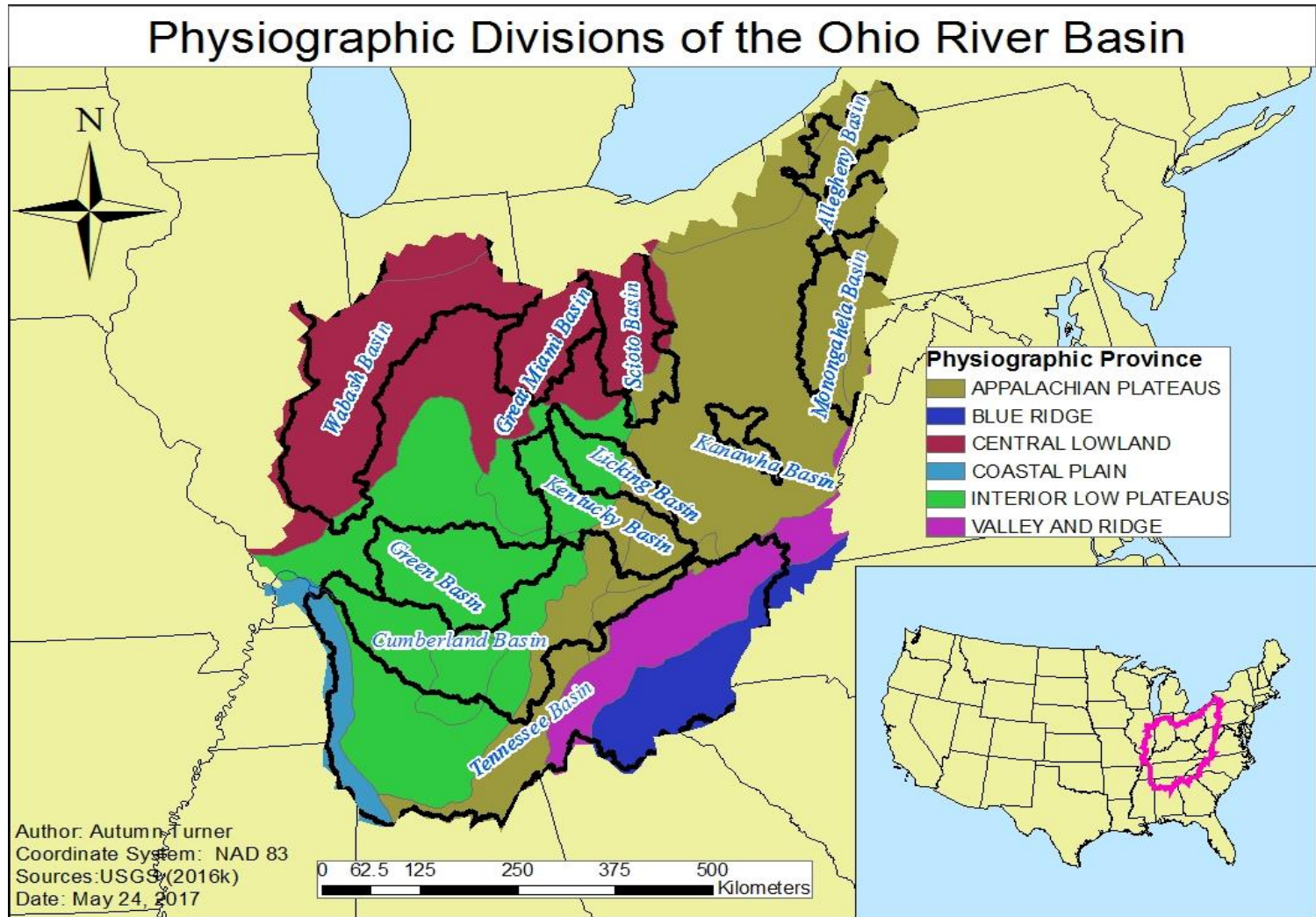


Figure 3.2. Physiographic provinces of the Ohio River Basin.  
 Source: Created by author from USGS (2016k) data.

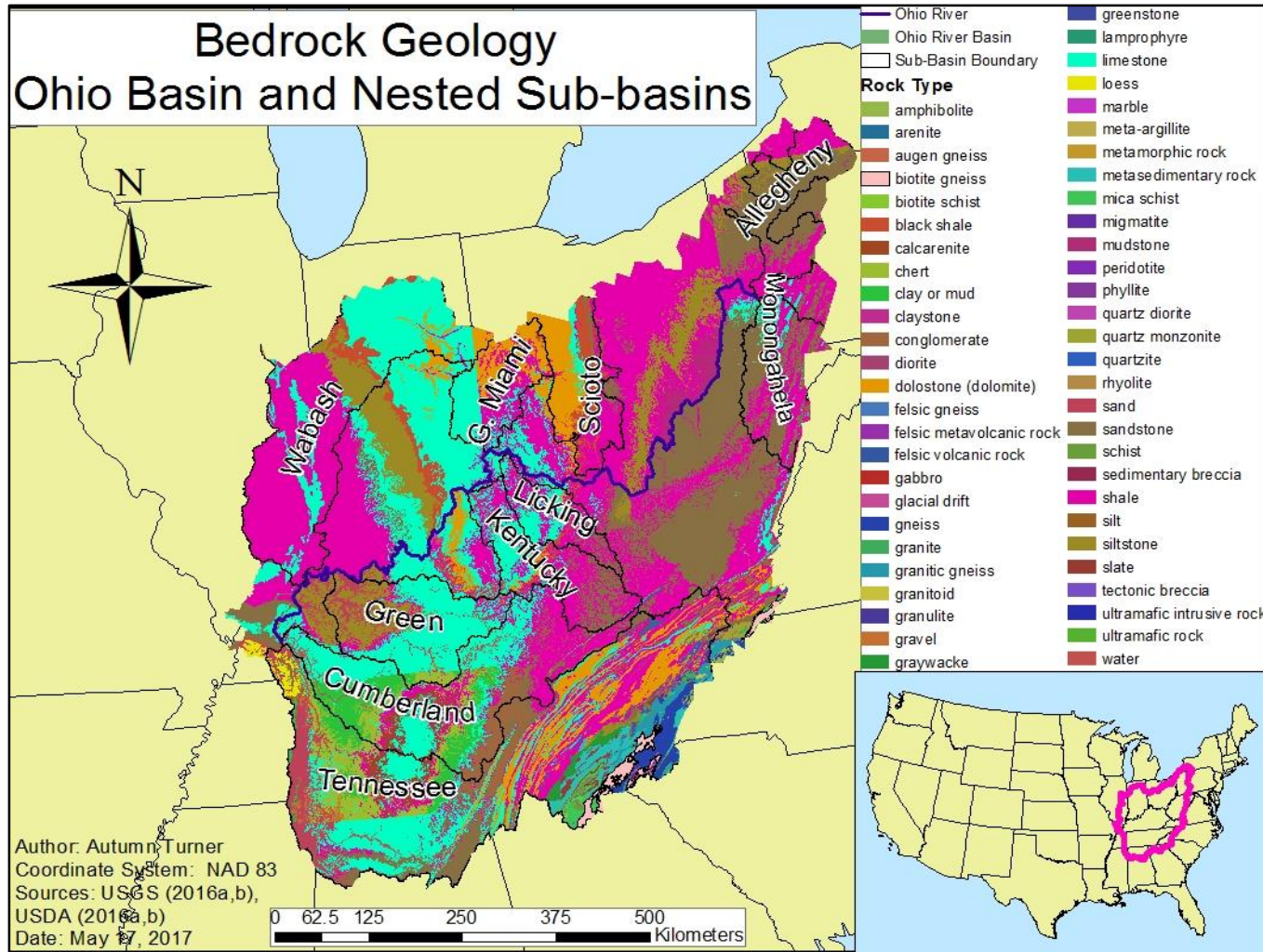


Figure 3.3. Bedrock geology of the Ohio River Basin and nested sub-basins.  
 Source: Created by author from USDA (2016a,b) and USGS (2016a,b) data.

# Carbonate Karst of the Conterminous United States

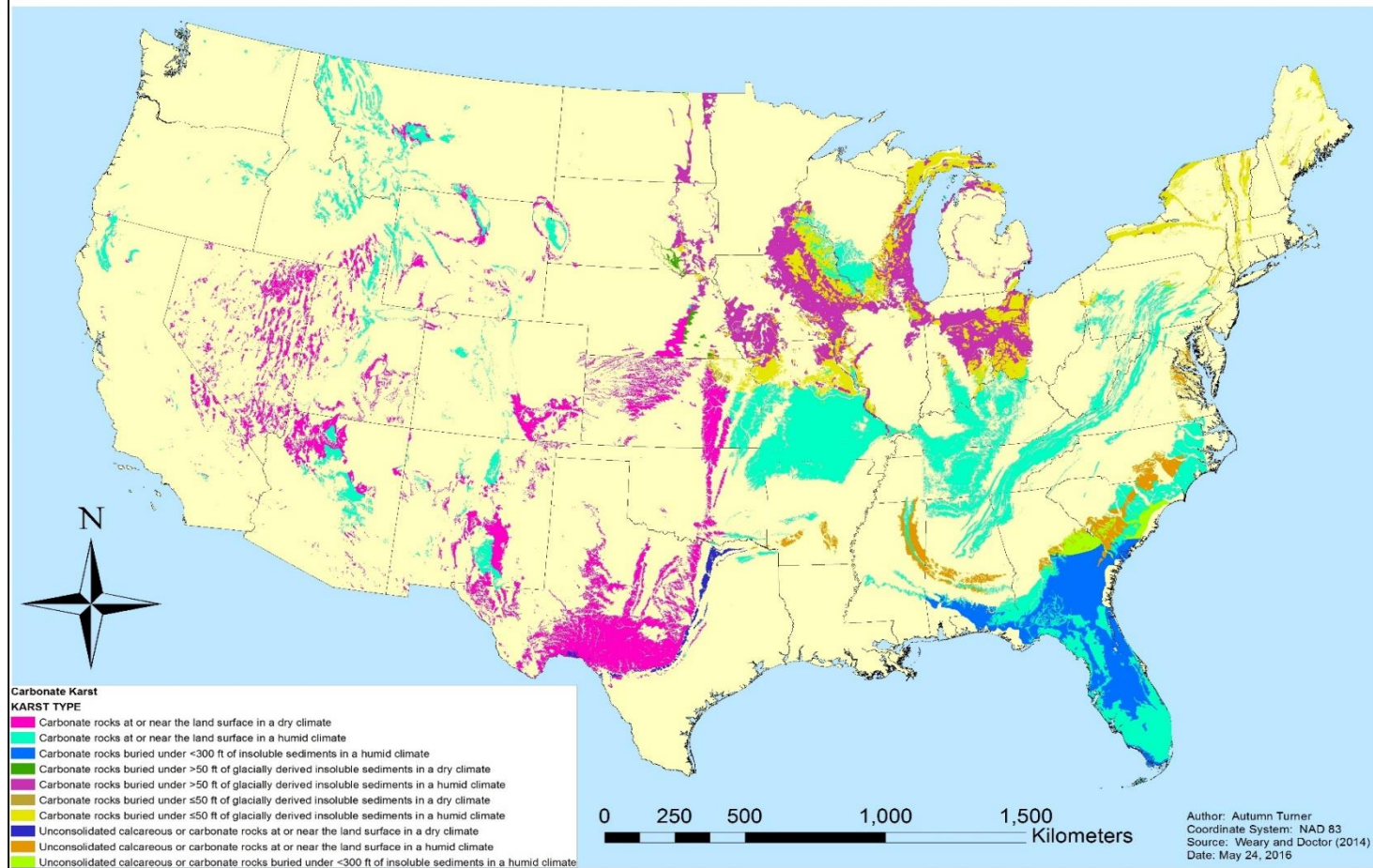


Figure 3.4. Carbonate karst of the conterminous United States.  
 Source: Modified by author from Weary and Doctor (2014).

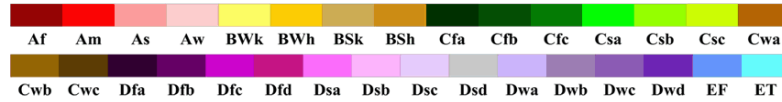
### 3.3 Climate

White et al. (2005) described the climate of the Ohio River basin as temperate with cool moist winters and warm humid summers. Mean monthly temperatures in the region range from  $-7^{\circ}\text{C}$  to  $10^{\circ}\text{C}$  in winter and  $24^{\circ}\text{C}$  to  $28^{\circ}\text{C}$  in the summer. Mean monthly precipitation is relatively consistent over the basin area, with significant snow accumulations in the north and Appalachian regions. Annual precipitation for the basin ranges from 94 cm in northern parts of the basin to about 135 cm in the southernmost part of the basin, with slightly increased measurements among high elevations (White et al., 2005; UTIA, 2016). The commonly referenced Köppen climate classification system that describes the climate of locations based on annual and monthly temperature and precipitation averages splits the basin into two climate categories. Regions above  $40^{\circ}\text{N}$  display moist mid-latitude climates with cold winters, warm summers, and year-round moist conditions. Regions between  $26^{\circ}$  to  $45^{\circ}\text{N}$  latitude exhibit moist mid-latitude climates with mild winters and warm-to-hot, humid summers. The Ohio River basin contains two climate regimes: fully humid regions that experience warm summers throughout most of the basin and fully humid regions that experience hot summers in the northern parts of the basin (Kottek et al., 2006) (Figure 3.5).



### Main Köppen-Geiger Climate Classes for US counties

updated with CRU TS 2.1 temperature and VASCLimO v1.1 precipitation data 1951 to 2000



#### Main climates

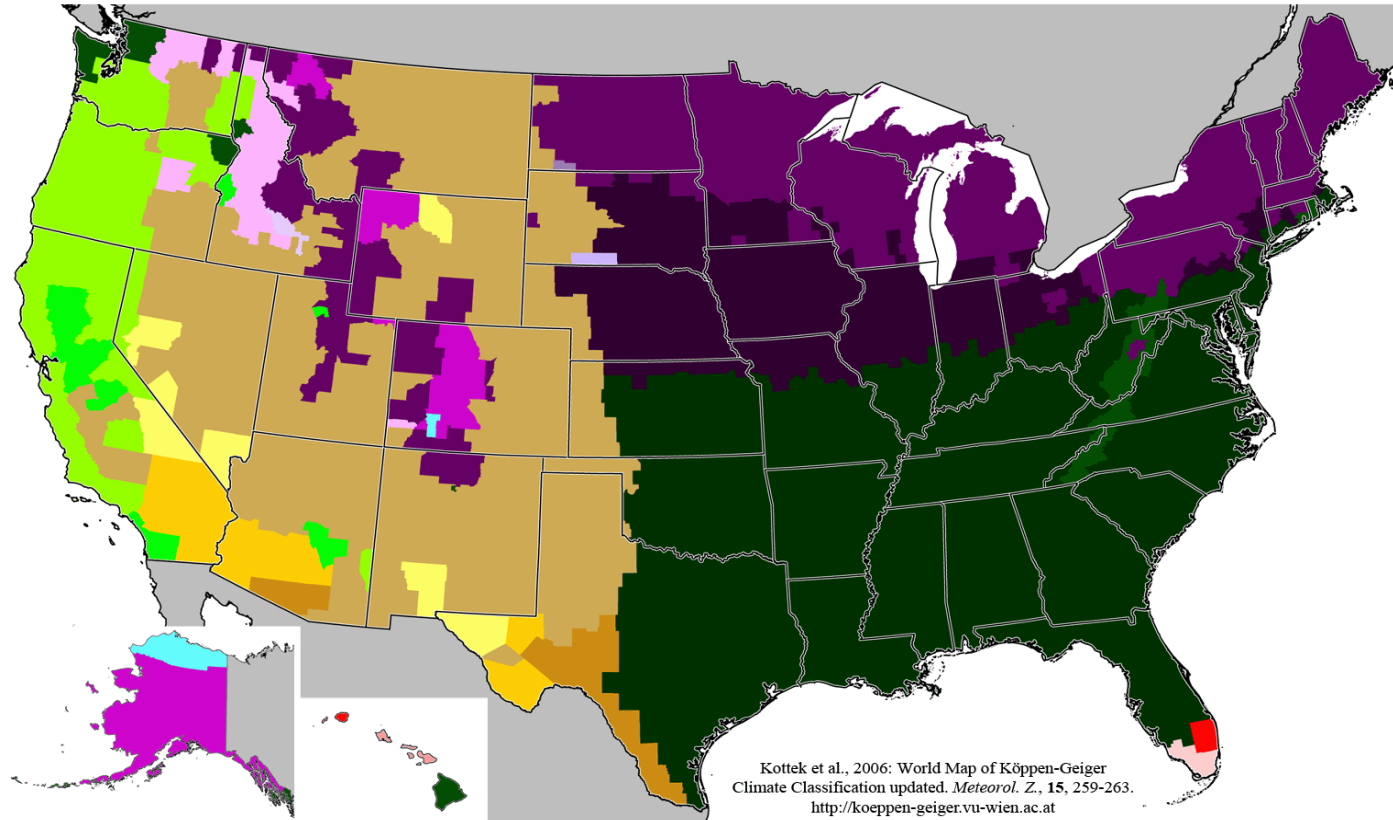
- A: equatorial
- B: arid
- C: warm temperate
- D: snow
- E: polar

#### Precipitation

- W: desert
- S: steppe
- f: fully humid
- s: summer dry
- w: winter dry
- m: monsoonal

#### Temperature

- h: hot arid
- k: cold arid
- a: hot summer
- b: warm summer
- c: cool summer
- d: extremely continental
- F: polar
- T: polar



Kottek et al., 2006: World Map of Köppen-Geiger Climate Classification updated. *Meteorol. Z.*, 15, 259-263. <http://koeppen-geiger.vu-wien.ac.at>

Figure 3.5. Köppen climate classification map of the United States. Source: Kottek et al. (2006).

### 3.4 Hydrologic and Geochemical Setting

The Ohio River is the main stem of the Ohio River basin system, formed by the confluence of the Allegheny and Monongahela Rivers in the northeast region of the basin running southwest approximately 1,575 km to the Mississippi River. Major tributaries of the Ohio River basin are the Allegheny, Monongahela, Muskingum, Kanawha, Scioto, Little Miami, Licking, Great Miami, Kentucky, Salt, Green, Wabash, Cumberland, and Tennessee rivers. The major tributaries constitute 84% of the overall drainage basin. An additional 57 tributary basins represent the remaining 16% of the basin area, all of which are rather small (<1000 km<sup>2</sup>).

Differences in geochemistry and land-use types within the Ohio basin have created a dichotomy in tributary characterizations. Those entering the Ohio from the north and indeed much of the Ohio main stem itself are geologically young, formed by Pleistocene glaciations. Rivers entering the basin from the south and east, such as the Tennessee, Cumberland, Green, Kentucky, Kanawha, Monongahela, and Allegheny, are much older (White et al., 2005). Differences in geomorphology and fauna in the basin have been categorized into two discrete aquatic ecoregions: the Teays—Old Ohio and the Tennessee—Cumberland (Abell et al., 2000). The rivers that make up the Teays—Old Ohio can be subdivided into three types according to stream gradient and physiography. The first category includes the Monongahela, Allegheny, Kanawha, Licking, and Kentucky rivers that drain the Appalachians. Here river slopes are relatively steep, with rock and cobble substrate typical. Alkalinity within these waters is naturally low. Relief in the region has resulted in commercial exploitation and extensive impoundment of water for the purposes of hydroelectric power generation, navigation, and flood control.

The second group under the Teays—Old Ohio ecoregion includes the Green and Salt rivers. Rivers here have moderate gradients among headwaters, and stream bottoms are characteristically composed of sand, sediments, and chert cobbles. These rivers also tend to display low natural alkalinity. The third group in the Teays—Old Ohio ecoregion is represented by the Wabash, Great Miami, and Scioto rivers (and several other smaller tributaries). These rivers flow southward from west-central Ohio becoming moderately to deeply incised across the gently sloping landscape. Here, river substrate is predominately sandy along with coarse glacial till. In contrast to the previous regions, the waters of this third group tend to have high alkalinity due to extensive exposures of carbonate rock, and high phosphate and nitrate concentrations associated with agricultural land-use patterns. The other ecoregion, the Tennessee—Cumberland, consists of the two rivers for which it is named. Both have steep gradients within their Appalachian headwaters and parallel each other through a series of flatter physiographic provinces to their entry to the Ohio main stem. These rivers are the most impounded major rivers in the nation and are threatened by agricultural, urban, industrial, and mining drainage (White et al., 2005).

## Chapter 4. Methods

### 4.1 Introduction

Previous attempts to evaluate the sink by dissolution have primarily relied on three basic methods. Mathematical modeling based on a recognized linear correlation between dissolution rates and precipitation/discharge has been used over broad-scale applications, particularly for global estimations (e.g. Amiotte Suchet and Probst, 1995; Liu and Zhao, 2000; Amiotte Suchet et al., 2003; Liu et al., 2008). Corrosion rates of limestone tablets buried in the soil have been used to calculate the CO<sub>2</sub> sink. These studies considered precipitation, primary production, soil respiration, and the area, type, and purity of carbonate rock exposed to create a regression describing carbonate corrosion at representative monitoring sites (Cao et al., 2011; Zhang, 2011). Finally, the hydrochem—discharge method utilizes high-resolution water chemistry data, along with discharge and basin area, to arrive at an estimate for the total carbon export from a basin (e.g., Groves and Meiman, 2001; Haryono, 2011; He et al., 2013; Osterhoudt, 2014; Salley, 2016). These studies concluded that the carbon sequestration processes occurring within a given basin are a product of the amount of discharge leaving the basin and the DIC present within the water. They stress the importance of high-resolution water chemistry and discharge data, particularly because flow rates and chemistry are commonly highly variable in carbonate rock flow systems (He et al., 2013). This variability reflects differences in carbonate type and purity that influence weathering rates. Recent investigations of carbon sequestration within the regional drainage basins of Kentucky (Osterhoudt, 2014; Salley, 2016) have sought to normalize the atmospheric carbon sink, either by time and area of carbonate rock outcrop (Osterhoudt, 2014), or by

time and volume of rainfall minus ET over an area of carbonate outcrop (Salley, 2016), to give an estimate that could be directly applied to other basins for determining carbon flux. Osterhoudt (2014) examined two nested watersheds within the upper Green River, Kentucky, using this normalization technique and found the magnitude of the atmospheric CO<sub>2</sub> sink between the two basins to be within 3% agreement. However, data acquisition relied upon high-resolution water chemistry and discharge measurements taken by data logger equipment, and required labor-intensive and, thus, relatively expensive field work. Salley (2016) employed a similar approach to estimating the carbon sink by carbonate rock weathering in the catchment of the Barren River, Kentucky. DIC flux was normalized by carbonate rock outcrop area, time, and the total depth of water available for dissolution and transport, using publicly accessible water chemistry, discharge, precipitation, and surface temperature data. The investigations performed by Osterhoudt (2014) and Salley (2016) were limited to surface water at base-level flow and did not consider non-carbonate contributions to the sink of atmospheric C from terrestrial weathering such as weathering of silicates, the presence of multiple stratigraphic units, or calcite cemented siliciclastics. When compared, the Salley (2016) and Osterhoudt (2014) results displayed a strong linear relationship ( $R^2=0.94$ ) for the flux as a function of those factors. This method holds promise for substantially improving the ease and accuracy with which carbon flux can be estimated on regional scales using secondary data. However, the approach has yet to be examined on large regional or global scales, and the range of conditions over which it is valid has not been evaluated prior to this study.

This investigation sought to determine the CO<sub>2</sub> dissolution sink for the roughly half-million km<sup>2</sup> Ohio River basin using an adaptation of the hydrochem-discharge method used by Salley (2016). The scope of this research does not include an investigation of the contributions of non-carbonate rocks to DIC flux or the atmospheric C sink from weathering of silicates, although these may be important considerations for future studies. A fundamental *a priori* hypothesis associated with this project contends that the weathering of carbonate minerals is the primary source of DIC flux observed in river basins and, because of this, non-carbonate sources of DIC were not considered. The study area was chosen for its size and because the basins used in previous studies, employing similar methods by Osterhoudt (2014) and Salley (2016), are nested drainages within the Ohio River basin. This allowed for direct comparison of results among small and large regional basins to determine if the factors of carbonate rock area, time, and discharge accounted for in the carbon flux normalization were sufficient considerations, or if additional factors should be evaluated as the scale of the study area increases. The data used in this research were secondary, such that successful implementation virtually eliminates the need for raw data collection in calculating carbon sink for a particular basin. The study area was defined by the Hydrologic Unit Code (HUC) basin boundaries available through the USDA Natural Resources Conservation Service (NRCS) Geospatial Data Gateway, and the area of carbonate rock within each HUC basin is determined from the U.S. karst map (Weary and Doctor, 2014). These have been overlain and clipped to the basin extent using ArcGIS 10.2.2 software. Public water chemistry data from municipal water-treatment facilities within the Ohio River basin and its tributaries were used to calculate total DIC present in solution. Precipitation and temperature data were

collected from individual weather stations within the study area operated by the National Oceanic and Atmospheric Administration (NOAA, 2016) National Centers for Environmental Information (NCEI), formerly known as the NOAA National Climatic Data Center (NCDC). Discharge data were obtained from the active U.S. Geological Survey (USGS) gauging stations located nearest the outlets of the Ohio River and its major tributaries (i.e., the Wabash, Great Miami, Scioto, Allegheny, Monongahela, Kanawha, Licking, Kentucky, Green, Cumberland, and Tennessee rivers) for each basin used in the study, for a total of 12 gauging stations.

#### 4.2 Water Chemistry and Discharge Data

A critical component in determining the carbon sink for a given basin is to know the total inorganic carbon present in the water that is discharged from the basin. This can be calculated from routine water-quality measurements taken by municipal treatment facilities. Hydrochemical data were evaluated from October 1, 2013, to September 30, 2014. This study period represents the water year following the study period used by Salley (2016) and coincides with the water year set by U.S. Geological Survey. Water chemistry data were collected from various public water treatment facilities (Figure 4.1). Preference was given to hydrochemical-sampling points located nearest to the river mouth. Priority was given to the highest resolution data available, which were adjusted to the degree of measurement precision for other parameters such as precipitation or discharge. Raw water chemistry data used for this study included pH, temperature, and total alkalinity (mg CaCO<sub>3</sub>/L), which was converted to bicarbonate alkalinity (mg HCO<sub>3</sub><sup>-</sup>/L). Methods for the analysis of water samples followed the protocols defined in Standard Methods for the Examination of Water and Wastewater (SM) (AWWA 2006a, b), by the

U.S. Environmental Protection Agency (EPA), or those of Hach, Inc. (Hach, 2012).

Water temperature was measured following SM 2550 with a thermometer (AWWA, 2006a). The total alkalinity of water was calculated by titration of sample with a strong acid such as sulfuric or hydrochloric acid (AWWA, 2006b, c).

Hydrochemical data were aggregated using the highest resolution available to represent daily values that were directly comparable to daily resolution discharge measurements. The influence of using aggregated and lower resolution data in making estimates of DIC flux was evaluated in two ways. First, by comparison of flux values calculated from daily resolution data from the Kentucky American Water Company for the Kentucky River at Pool 3 for all of WY 2014. Available monthly water-chemistry measurements were taken from the Kentucky River at Lockport, KY, between March and September, 2014. Second, by comparison of time-area normalized flux calculated from high-resolution direct measurements of water chemistry in the Green River for the period October 21, 2012, to January 27, 2013, with the analogous period in 2013-2014 as calculated from secondary water chemistry data acquired from the EPA Storage and Retrieval (STORET) database.

Discharge data were obtained from USGS gauging stations via the National Water Information System (NWIS) for the Ohio River and major tributaries. Daily resolution discharge measurements ( $\text{ft}^3/\text{s}$ ) were assembled for the study period of WY 2014 and units converted to liters per day (L/day). Discharge monitoring locations were selected based on the distance of each gauging station from the river outlet and the sampling site of hydrochemical measurements. Hydrochemical data were aggregated to match discharge sampling frequency. This approach was chosen over averaging of high



resolution discharge data to match lower resolution chemistry measurements, since the range of discharge measurements varied more greatly than hydrochemical data over the year.

#### 4.3 Precipitation and Temperature Data

Annual air temperature and precipitation data, for determination of rainfall and evapotranspiration, were collected for the Ohio River drainage basin for the duration of the study period. The NOAA National Climate and Environmental Information database (NOAA, 2016) provided annual summaries of monthly precipitation totals (cm) and mean monthly air temperature (°C) data reported from various stations located throughout the study area. The locations of the weather stations where precipitation and temperature data were obtained are shown in Figure 4.2. The climate data selected for this study were reported from Cooperative Observer Program (COOP) stations in the Ohio River basin. The NCEI Annual Climatological Summary is derived from the National Climate Data Centers (NCDC) Summary of the Month dataset (DSI-3320). The NCEI was launched by NOAA on April 22, 2015, as a merging of the NCDC, National Geophysical Data Center (NGDC), and National Oceanographic Data Center (NODC), including the National Coastal Data Development Center (NCDDC), per the Consolidated and Further Continuing Appropriations Act, 2015, Public Law 113-235 (NOAA, 2016). This information, along with weather-station coordinates, was used in calculating the total amount of water available for carbonate-rock dissolution for the Ohio River drainage and its major sub-basins.

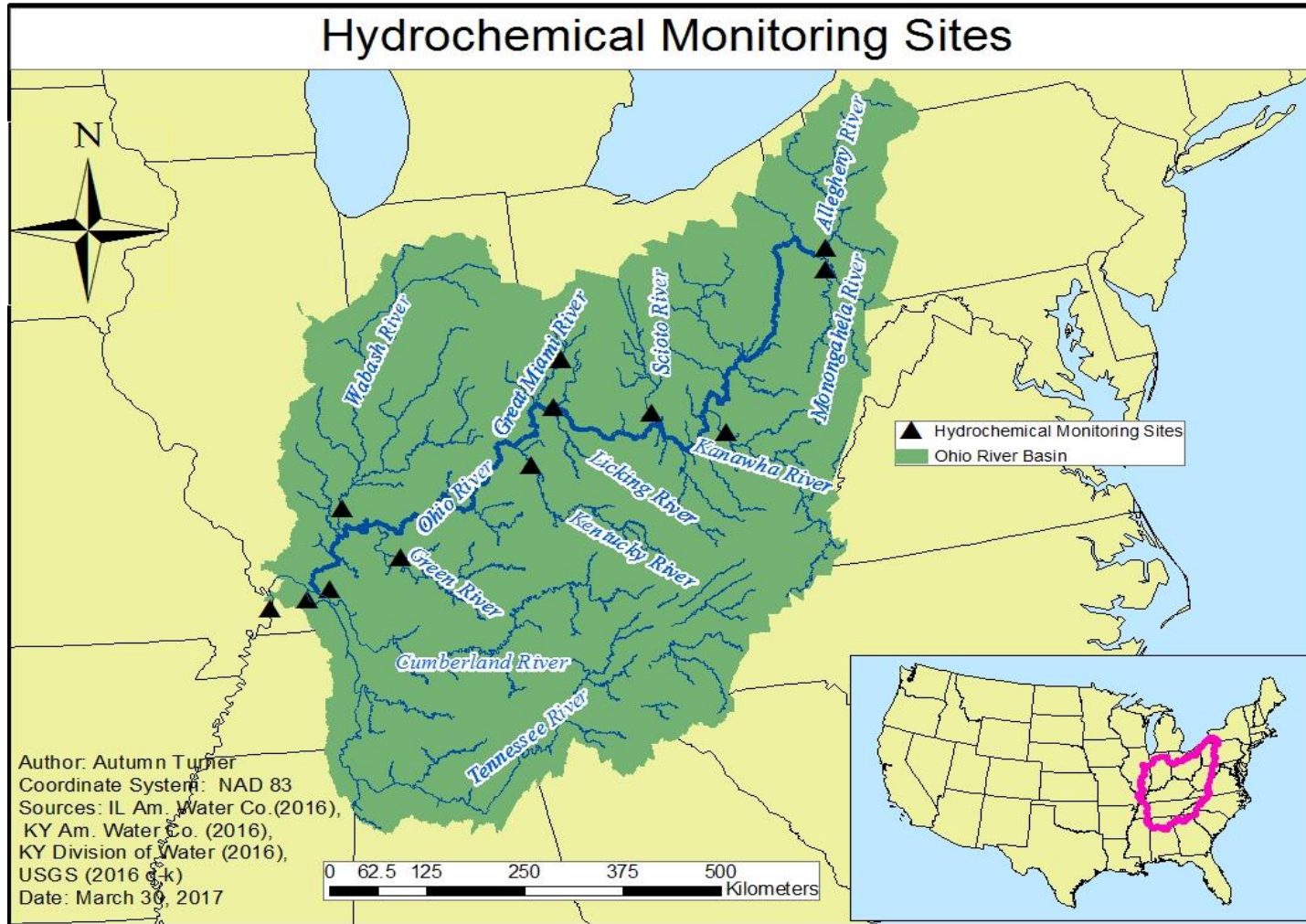


Figure 4.1. Location of hydrochemical monitoring points. Source: Created by the author from IAWC (2016), KAWC (2016), KDOW (2016a, b, c); and USGS (2016d-k) data.

### 4.3 Precipitation and Temperature Data

Annual air temperature and precipitation data, for determination of rainfall and evapotranspiration, were collected for the Ohio River drainage basin for the duration of the study period. The NOAA National Climate and Environmental Information (NCEI) database provided annual summaries of monthly precipitation totals (cm) and mean monthly air temperature (°C) data reported from various stations located throughout the study area. The locations of the weather stations where precipitation and temperature data were obtained are shown in Figure 4.2. The climate data selected for this study were reported from Cooperative Observer Program (COOP) stations in the Ohio River basin. The NCEI Annual Climatological Summary is derived from the National Climate Data Centers (NCDC) Summary of the Month dataset (DSI-3320). The NCEI was launched by NOAA on April 22, 2015 as a merging of the NCDC, National Geophysical Data Center (NGDC) and National Oceanographic Data Center (NODC), including the National Coastal Data Development Center (NCDDC), per the Consolidated and Further Continuing Appropriations Act, 2015, Public Law 113-235 (NOAA, 2016). This information, along with weather-station coordinates, was used in calculating the total amount of water available for carbonate-rock dissolution for the Ohio River drainage and its major sub-basins.

## NOAA COOP Weather Stations

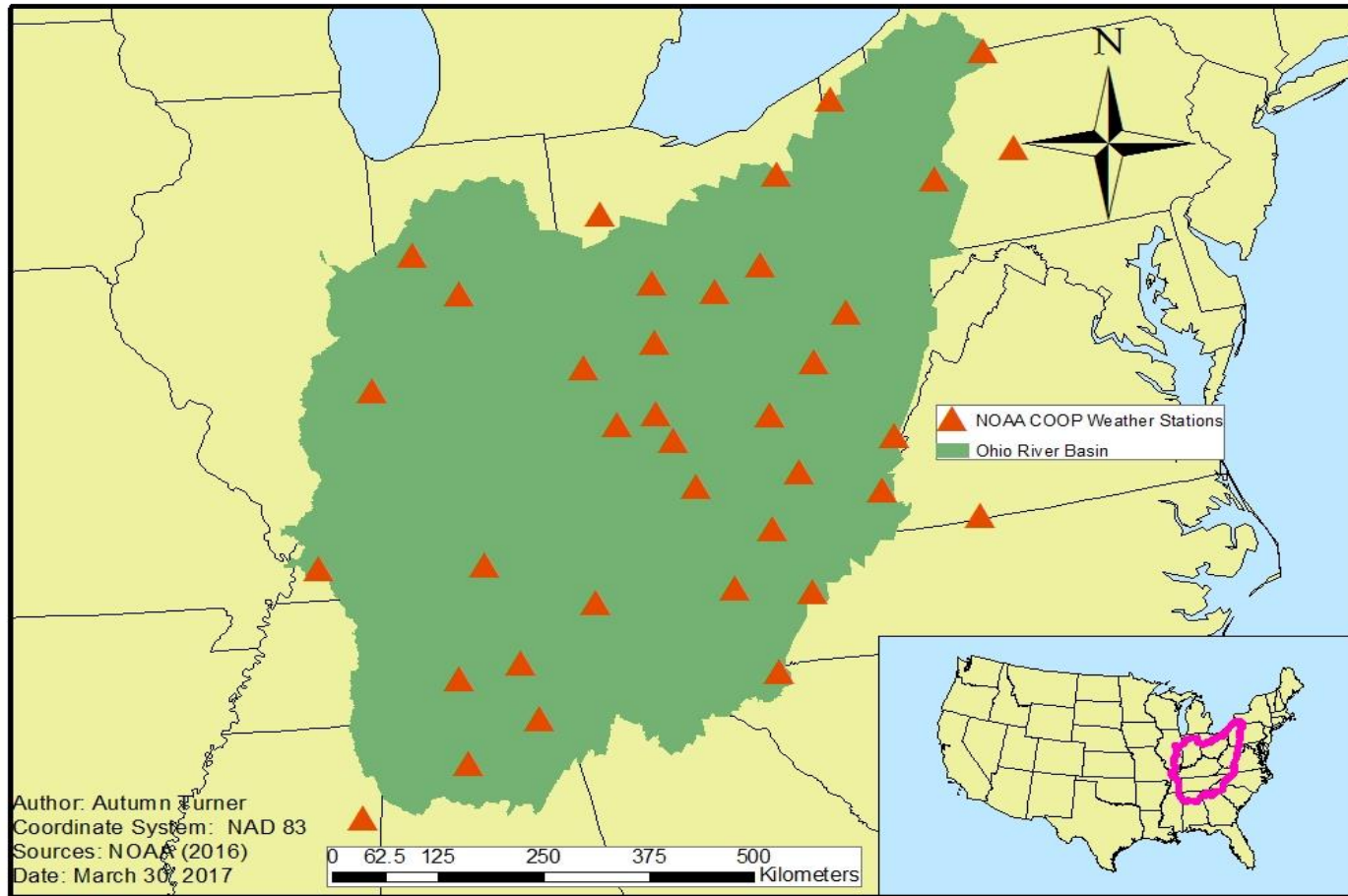


Figure 4.2. Location of NOAA COOP weather stations.  
Source: Created by the author from NOAA (2016) data.

#### 4.4 GIS Data

Several forms of GIS spatial data were used to represent the geologic, hydrologic, topographic, basin delineation, and county boundaries within the study area. These data were obtained using the U.S. karst map (Weary and Doctor, 2014), USDA NRCS Geospatial Data Gateway, Advanced Spaceborne Thermal Emission and Reflection Radiometer (ASTER) Global Digital Elevation Model (GDEM), USGS Open-File Report 2014-1156, and NOAA NCEI Annual Climatological Summaries Database (NOAA, 2016). Data were imported into ArcMap 10.2.2 and clipped to the basin extent. Drainage basin boundaries for the Ohio River and major tributaries were delineated using Hydrologic Unit Code (HUC) shapefiles available via the U.S. National Hydrography Watershed Boundary Dataset (USGS, 2016a) and ASTER GDEM topographic data (NASA, 2016). The carbonate outcrop area was defined by the extent of exposed carbonate rock within a basin. A geologic shapefile representing carbonate rock distribution was accessed from the U.S. karst map (Weary and Doctor, 2014), and the area was calculated in ArcMap 10.2.2 using geoprocessing and summary tools. User-defined Kriging interpolation of precipitation minus evapotranspiration (P-ET) data taken from selected weather stations throughout the Ohio River drainage basin was conducted. Kriging interpolation is a spatial statistics tool available in ArcGIS that averages values for areas that do not have a direct measurement using the measurements taken at nearby points as a function of distance. The results of the Kriging analysis were mapped to show contour lines of equal water availability (cm). All GIS data were represented using the North American Datum 1983 (NAD 83) geographic coordinate system and the Albert Equal Area Conic projected coordinate system.

#### 4.5 Data Processing

Data processing involved several components, including mapping and spatial analysis using ArcGIS, spreadsheet data management, and calculations performed in Microsoft Office Excel 2013 or Systat Software Sigma Plot 11.0, and graphing and statistical analysis using Sigma Plot 11.0. Water chemistry, discharge, precipitation, and surface temperature records and calculations were managed and carried out using Excel 2013 and Sigma Plot 11.0. The ESRI ArcGIS 10.2.2 GIS platform was used to delineate the Ohio River basin and sub-basin spatial extents, process geologic data, and implement Kriging interpolation of precipitation. As described, Kriging is a means of estimating values for points without measurement using measurements from nearby points. Salley (2016) compared two methods of interpolation for precipitation-evapotranspiration data points within the Barren River drainage basin and found that the more technically complex Kriging method of interpolation did not significantly improve the accuracy compared to Inverse Distance Weighted (IDW) interpolation. This study also compared interpolation surfaces produced by IDW and Kriging interpolation. The contour surface produced by the Kriging interpolation was chosen for the improved smoothness of the contours versus the IDW surface.

#### 4.6 Drainage Basin Delineation

The drainage boundaries for the Ohio, Wabash, Great Miami, Scioto, Allegheny, Monongahela, Kanawha, Licking, Kentucky, Green, Cumberland, and Tennessee river basins were delineated using HUC shapefiles and represented in ArcMap 10.2.2. Basin polygons were adjusted based on the location where hydrochemical measurements were taken, such that basin areas downstream of a hydrochemical monitoring point were

excluded (see Figure 5.1). In other words, basins were considered to “end” at the point where the hydrochemical data were collected. Drainage basin corrections were delineated along drainage divides as indicated by elevation contours. Coarse elevation contours were acquired from ASTER GDEM version 2.0 data. ASTER GDEM v2 is a product provided by the Land Processes Distributed Active Archive Center (LP DAAC) managed by the NASA Earth Science Data and Information System (ESDIS) project. Elevation contours were manually digitized to create basin polygons that reflect only the basin area upstream of the hydrochemical sampling locations. The resulting corrected basins more accurately reflect the area of the basin where carbonate rocks may contribute alkalinity to the river water at a given monitoring location. Adjustment of basin boundaries to represent subsurface flow was also considered, but not applied. Among hydrologic environments where rock permeability is low (that is, not enhanced by the presence of dissolution conduits or rock fractures), basin delineation reflects topographical divides. In contrast, rocks that display high permeability can allow for the extension of drainage basins beyond those delineated from surface features. Similarly, among karst environments, groundwater basins do not necessarily follow surface topography. Previous studies (see Salley, 2016) adjusted drainage basins to account for known karst groundwater flow paths among smaller basins that alter the effective area of the basins determined from surface topography only. The corrected basin delineations added a total of 464.6 km<sup>2</sup>, or roughly 11% of the total 4247.7 km<sup>2</sup> drainage area of the Barren River upstream from Bowling Green. Basin area extension from groundwater flow paths proves to be an important factor in delineating drainage areas for basins that are hundreds of square miles, but these considerations may be of less consequence for the 490,600 km<sup>2</sup> Ohio

River basin. Basin extensions of hundreds of miles would not significantly increase the area of a basin the size of the Ohio River drainage and, as such, corrections for basin extension from subsurface karst conduits are not be considered within the scope of this study.

#### 4.7 Calculation of Water Volume Available for Carbonate Dissolution

Average monthly temperature (°C), monthly precipitation totals (cm), and station coordinates were collected from 37 Cooperative Observer Network (COOP) weather stations distributed throughout the study area, as well as a buffer beyond the basin boundaries to avoid edge effect and provide a suitable number of neighboring points for interpolation of precipitation values. These averages were adjusted to account for monthly volumetric loss due to evapotranspiration at given average monthly air temperatures for each weather station evaluated in the study area, such that: precipitation-evapotranspiration = volume available for dissolution. The calculation for potential evapotranspiration (PET) was performed per the methods of Thornthwaite and Mather (1957) as follows:

$$PET = 1.6x \left( \frac{10T_a}{i} \right)^a \quad (13)$$

Where  $T_a$  is the mean monthly air temperature (°C),  $a$  is an empirically-derived exponent that is a function of  $i$ , given by  $a = [0.49 + 0.0179 * (I - 0.0000771) * I^2 + 0.000000675 * I^3]$  and  $I$  is the heat index summed over a 12-month period where:

$$I = \sum_{i=1}^{12} \left( \frac{T_{ai}}{5} \right)^{1.5} \quad (14)$$



Moisture excess or deficiency was determined as the difference of precipitation and PET with negative values representing potential deficiency of water (Thornthwaite and Mather, 1955, 1957; Sellinger, 1996).

#### 4.8 Calculation of Dissolved Inorganic Carbon (DIC)

To calculate the carbon flux from a basin, it was necessary first to determine the total alkalinity and dissolved organic carbon (DIC) of the water discharged from the basin. Total alkalinity is the equivalent sum of bases titratable with strong acid (Stumm and Morgan, 1981). Although other sources of non-carbonate alkalinity are present in natural waters, in carbonate rock flow systems these are typically of small consequence relative to carbonate species. Waters substantially influenced by limestone are dominated by  $\text{HCO}_3^-$  (Dreybrodt, 1988) and, thus, carbonic acid ( $\text{H}_2\text{CO}_3$ ), bicarbonate ( $\text{HCO}_3^-$ ), and carbonate ( $\text{CO}_3^{2-}$ ) ions are considered primary species present in the system. Relative concentrations of carbonate species in solution were calculated from pH, temperature, and alkalinity ( $\text{mg/l HCO}_3^-$ ) measurements of surface waters from routine monitoring programs at water treatment facilities located near basin outlets. Bicarbonate ( $\text{HCO}_3^-$ ) species activity ( $a_i$ ) was calculated using the extended Debye-Hückel expression (Debye-Hückle, 1923; Harned and Owen, 1958; Stumm and Morgan, 1981):

$$-\log \gamma_i = \frac{Az_i^2\sqrt{I}}{1+\alpha_i^{\circ}B\sqrt{I}} \quad (15)$$

$$a_i = m_i\gamma_i \quad (16)$$

where a and b are constants for a given temperature and solvent,  $\alpha^{\circ}$  is the effective diameter of the  $\text{HCO}_3^-$  ion complex,  $z_i$  is the formal charge of  $\text{HCO}_3^-$ , and  $I$  is the ionic strength of the solution, given by:

$$I = \frac{1}{2} \sum m_i z_i^2 \quad (17)$$

Activities of carbonic acid ( $H_2CO_3$ ) and carbonate ( $CO_3^{2-}$ ) were calculated using acid-base equilibria as follows:

$$[H_2CO_3] = \frac{[H^+][HCO_3^-]}{K_1} \quad (18)$$

$$[CO_3^{2-}] = \frac{[K_2][HCO_3^-]}{H^+} \quad (19)$$

where  $k_1$  and  $k_2$  are temperature dependent solubility product constants. DIC is the sum of carbonate species in solution given by:

$$\sum H_2CO_3^*, HCO_3^-, CO_3^{2-} \quad (20)$$

Daily resolution discharge (Q) measurements were obtained from US Geological Survey stations located at or very near locations where hydrochemical measurements were taken. Dissolved inorganic carbon (DIC) export from each basin was calculated as the product of the sum inorganic carbon species in solution and discharge.

$$DIC \text{ Export} = (\sum H_2CO_3^*, HCO_3^-, CO_3^{2-}) \times Q \quad (21)$$

Annual and monthly DIC flux values were calculated for the Ohio basin. Annual DIC flux was calculated for the major tributaries during WY 2014.

#### 4.9 Calculation of Atmospheric Carbon Sink

The atmospheric carbon sink by carbonate rock dissolution for the Ohio River drainage and major sub-basins was estimated for WY 2014 as one-half of the total DIC flux leaving the basin per appropriate chemical mass balances (Jiang and Yuan, 1999; Liu

and Zhao, 2000; Groves and Meiman, 2001; Groves et al, 2002; Amiotte Suchet et al., 2003; He et al., 2013). Inorganic carbon flux from the atmosphere to the terrestrial reservoir is one-half of the total DIC export from a basin. This is related to the fundamental assumption that for every two moles of carbon produced in equation (1), one mole of carbon originated as CO<sub>2</sub> in the atmosphere and the other mole was derived from the carbonate rock itself.

#### 4.10 DIC Flux Normalization Procedure

The DIC flux leaving the Ohio basin and sub-basins was normalized by time and the volume of water available for dissolution of carbonate minerals (rainfall minus ET over the area of carbonate rock), as in Salley (2016). The annual DIC mass exported per basin was divided by the product of days in the sample period, area of exposed carbonate rock, and depth of precipitation minus ET to achieve normalized DIC flux per time-volume unit. The competence of the calibration in direct estimation of DIC flux as a function of time-volume normalization parameters was tested by statistical correlation. DIC flux values were plotted for each basin and compared using linear regression analysis to previous work conducted by Osterhoudt (2014) and Salley (2016).

## Chapter 5. Results

### 5.1 Basin Delineation and Geologic Mapping

The total area of the Ohio River basin is 460,901 km<sup>2</sup> (White et al., 2005) and includes 11 major sub-basins ranging in area, from 9479 km<sup>2</sup> for the Licking River basin to 245194.2 km<sup>2</sup> for the Tennessee River basin (USGS, 2016c). Sub-basins were delineated to exclude areas below the location where hydrochemical samples were taken to improve accuracy and avoid inclusion of carbonate areas that did not act as a source of alkalinity at the monitoring point (Figure 5.1). Delineation was performed in a Geographic Information System (GIS) using ASTER GDEM (NASA, 2016) topographic raster files. Geologic maps of carbonate distribution (Weary and Doctor, 2014) were manipulated in ArcMap 10.2.2 to match the adjusted basin extents, and the area of exposed carbonate rocks present within each corrected basin was calculated. The total area of carbonate exposed carbonate rock for the Ohio River basin was 120,401 km<sup>2</sup> (Figure 5.2). The area of exposed carbonate rock among the sub-basins ranged from 0 km<sup>2</sup> in the Kanawha River basin to 44308 km<sup>2</sup> in the Tennessee River basin. Values for the total basin area and for the corrected carbonate area are given in Table 3.

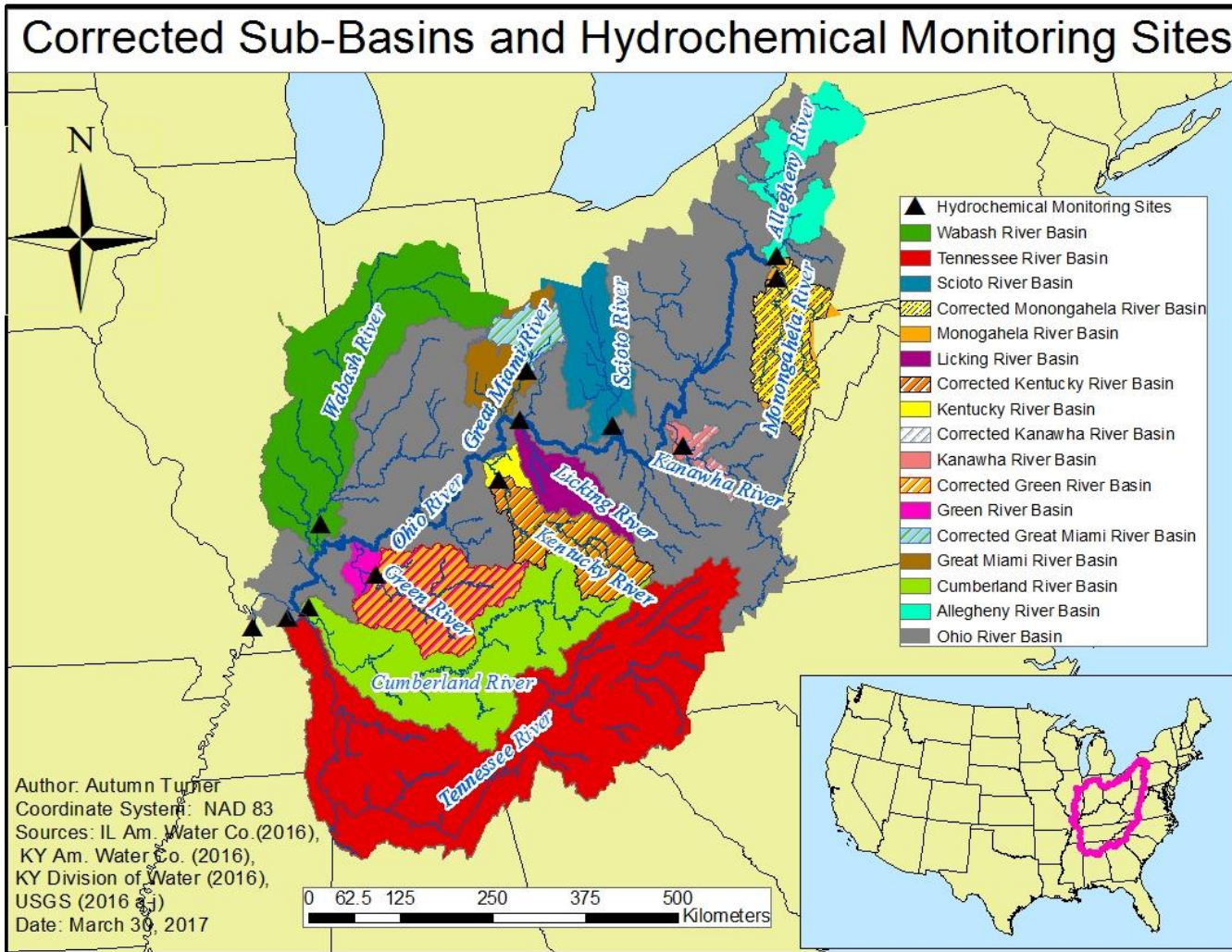


Figure 5.1. Corrected sub-basins reflecting drainage upstream of hydrochemical monitoring locations.  
 Source: Created by the author from IAWC (2016), KAWC (2016), KDOW (2016a,b,c), and USGS (2016a-j).

## Near Surface Carbonate Rocks of the Ohio River Basin

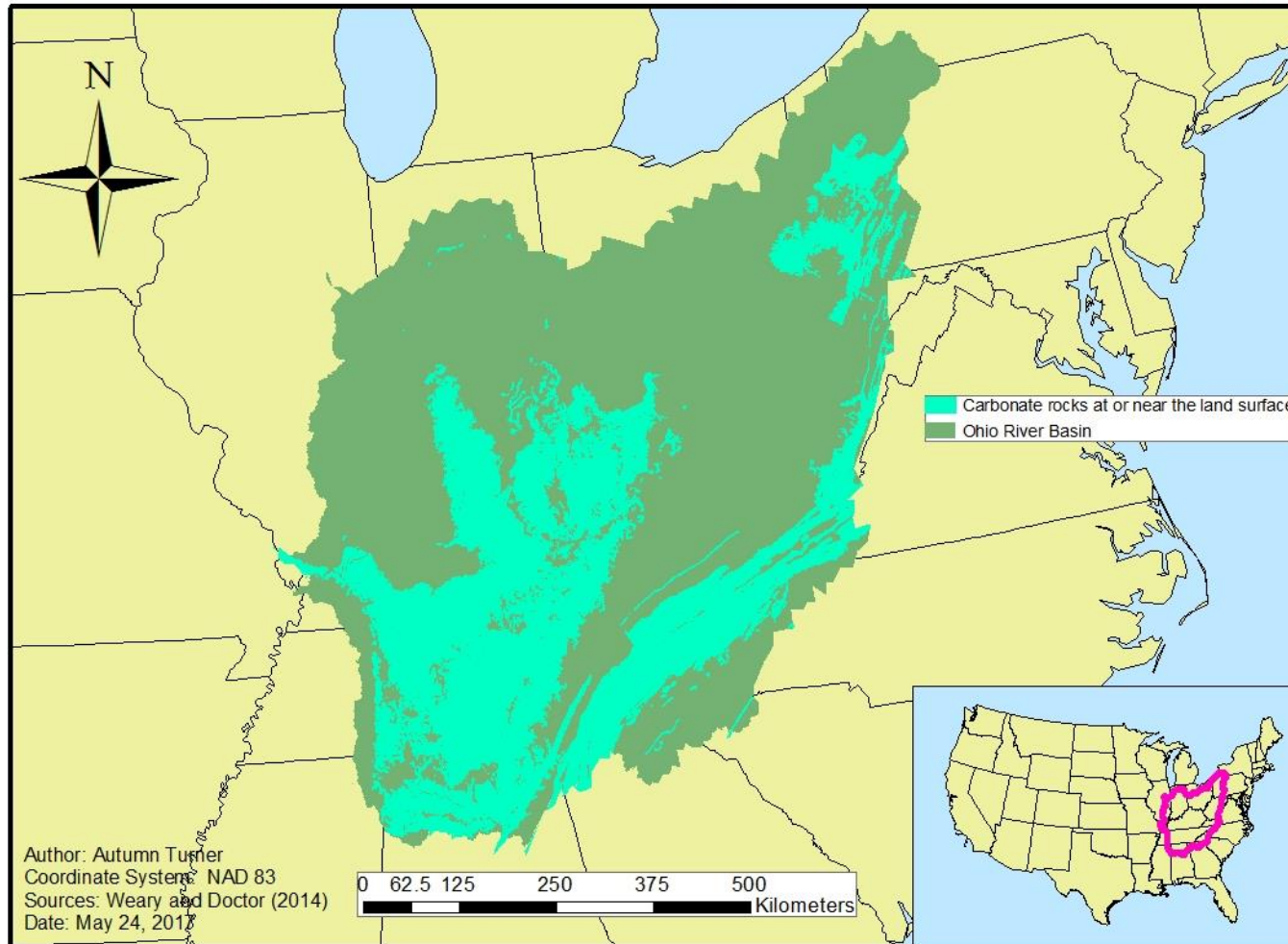


Figure 5.2. Geographic distribution of exposed carbonate rock surface within the Ohio River Basin.  
Source: Created by the author from Weary and Doctor (2014) data.

## 5.2 Precipitation (P), Evapotranspiration (ET), and (P-ET) Kriging Interpolation

Mean monthly precipitation for the Ohio River basin ranged from 5.67 cm in January to 13.6 cm in June. Monthly means for evapotranspiration ranged from  $5.72 \times 10^{-3}$  cm in January to 13.1 cm in June. The balance of water remaining after volumetric losses due to ET were subtracted from total precipitation was considered the amount of water available to participate in carbonate-rock dissolution. Comparison of the water balance relative to average monthly precipitation and ET values reveals a strong seasonal influence of ET on the amount of water available for dissolution processes (Figure 5.3). In general, ET is at a minimum during the winter months and rises steadily throughout the spring to reach peak levels in the summer before waning during the fall. Therefore, the calculated water balance was less than 1 cm during the months of May, June, July, August, and September. The effects of ET were especially evident during the months of July and September when the calculated water balance was negative. The average depth of precipitation over the Ohio River basin for the hydrologic year 2014 was 118.9 cm, and the average depth lost to evapotranspiration was 69.2 cm. The balance of water calculated at 37 COOP weather stations was interpolated by user-defined Kriging and mapped in ArcMap 10.2.2 to represent contours of equal water availability in the Ohio River and major sub-basins (Figure 5.4). These data were then converted to raster format and clipped to the extent of exposed carbonate rock in each basin. The depth of water (cm) that fell on exposed carbonates was calculated, converted to kilometers, and multiplied by the total carbonate rock area per basin to arrive at the total volume of water available for carbonate dissolution. The average depth of water available for carbonate dissolution for the Ohio basin during WY 2014 was  $5.1 \times 10^{-4}$  km (51 cm).

Precipitation (P), Potential Evapotranspiration (ET), and P-ET  
Ohio River Basin Water Year 2014

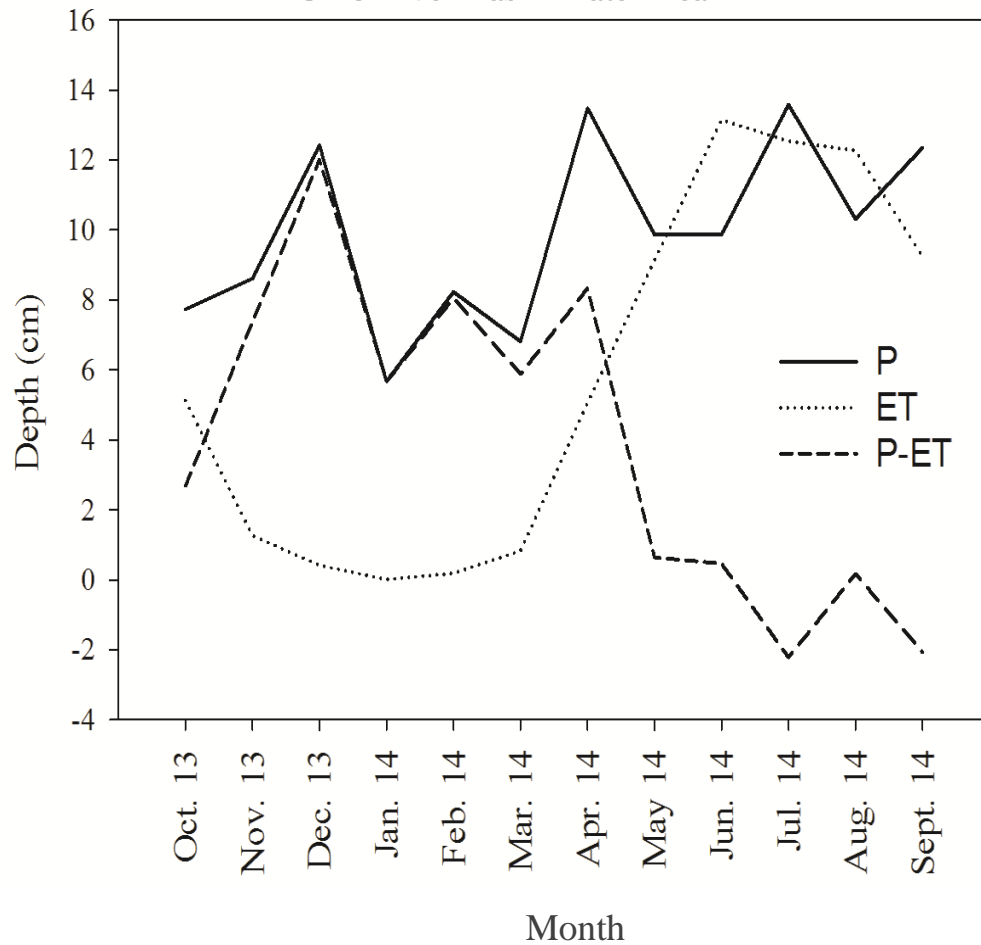


Figure 5.3. Monthly average water balance available for dissolution, relative to precipitation and water lost to evapotranspiration.  
Source: Created by the author from NOAA (2016) data.



## Interpolated Precipitation-Evapotranspiration Surface

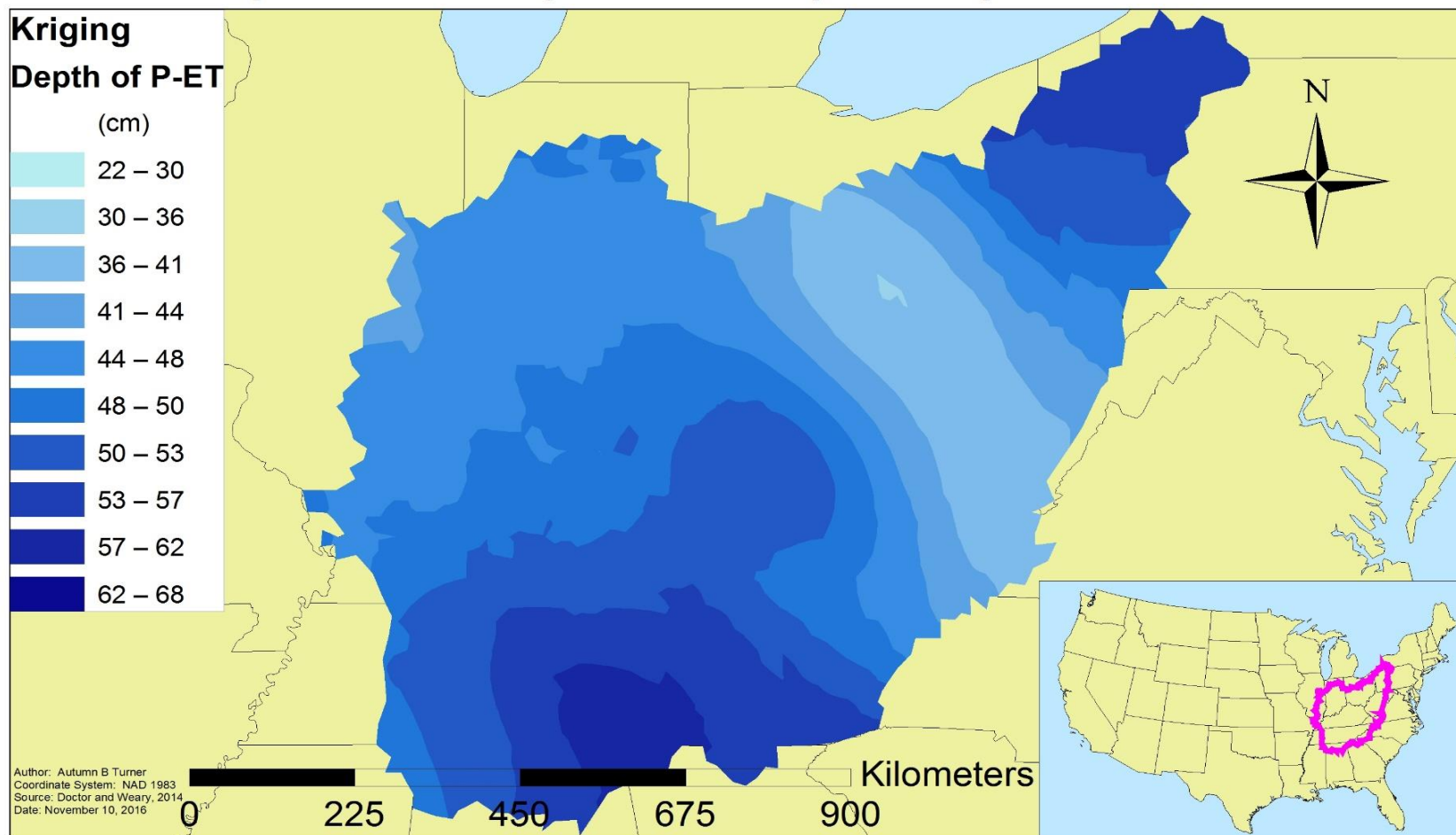


Figure 5.4. P-ET surface for depth of water available for carbonate rock dissolution.  
Source: Created by the author from NOAA (2016) data.

### 5.3 Hydrophysical Data

Discharge measurements were obtained for the period October 1, 2013, through September 30, 2014 (Figures 5.5-5.8). Discharge of the Ohio River varied considerably, ranging from  $1.79 \times 10^6$  L/s to  $2.14 \times 10^7$  L/s, with a mean discharge of  $8.64 \times 10^6$  L/s. The total volume discharged from the Ohio River during the study period was  $2.72 \times 10^{14}$  L. In general, discharge reflects seasonal variations in precipitation. Peak discharge measurements were observed between late December, 2013, and late April, 2014. This period of maximum discharge corresponds to increased precipitation events during winter and spring. Lower discharge values were observed among summer and fall months, consistent with decreased precipitation. Discharge measurements for sub-basins ranged from 2,888 L/s to 4,847,759 L/s. Discharge for all basins are summarized in Table 5.1.

<b>Basin</b>	<b>Minimum Discharge (L/s)</b>	<b>Maximum Discharge (L/s)</b>	<b>Mean Discharge (L/s)</b>
Ohio	1795288	21435853	8639485
Tennessee	187457	4847759	1598577
Wabash	67960	4360794	987158
Cumberland	73623	2755229	736160
Allegheny	128275	2616476	649352
Kanawha	63429	2271011	409152
Green	15574	1517782	392015
Kentucky	8636	1832100	271842
Monongahela	33697	1506456	233454
Scioto	19935	1101525	202246
Great Miami	19397	1554594	144749
Licking	2888	645624	92872

Table 5.1. Minimum, maximum, and average discharge for the Ohio River and major tributaries.

Source: Created by the author from USACE (2016a, b) and USGS (2016l, m, n, o, p, q, r, s, t, u) data.

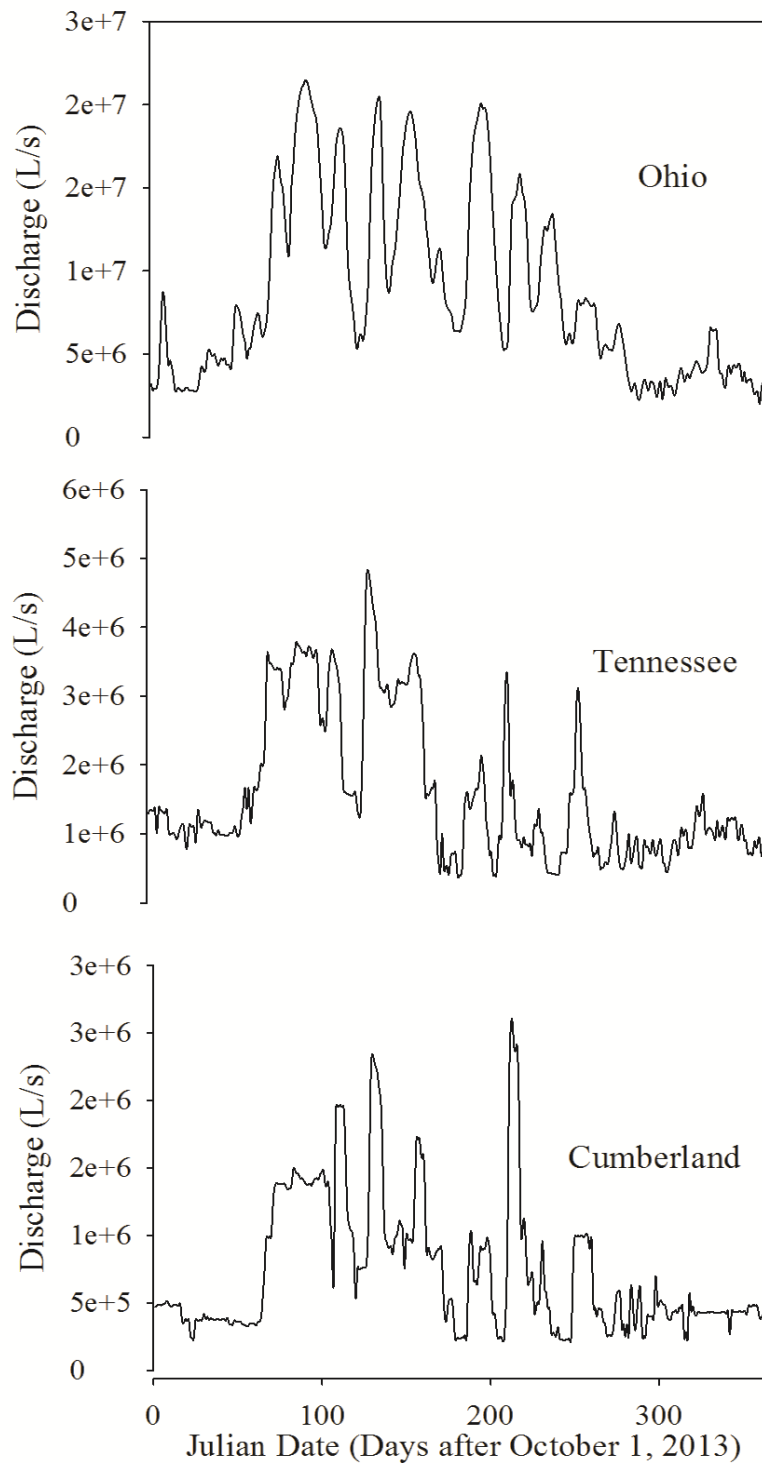


Figure 5.5. Discharge for the Ohio, Tennessee, and Cumberland rivers.  
 Source: Created by the author from USGS (2016s) and USACE (2016a, b) data.

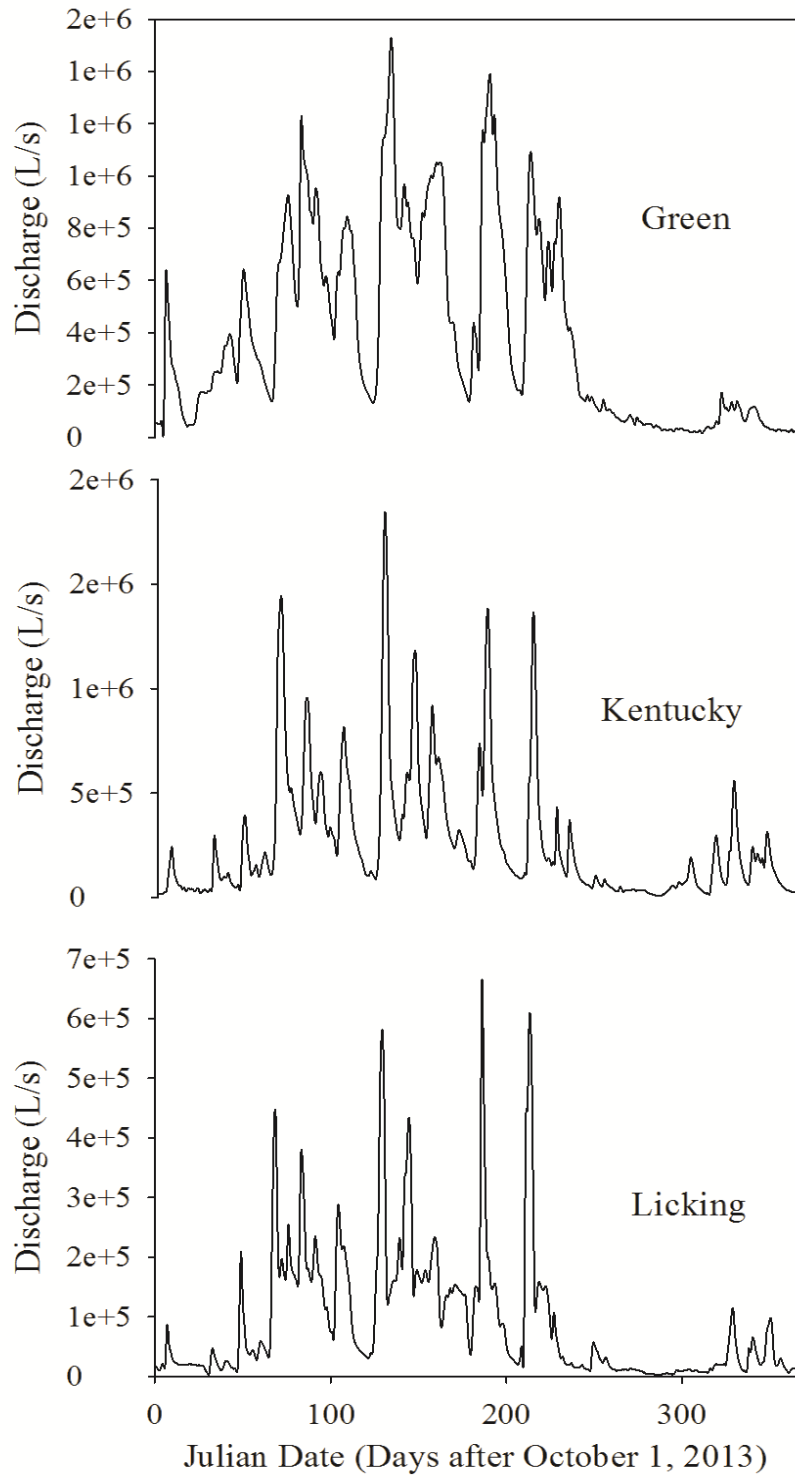


Figure 5.6. Discharge for the Green, Kentucky, and Licking rivers. Source: Created by the author from USGS (2016n, p, q) data.

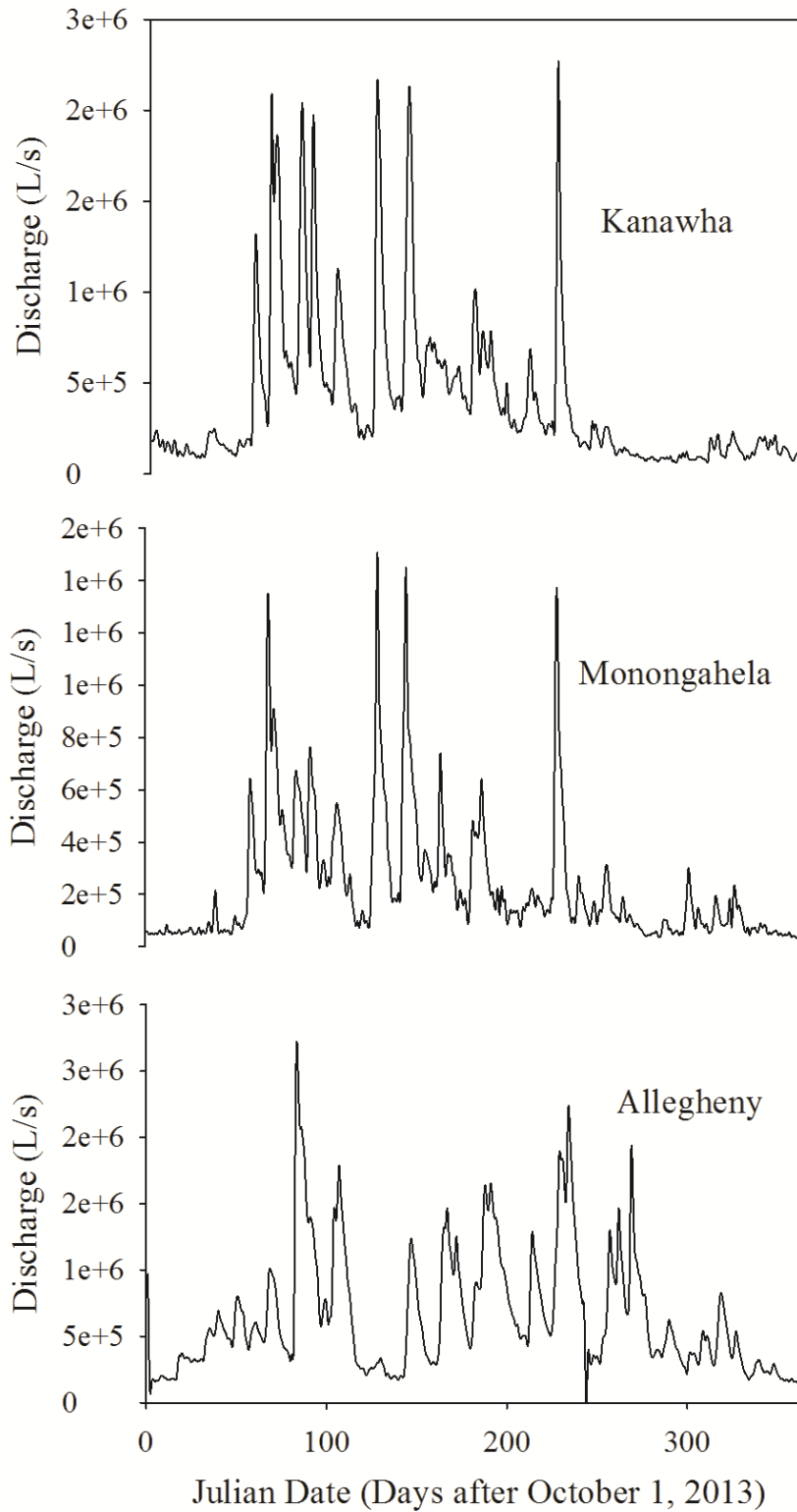


Figure 5.7. Discharge for the Kanawha, Monongahela, and Allegheny rivers. Source: Created by the author from USGS (2016l, o, r) data.

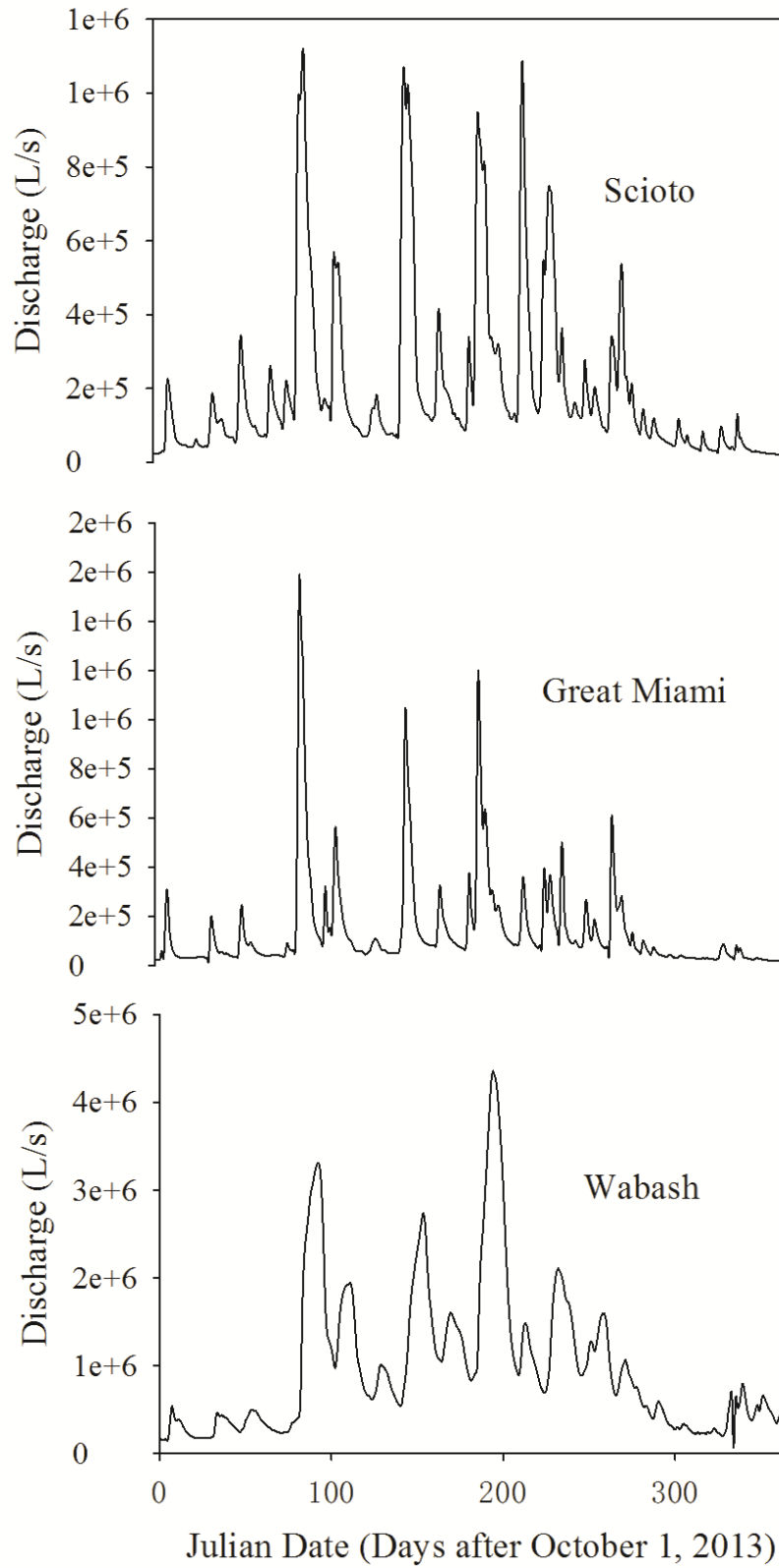


Figure 5.8. Discharge for the Scioto, Great Miami, and Wabash rivers. Source: Created by the author from USGS (2016m, t, u) data.

## 5.4 Hydrochemical Data

Daily resolution water-quality measurements for the parameters of pH, temperature, and alkalinity were acquired for the Ohio River and each of the major sub-basins for use in the calculation of total DIC concentration (Figure 5.9). Alkalinity data may be used in the calculation of DIC concentrations based on the assumption that, among carbonate dominated waters, alkalinity measurements reflect the basic carbonate species (bicarbonate and carbonate ions) in solution (Stumm and Morgan, 1981; Drever, 1988). The exact proportion of these species is a function of pH; for waters with pH values in the range of 7 to 9, bicarbonate species dominate. Water temperature and pH measurements were used in conjunction with bicarbonate alkalinity data to provide a more accurate calculation of DIC concentration in water.

The water temperature of the Ohio River during the study period ranged from 1.11 to 26.7 °C, with an average value of 13.7 °C. (Figure 5.10). Among the major sub-basins, water temperatures ranged from 0.170 to 35.2 °C (Figure 5.11). Coolest average temperatures were observed for the Allegheny River (12.7 °C) and warmest average temperatures were associated with the Cumberland River (19.2 °C). Minimum, maximum, and mean water temperatures for all sub-basins are presented in Figure 5.12. Temperature fluctuations for the Ohio and all evaluated sub-basins follow expected seasonal variations for the region. Throughout the hydrologic year under investigation, the lowest water temperatures were observed during the winter months, followed by a gradual rise throughout the spring, peak temperature conditions in the summer, and a gradual decline in water temperature during the fall.

The pH measurements within the Ohio River exhibited relatively stable conditions throughout the hydrologic year, with values ranging from 7.5 to 8.0 pH units and an

average value of 7.76 pH units (Figure 5.13). The sub-basin waters exhibited greater variation in pH than the Ohio River, with values ranging from 6.93 pH units to 12.5 pH units (Figure 5.14). The highest average pH values for WY 2014 were observed in the Monongahela River (7.60 pH units), while the lowest average pH values were observed in the Kanawha River (8.41 pH units). Minimum, maximum, and average pH values for each sub-basin are represented in Figure 5.15. Although the range of pH values varied considerably less than temperature among all the basins evaluated, the observed variations in pH occurred on shorter time scales without a clear influence on pH signal based on time of year.

Alkalinity measurements were reported as milligrams per liter calcium carbonate ( $\text{mg/L CaCO}_3$ ) and converted to milligrams per liter bicarbonate ( $\text{mg/L HCO}_3^-$ ). Bicarbonate alkalinity values for the Ohio River ranged from 109.8 to 175.7  $\text{mg/L HCO}_3^-$ , with a mean value of 139.2  $\text{mg/L HCO}_3^-$  (Figure 5.16). Within the sub-basins, bicarbonate alkalinity ranged from 34.6 to 502  $\text{mg/L HCO}_3^-$  representing a much greater range than analogous measurements from the Ohio River (Figure 5.17). The lowest average bicarbonate alkalinity values were found in the Allegheny River (47.0  $\text{mg/L HCO}_3^-$ ), while the highest average bicarbonate alkalinities were observed in the Great Miami River (378  $\text{mg/L HCO}_3^-$ ). Overall, bicarbonate alkalinity displayed a similar trend as pH, which is to be expected per the relationship between pH and alkalinity. Variations in bicarbonate alkalinity occurred at intervals closely aligned to that of pH, rather than exhibiting the seasonal fluctuations observed among temperature measurements. The patterns of variation among pH and alkalinity measurements may be substantially influenced by changes in discharge over smaller timescales.



Temperature for the Ohio River at Olmsted, IL  
Water Year 2014

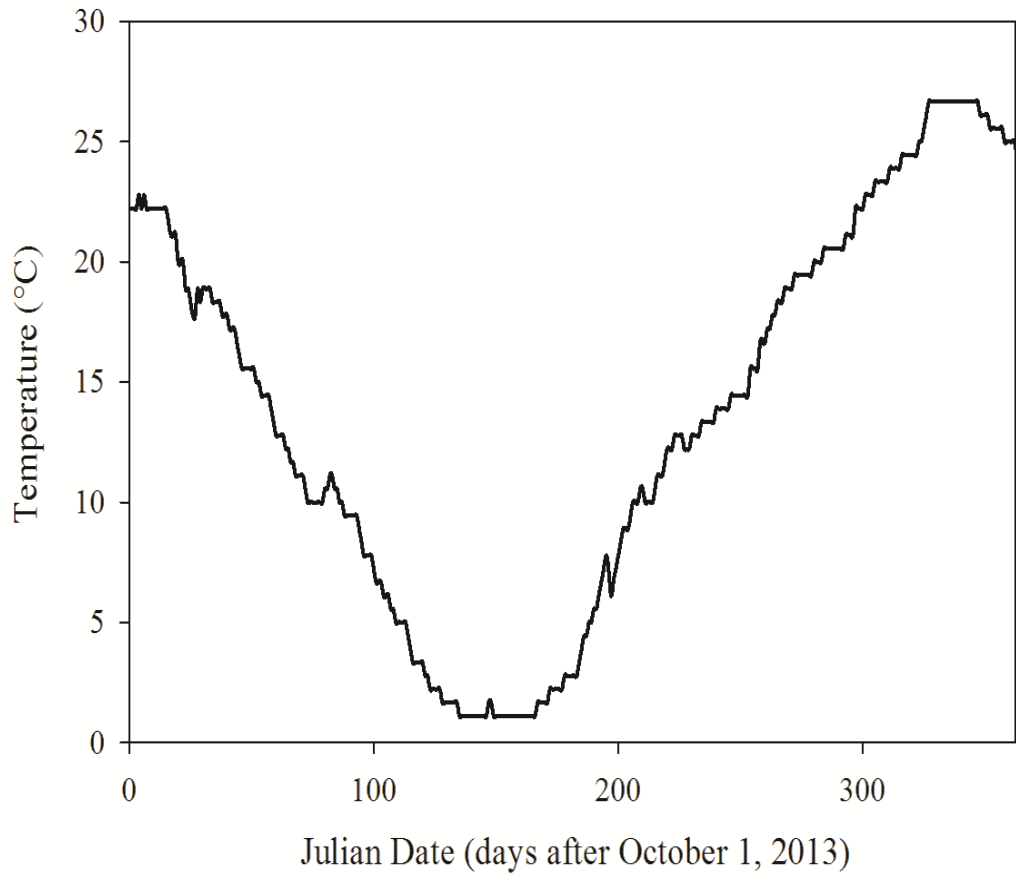


Figure 5.9. Water temperature for the Ohio River.  
Source: Created by the author from IAWC (2016) data.

## Mean Temperature for Major Sub-basins Water Year 2014

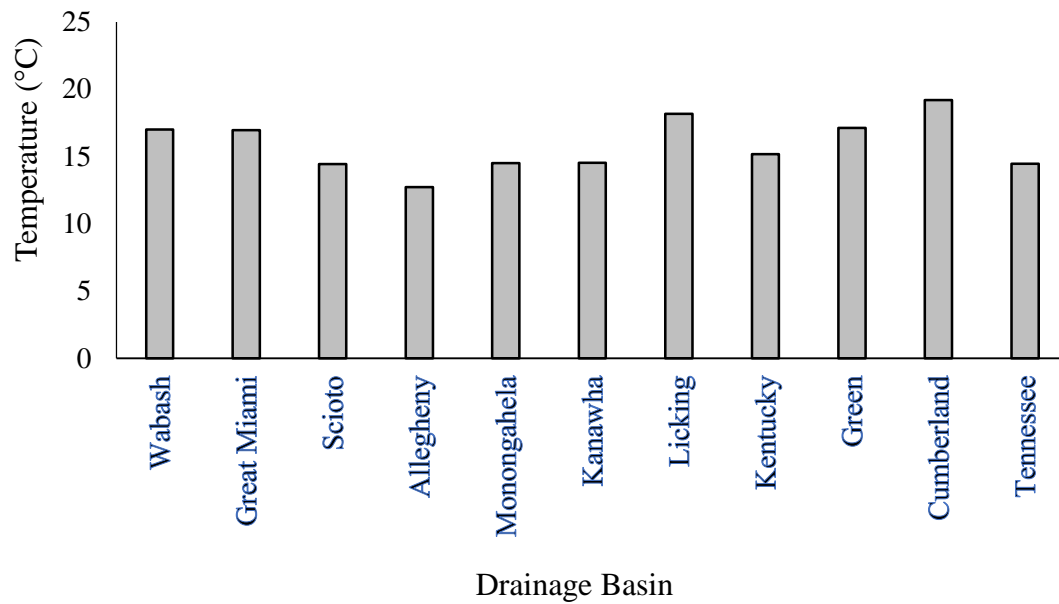


Figure 5.10. Mean water temperature for the major sub-basins.

Source: Created by the author from KAWC (2016), KDOW (2016a, b, c), and USGS (2016d, e, f, g, h, I, j, k) data.

pH for the Ohio River at Olmsted, IL  
Water Year 2014

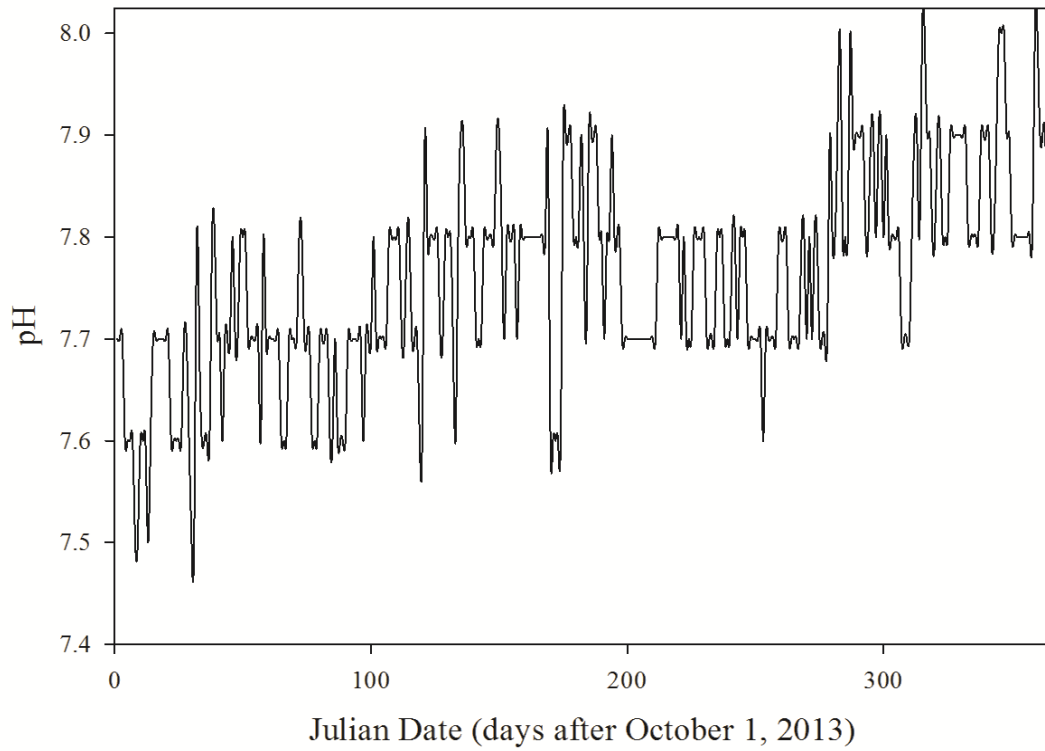


Figure 5.11. Recorded pH values for the Ohio River.  
Source: Created by the author from IAWC (2016) data.

## Mean pH for Major Sub-basins Water Year 2014

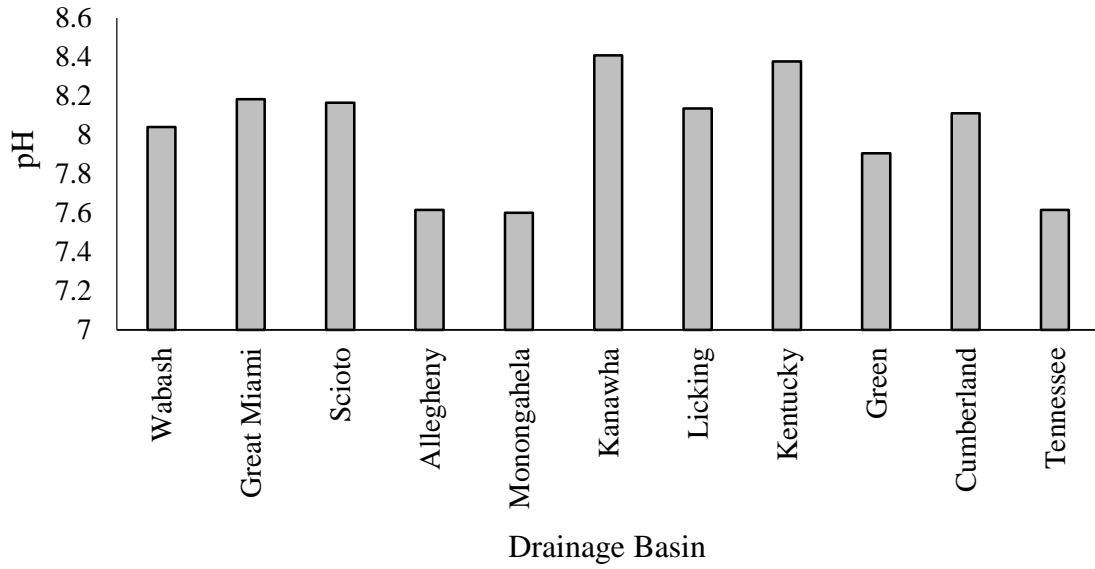


Figure 5.12. Mean pH values for the major tributaries to the Ohio River.  
Source: Created by the author from KAWC (2016), KDOW (2016 a, b, c), and USGS (2016d, e, f, g, h, I, j, k) data.

### Alkalinity for the Ohio River at Cairo, IL Water Year 2014

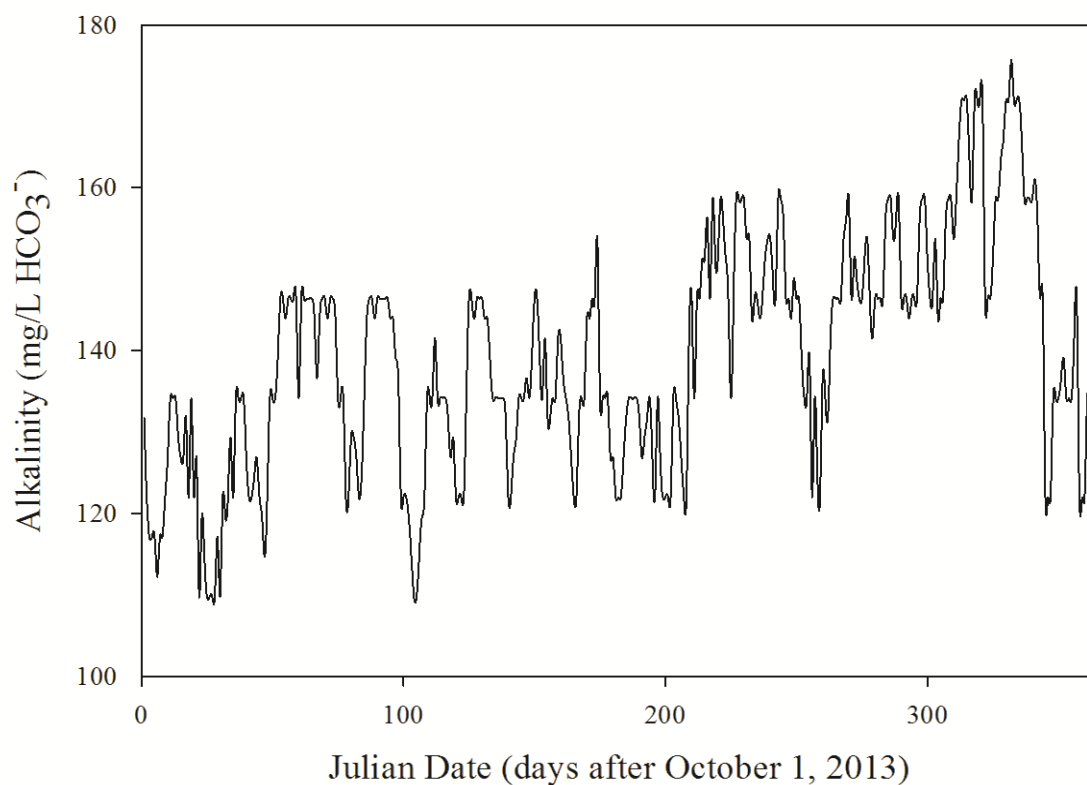


Figure 5.13. Recorded alkalinity values for the Ohio River.  
Source: Created by the author from IAWC (2016) data.

## Mean Alkalinity for Major Sub-basins Water Year 2014

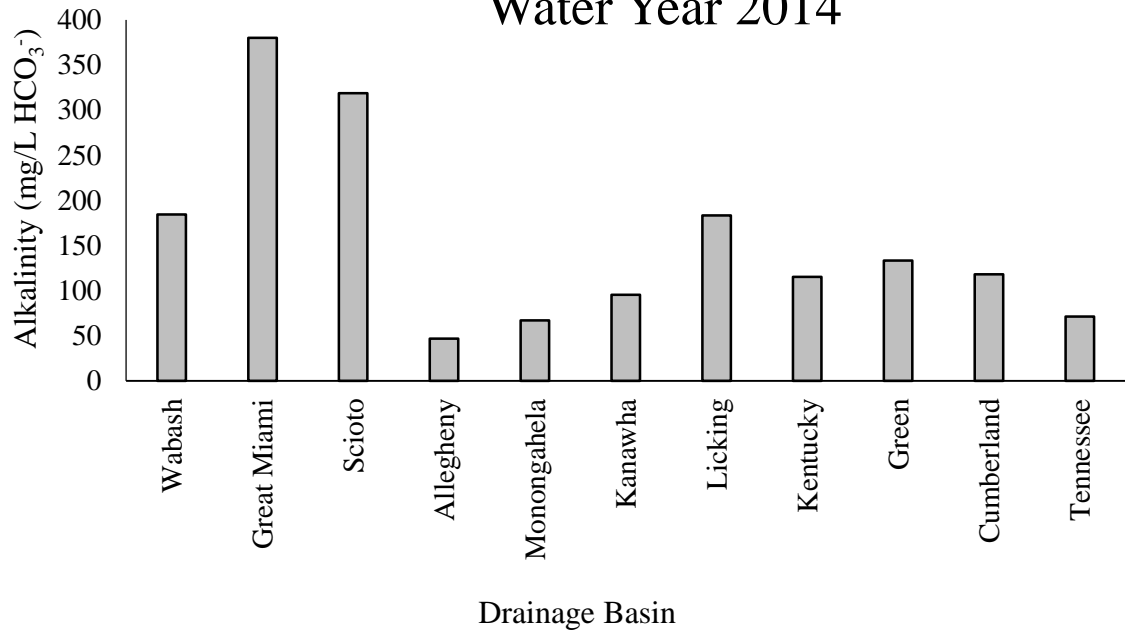


Figure 5.14. Mean bicarbonate alkalinity values for the major tributaries to the Ohio River.

Source: Created by the author from KAWC (2016), KDOW (2016a, b, c), and USGS (2016d, e, f, g, h, I, j, k) data.

## 5.5 Annual DIC Flux

The DIC flux, or amount of DIC discharged from a given basin, was calculated using existing discharge and hydrochemical data available to the public for each basin in study. The total mass of DIC removed from the Ohio River basin for WY 2014 was estimated at  $7.54 \times 10^{12}$  g C (Figure 5.15). Monthly DIC flux values were also calculated for the Ohio River basin. The average mass of DIC export among the major sub-basins during WY 2014 ranged from  $8.90 \times 10^{10}$  g C to  $1.15 \times 10^{12}$  g C (Figure 5.16). DIC values followed a similar pattern as alkalinity measurements. This was expected since the range of pH in each basin fell between 7.2 and 8.8 pH units and is well within the range of pH where bicarbonate ions are dominant in solution (7 to 9 pH units), thereby contributing most of the measured alkalinity (Drever, 1988). DIC flux ranged from  $9.3 \times 10^4$  to  $8.6 \times 10^6$  L/s (Figures 5.17 to 5.20).

## DIC for the Ohio River Water Year 2014

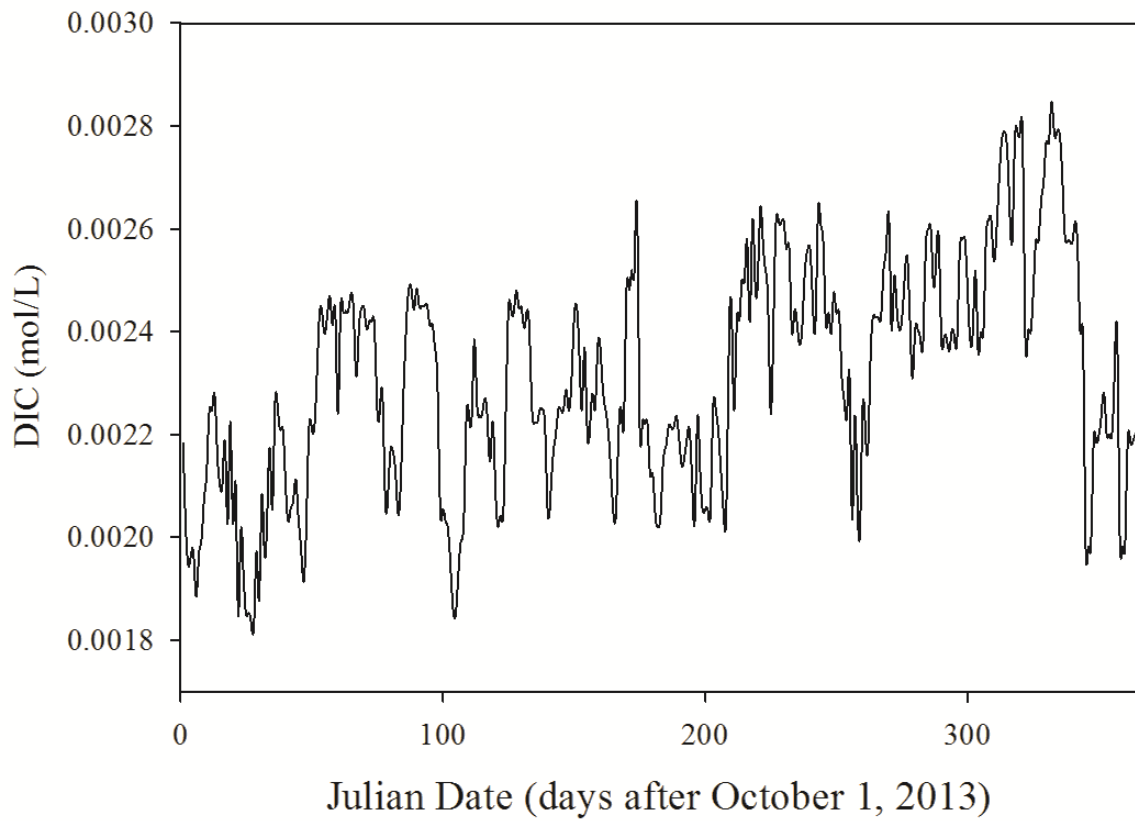


Figure 5.15. Sum DIC for the Ohio River.  
Source: Created by the author from IAWC (2016) and USGS (2016s) data.



### Mean DIC for Major Sub-basins Water Year 2014

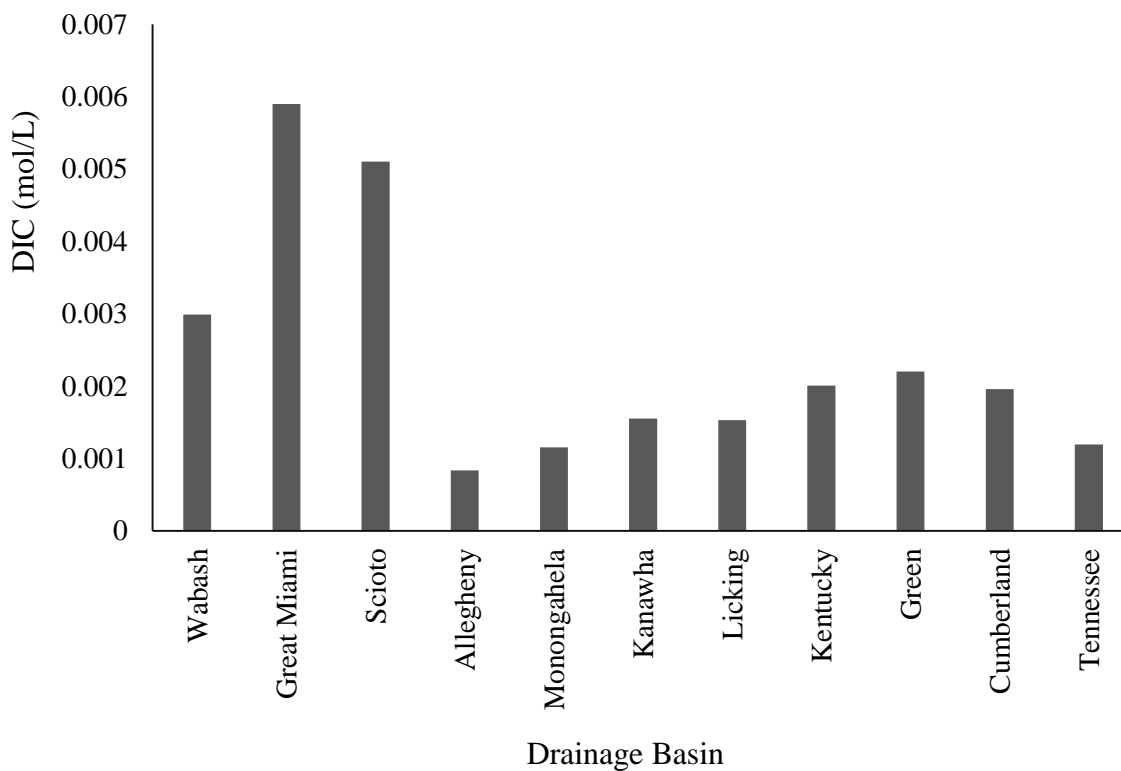


Figure 5.16. DIC for the major sub-basins of the Ohio River.

Source: Created by the author from KAWC (2016), KDOW (2016 a, b), USACE (2016a, b), USGS (2016a, b, c, d, e, f, g, h, I, j, k, l, m, n, o, p, q, r, s, t, u), and NOAA (2016) data.

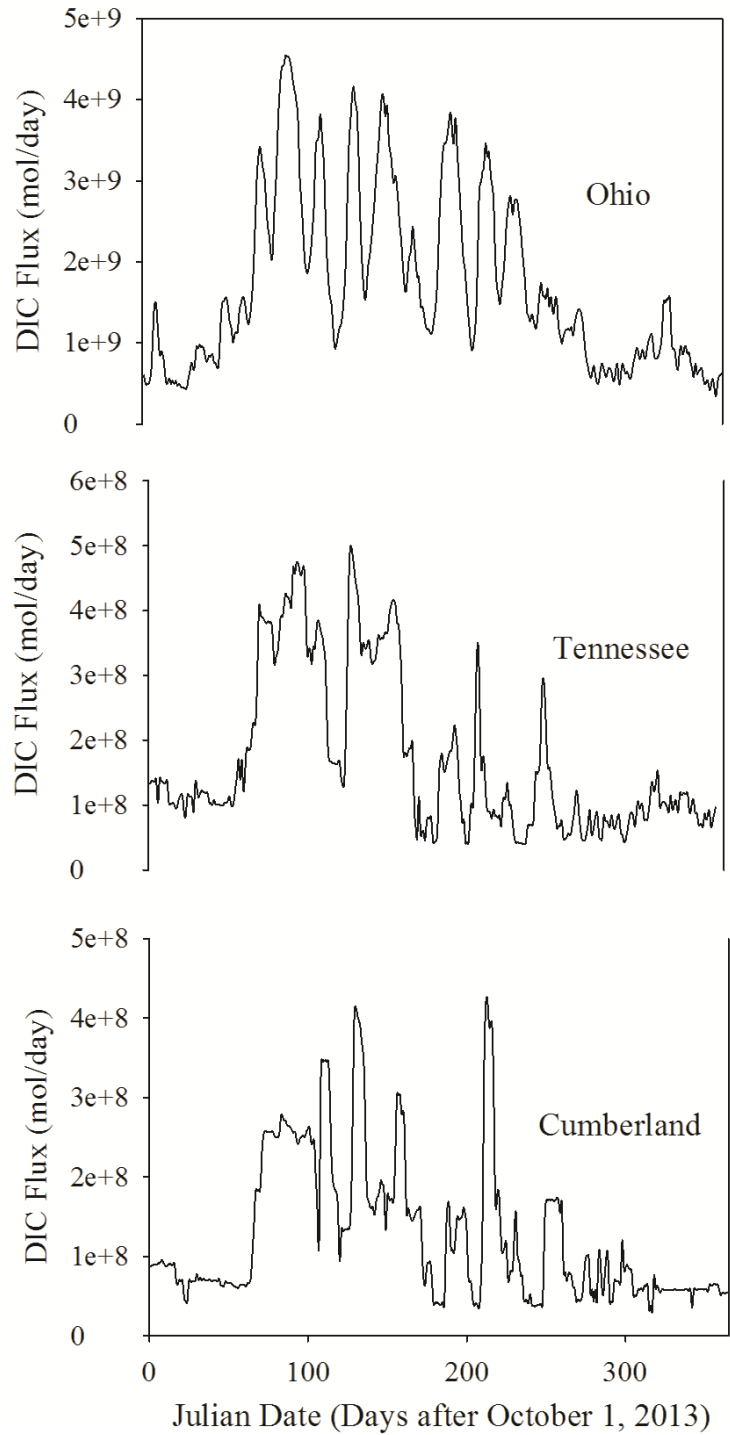


Figure 5.17. DIC flux for the Ohio, Tennessee, and Cumberland rivers. Source: Created by the author from IAWC (2016), USACE (2016a, b), USGS (2016e, s), and NOAA (2016) data.

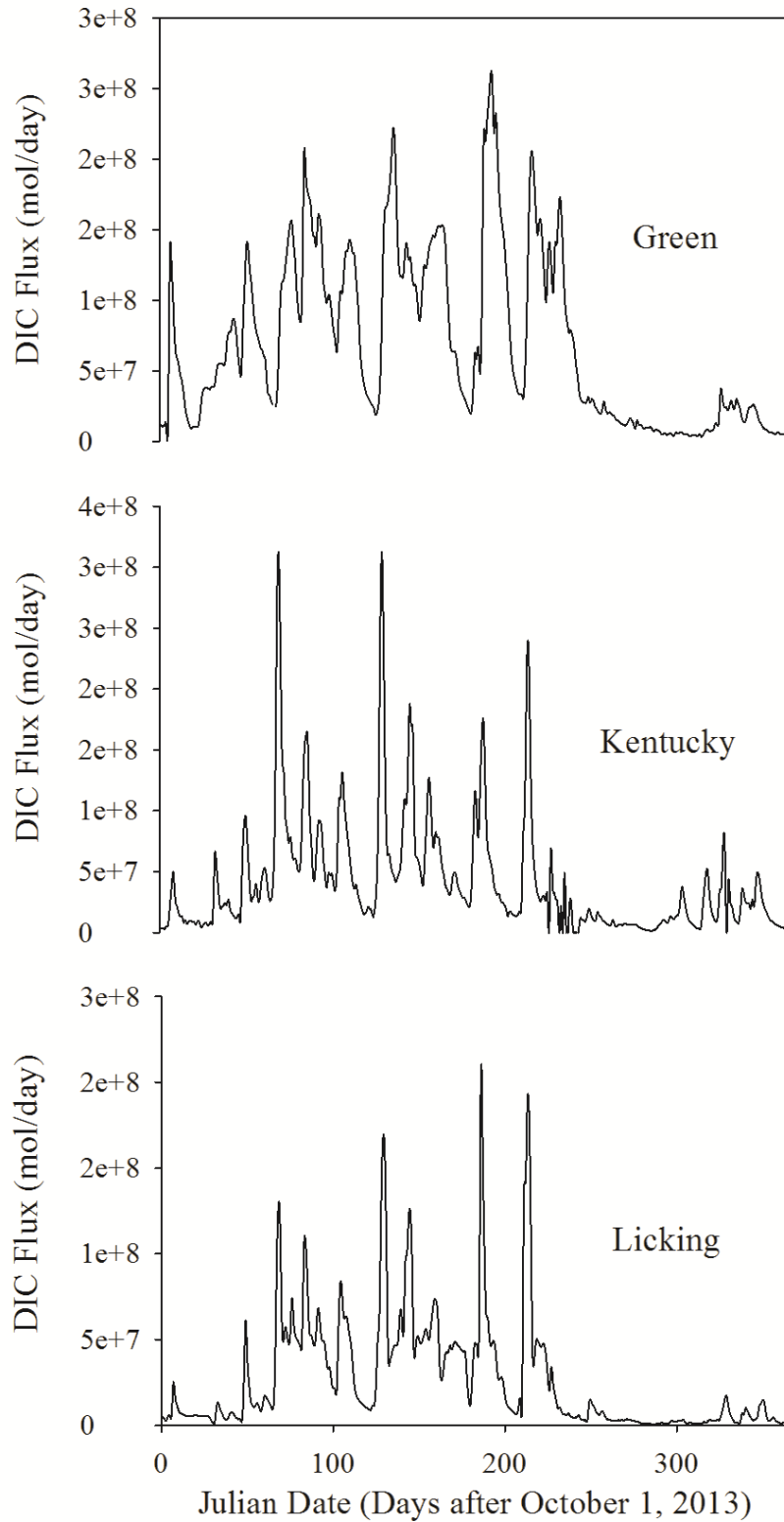


Figure 5.18. DIC flux for the Green, Kentucky, and Licking rivers.  
 Source: Created by the author from, KAWC (2016), KDOW (2016 a, b), USACE (2016a, b), USGS (2016m. h. p), and NOAA (2016) data.

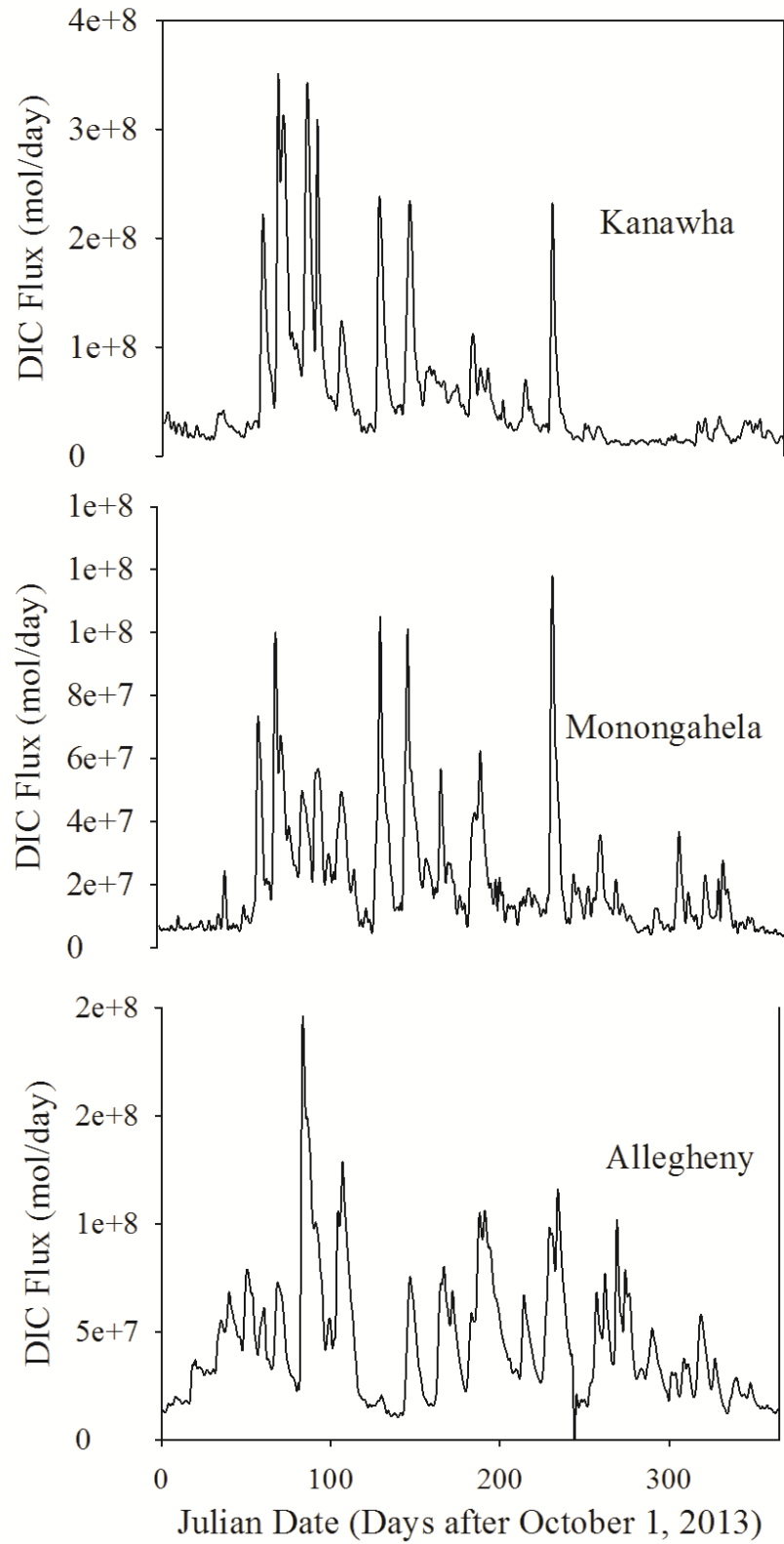


Figure 5.19. DIC flux for the Kanawha, Monongahela, and Allegheny rivers.  
 Source: Created by the author from, USGS (2016d, g, i, l, o), and NOAA (2016) data.

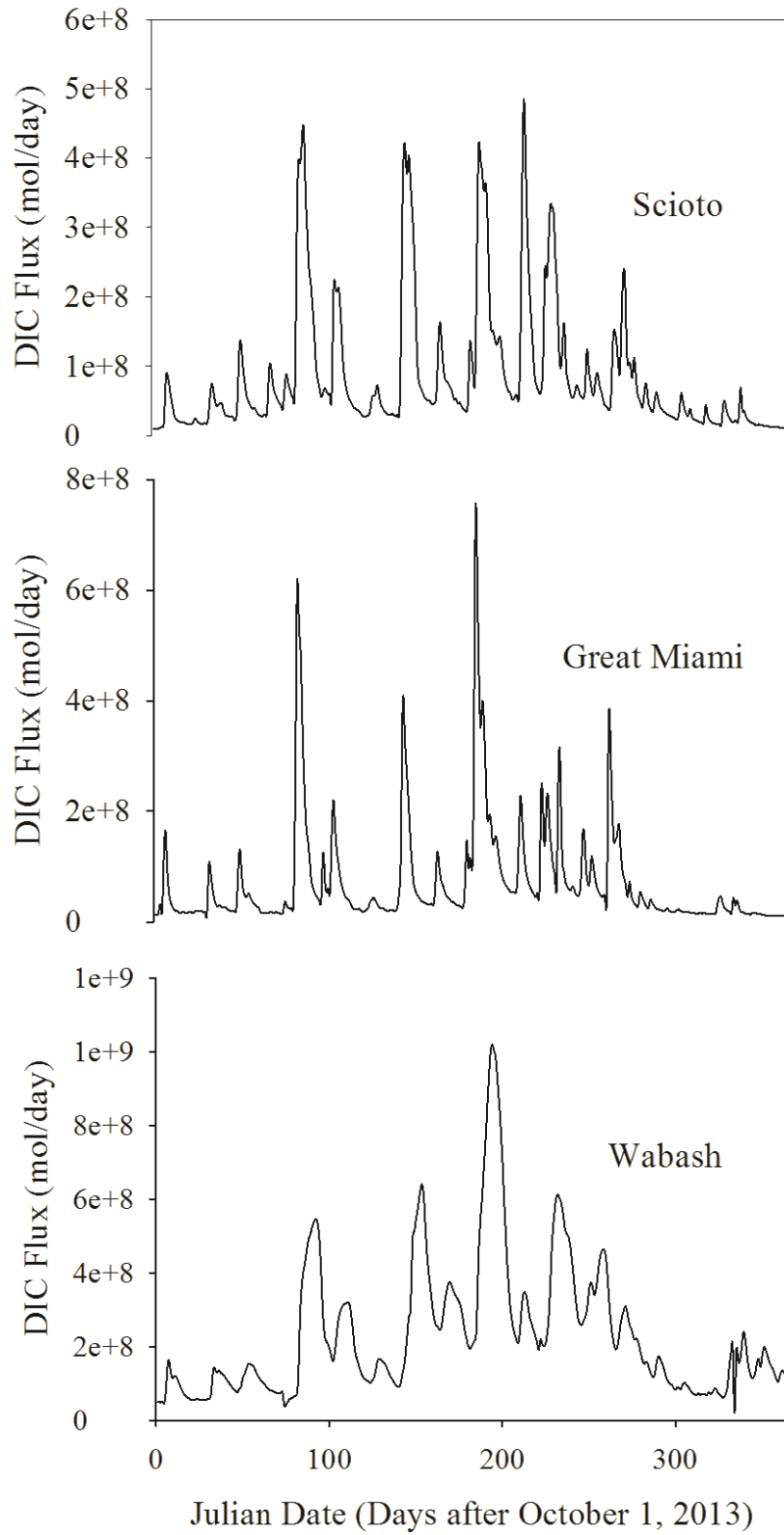


Figure 5.20. DIC flux for the Scioto, Great Miami, and Wabash rivers.  
 Source: Created by the author from USGS (2016f, j, k, m, u, t), and NOAA (2016) data.

## 5.6 Agreement Comparisons of Normalized DIC Flux

The main objective of the study was to evaluate the efficacy of the normalization technique involving time and volume of water available for carbonate dissolution to predict DIC flux with suitable precision to be applied at larger scales. Time and volume (where volume is the average depth of water of the area of carbonate rock for the basin) normalized DIC flux values for the Ohio River basin were estimated from existing data and evaluated against flux values obtained from the use of secondary hydrochemical and discharge data for the Barren River and Green River employed by Salley (2016). The use of time and volume normalization parameters attempts to account for the chief variables that affect DIC, without using discharge or water chemistry data, by establishing a statistical relationship between DIC flux and the time and volume of water available to the system. Agreement of normalized flux values, combined with a strong statistical correlation between flux and normalization parameters, would offer support to the hypothesis that time and volume are sufficient considerations for estimating DIC flux over large basins using climate and geologic data exclusively.

The normalized DIC flux for the Ohio River was estimated at  $3.36 \times 10^8 \text{ g C km}^{-3} \text{ day}^{-1}$  (grams of carbon per cubic kilometer of water, per day). Relative to previous estimates of  $5.61 \times 10^7 \text{ g C km}^{-3} \text{ day}^{-1}$  and  $7.43 \times 10^7 \text{ g C km}^{-3} \text{ day}^{-1}$  for the Barren and Green River (Salley, 2016), respectively, the Ohio River exports  $2.80 \times 10^8 \text{ g C km}^{-3} \text{ day}^{-1}$  more DIC than the Barren River and an additional  $2.62 \times 10^8 \text{ g C km}^{-3} \text{ day}^{-1}$  more DIC than the Green River. Normalized flux values for the Ohio River were not considered to be in close agreement with previous estimates of the Barren and Green River basins. The time-volume normalized DIC flux for the Ohio demonstrated 28.6% agreement with the

Barren River and 36.1% agreement with the normalized flux calculated for the Green River (Salley, 2016). This suggests that factors other than time and the final volume of water available to the carbonate system may account for over 70% error in the estimation of DIC flux.

Normalized flux values of the major sub-basins were also compared to normalized flux values calculated by Salley (2016) for the Green and Barren rivers. The normalized flux for the Cumberland River ( $1.13 \times 10^8 \text{ g C km}^{-3} \text{ day}^{-1}$ ) agreed 66.4% and 79.3% with the normalized flux for the Barren and Green Rivers, respectively. Normalized flux calculated for the Tennessee River ( $8.79 \times 10^7 \text{ g C km}^{-3} \text{ day}^{-1}$ ) agreed reasonably well with flux calculated for the Barren and Green Rivers (77.9% and 91.6% agreement, respectively). Comparison of the normalized flux from the Green River for WY 2014 ( $2.88 \times 10^8 \text{ g C km}^{-3} \text{ day}^{-1}$ ) compared to normalized flux for the Barren and Green rivers for WY 2013 did not yield results in close agreement (32.6% and 41% agreement, respectively). The normalized flux of the Kentucky River ( $2.34 \times 10^8 \text{ g C km}^{-3} \text{ day}^{-1}$ ) agreed 38.7% with the Barren River and agreed 48.2% with the normalized DIC flux of the Green River. The normalized flux for the Licking River ( $3.28 \times 10^8 \text{ g C km}^{-3} \text{ day}^{-1}$ ) exhibited only 29.2% agreement with the Barren River and 36.9% with the Green River. The normalized flux of the Monongahela River ( $2.50 \times 10^8 \text{ g C km}^{-3} \text{ day}^{-1}$ ) agreed 36.6% with the Barren River and 45.8% with the Green River. The Allegheny River normalized DIC flux ( $4.18 \times 10^8 \text{ g C km}^{-3} \text{ day}^{-1}$ ) was in poor agreement (23.7% and 30.2%) with the Barren and Green Rivers, respectively. Normalized flux values for the Kanawha, Scioto, Great Miami, and Wabash rivers exhibited very little agreement to

previous estimates of the Barren and Green Rivers, with less than 2% agreement for said basins.

The normalized values for DIC flux among the major sub-basins ranged from  $8.79 \times 10^7 \text{ g C day}^{-1}\text{km}^{-3}$ ) for the Tennessee River to  $1.22 \times 10^{11} \text{ g C km}^{-3} \text{ day}^{-1}$  for the Wabash River. Normalized flux values were compared between the Ohio River basin and the major sub-basins for WY 2014. In general, DIC flux of sub-basins containing substantial amounts of exposed carbonates (Tennessee, Cumberland, Green, Kentucky, Licking, Monongahela, and Allegheny) were in strong agreement with the DIC flux of the Ohio River basin, whereas basins with little or no near-surface carbonates (Wabash, Great Miami, Scioto, and Kanawha) yielded extremely poor agreement. The normalized DIC flux of the Cumberland River basin ( $1.13 \times 10^8 \text{ g C day}^{-1}\text{km}^{-3}$ ) exhibited 50.3% agreement with the Ohio River basin ( $3.36 \times 10^8 \text{ g C day}^{-1}\text{km}^{-3}$ ). The normalized flux for the Tennessee River basin ( $8.79 \times 10^7 \text{ g C day}^{-1}\text{km}^{-3}$ ) agreed 41.8% with the Ohio River basin. For the Green River basin, normalized flux ( $2.88 \times 10^8 \text{ g C day}^{-1}\text{km}^{-3}$ ) agreed 92.3% with the value estimated for the Ohio River basin. In the Kentucky River basin, normalized DIC flux ( $2.34 \times 10^8 \text{ g C day}^{-1}\text{km}^{-3}$ ) was found to be within 82.1% agreement of the Ohio River basin DIC flux. The Licking River basin flux ( $3.28 \times 10^8 \text{ g C day}^{-1}\text{km}^{-3}$ ) was in very close agreement (98.8 %) with the DIC flux from the Ohio River basin. The Monongahela River basin DIC flux ( $2.50 \times 10^8 \text{ g C day}^{-1}\text{km}^{-3}$ ) agreed 92.3% with the Ohio River basin. DIC flux estimated for the Allegheny River basin ( $4.18 \times 10^8 \text{ g C day}^{-1}\text{km}^{-3}$ ) agreed 89.1% with the Ohio River basin flux. DIC flux for the Great Miami River basin ( $3.46 \times 10^{10} \text{ g C day}^{-1}\text{km}^{-3}$ ) showed only 1.7% agreement with the Ohio River basin. Similarly, DIC flux in the Scioto River basin had just 1.5% agreement with the



flux from the Ohio River basin. The Wabash River basin normalized flux ( $1.22 \times 10^{11} \text{ g C day}^{-1}\text{km}^{-3}$ ) had virtually no agreement (0.30%) with the flux observed for the Ohio River basin. The Kanawha River basin was completely devoid of exposed carbonates and, as such, no normalization of DIC flux was possible to compare to the Ohio River basin, so it is considered to share zero agreement. Several possible explanations for this are discussed in the following section. Annual DIC flux, normalization parameters, and normalized flux values for the all basins evaluated are summarized in Table 5.2.

Lastly, the percent agreement of normalized DIC flux was compared among the major tributary basins of the Ohio River. Similar trends were observed as with comparisons of sub-basins with the Ohio River. Generally, high percentage agreement existed among the river basins that were represented by extensive carbonate surface geology; all normalized flux values were in at least 35% agreement, with all but four basins in 63% agreement. Basins with limited carbonate rock area were in moderate agreement with one another; all normalized flux values were in 44% agreement. Agreements were much weaker between the carbonate dominated basins and those with little exposed carbonates:  $\leq 3\%$  agreement.

The basins in closest agreement with respect to normalized DIC flux during WY 2014 included the Cumberland, Tennessee, Green, Licking, Kentucky, Monongahela, and Allegheny rivers. The normalized DIC flux from the Kentucky River was in 99.4% agreement with the flux in the Monongahela River, 91% with the Licking River, 71% with the Allegheny River, 55.3% with the Tennessee River, 1.1% with the Scioto River, 0.4% with the Wabash River, and 0.1% with the Great Miami River. The Licking River normalized flux was found to be in 9.6% agreement with the Monongahela River, 85.4%

with the Green River, 63% with the Allegheny, 62.8% with the Tennessee River, 1.7% with the Wabash River, 1.1% with the Great Miami River, and 0.9% with the Scioto River. The normalized DIC flux in the Cumberland River was in 88.3% agreement with the Green River, 87.5% with the Tennessee River, 74.1% with the Licking River, 65.9% with the Kentucky River, 65.3% with the Monongahela River, 42.6% with the Allegheny River, 0.7% with the Great Miami River, 0.6% with the Scioto, and 0.2% with the Wabash River. Normalized DIC flux for the Green River was in 76.7% agreement with the Kentucky River, 76.2% with the Tennessee River, 76.1% with the Monongahela River, 51% with the Allegheny River, 0.8% with the Great Miami River, 0.7% with the Scioto River and 0.2% with the Wabash River. For the Tennessee River, normalized flux was in 73.8% agreement with the Monongahela River, 34.8% with the Allegheny River, 0.5% with the Great Miami River, 0.4% with the Scioto River, and 0.1% with the Wabash River. The normalized DIC flux of the Monongahela River was in 71.6% agreement with the Allegheny River, 0.3% with the Great Miami River, 0.2% with the Scioto River, and 0.4% with the Wabash River. The normalized DIC flux for the Allegheny River agreed 2.6% with the Great Miami River, 2% with the Scioto River and 0.7% of the Wabash River basin. The normalized DIC flux of the Great Miami River was in 91.8% agreement with the Scioto River and in 44.2% agreement with the Wabash River. The normalized DIC flux of the Wabash and Scioto basins was in 50.1% agreement.

<b>Drainage Basin</b>	<b>DIC Flux (g C)</b>	<b>Total Area (km<sup>2</sup>)</b>	<b>Carbonate Rock Area (km<sup>2</sup>)</b>	<b>Percent Carbonate Area (%)</b>	<b>P-ET on Carbonate Rock (km)</b>
Wabash	1.15 x 10 <sup>12</sup>	84433.6	56.8	0.10	4.55 x 10 <sup>-4</sup>
Scioto	3.78 x 10 <sup>11</sup>	16679.5	55.6	0.30	4.56 x 10 <sup>-4</sup>
Great Miami	3.20 x 10 <sup>11</sup>	13804.6	52.9	0.40	4.78 x 10 <sup>-4</sup>
Allegheny	1.92 x 10 <sup>11</sup>	30043.8	2374.3	7.90	5.29 x 10 <sup>-4</sup>
Ohio	7.54 x 10 <sup>12</sup>	400, 901.0	120401.8	30.0	4.90 x 10 <sup>-4</sup>
Licking	1.19 x 10 <sup>11</sup>	9479.4	3353.0	35.4	5.06 x 10 <sup>-4</sup>
Green	3.00 x 10 <sup>11</sup>	23672.5	11506.1	48.6	5.00 x 10 <sup>-4</sup>
Monongahela	8.94 x 10 <sup>10</sup>	18932.8	2173.3	11.5	4.84 x 10 <sup>-4</sup>
Kentucky	1.92 x 10 <sup>11</sup>	17793.2	4415.4	24.8	5.10 x 10 <sup>-3</sup>
Cumberland	5.55 x 10 <sup>11</sup>	45842.8	25181.0	54.9	5.33 x 10 <sup>-4</sup>
Tennessee	7.49 x 10 <sup>11</sup>	245194.2	44308.6	18.1	5.27 x 10 <sup>-4</sup>
Kanawha	2.31 x 10 <sup>11</sup>	31597.8	0.00	0.0	0.00

Table 5.2. Summary table for the Ohio River and major sub-basins.

Source: Created by the author from Weary and Doctor (2014), NASA (2016), IAWC (2016), KAWC (2016), KDOW (2016 a, b), USACE (2016a, b), USGS (2016a, b, c, d, e, f, g, h, i, j, k, l, m, n, o, p, q, r, s, t, u), and NOAA (2016) data.

## 5.7 Statistical Correlation by Regression Analysis

The strength of the relationship between DIC flux and time-volume normalization parameters at various basin scales was tested using linear-regression analysis. Linear regressions evaluate the closeness of fit for a statistical model based on the variation of individual data points from the line of best fit to the entire data set. In regression,  $R^2$  coefficients are used to approximate the agreement of the regression line with the data. A model in which the line agrees perfectly with all points in a data set has an  $R^2$  value of 1.0, whereas no agreement between the line and the data points would yield an  $R^2$  value of 0.0 (Kleinbaum et al., 2013).

The Wabash, Great Miami, and Scioto sub-basins exhibit elevated normalized flux values relative to other basins evaluated. Here, the distribution of carbonate rocks is diffuse, with geology characterized by quaternary glacial deposits (e.g., Call, 1882; Thornbury, 1940; Ray, 1965). The Kanawha River basin was found to be entirely devoid of exposed carbonates, such that zero DIC flux is contributed by carbonate rock dissolution. To remove the influence of these basins, which were determined to be inappropriate for application of this technique, regression analysis was performed on a data sub-set that excluded the Wabash, Great Miami, Scioto, and Kanawha River basins. The remaining sub-basins (Tennessee, Cumberland, Green, Kentucky, Licking, Monongahela, and Allegheny) were considered to have significant amounts of exposed carbonates. When the regression treatment was applied to carbonate dominated sub-basins for WY 2014, a strong statistical correlation ( $R^2=0.97$ ,  $p = <0.001$ ) (Figure 5.21) was revealed.

## Sub-Basins with at least 8% Surface Carbonates Water Year 2014

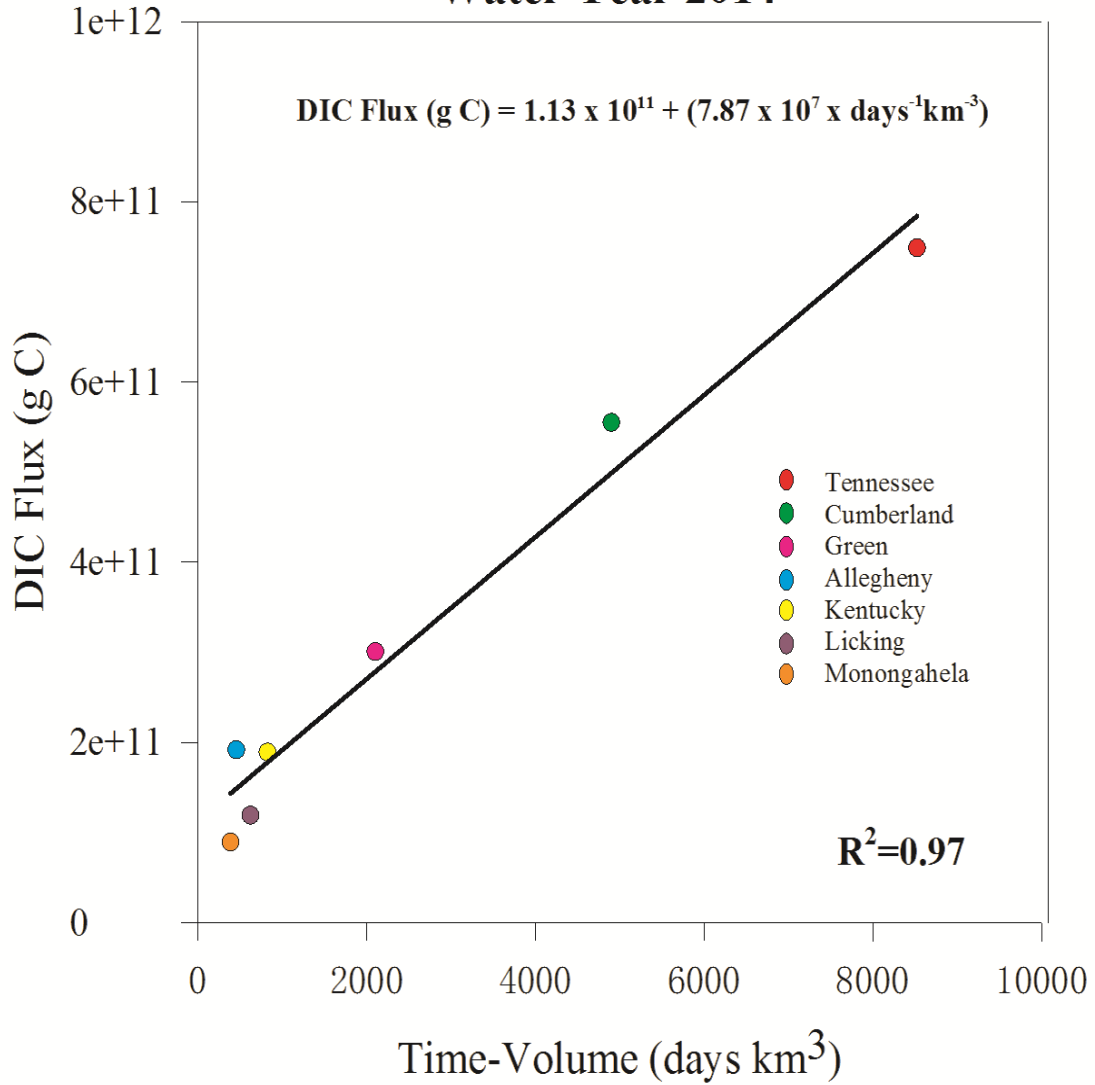


Figure 5.21. Regression analysis of DIC flux vs. time-volume for sub-basins, with  $\geq 8\%$  of total areas as carbonate outcrops.

Source: Created by the author from KAWC (2016), KDOW (2016 a, b), USACE (2016a, b), USGS (2016a, b, c, d, e, f, g, h, i, j, k, l, m, n, o, p, q, r, s, t, u), and NOAA (2016) data.

## 5.8 Magnitude of Atmospheric Carbon Sink by Carbonate Dissolution

The magnitude of the atmospheric sink from carbonate rock dissolution for the Ohio River basin was  $1.68 \times 10^8 \text{ g C km}^{-3} \text{ day}^{-1}$ , or one-half the normalized DIC flux. Recall that the atmospheric sink is considered as half the total flux for each basin because of the stoichiometric relationship described in Equation 5. For every two moles of carbon produced as bicarbonate, one mole was derived from the atmosphere as  $\text{CO}_2$  (this represents the atmospheric sink) and one mole was contributed from the rock as  $\text{CaCO}_3$ .

## 5.9 Influence of Hydrochemical Data Resolution on Flux Estimates

The influence of data resolution on DIC flux was evaluated in two ways: 1) comparison of flux values generated from fine and coarse resolution datasets obtained from different organizations conducting hydrochemical monitoring near the confluence of the Kentucky River with the Ohio, and 2) comparison of flux values calculated from high resolution data for the Green River collected by Osterhoudt (2014) to fluxes as calculated from lower resolution data for the Green River obtained from secondary sources as part of this study.

To test the usefulness of coarse resolution hydrochemical monitoring programs employed by treatment facilities, a pair of hydrochemical datasets collected from the Kentucky River were compared. The data represented high resolution daily monitoring for all of WY 2014 (KAWC, 2016) and a low resolution monthly dataset for the period March 26, 2014, through September 25, 2014 (KDOW, 2016b). The annual DIC flux for the Kentucky River basin calculated from the high-resolution KAWC (2016) data was  $1.92 \times 10^{11} \text{ g C year}^{-1}$ . The same calculation using the low-resolution Kentucky Division of Water (KDOW, 2016b) data yielded an annual flux of  $1.99 \times 10^{11} \text{ g C year}^{-1}$  for the

Kentucky River basin. The normalized flux calculated from the high-resolution dataset was equal to  $2.34 \times 10^8 \text{ g C km}^{-3} \text{ day}^{-1}$ , and the low-resolution data yielded a normalized flux of  $2.42 \text{ g C km}^{-3} \text{ day}^{-1}$ . The normalized flux values generated by the high and low-resolution datasets were in 98.2% agreement. The very close agreement of the normalized flux values for the Kentucky River derived from the high and low-resolution data suggests that lower resolution secondary data can be used with confidence, where high resolution direct measurement is unavailable. This is of substantial value, as in most cases it is not practical, economical, or desirable to make direct measurement for large basins or among many basins in an attempt to arrive at global flux estimates.

An attempt was also made to evaluate the difference in flux estimated from high resolution direct measurement techniques relative to lower resolution monitoring systems implemented at treatment facilities. Time-volume normalized DIC flux could not be used to evaluate agreement of normalized flux between high resolution hydrochemical measurements taken using data loggers (Osterhoudt, 2014) and existing chemical data from water treatment facilities along the Ohio River and major tributaries during this study. The flux values calculated from direct water chemistry measurements by Osterhoudt (2014) were normalized per time and area of carbonate rock, rather than time and volume, since the basins evaluated in the study were nested and considered to have received approximately equal precipitation. Moreover, the study period used by Osterhoudt (2014) represented flux values calculated between October 21, 2012, and January 27, 2013, rather than the Water Year 2014 (October 1, 2013, through September 30, 2014) used to study the Ohio River and its major sub-basins.

## Chapter 6. Discussion and Conclusions

### 6.1 Review of Research Objectives

The objectives of this study were as follows: 1) determine the magnitude of the inorganic carbon flux for the Ohio River basin; 2) evaluate whether the variables of area of carbonate rock outcrop, depth of P-ET, and duration of exposure (time) are suitable considerations in normalization of DIC flux for large drainage basins; and 3) assess the use of secondary hydrochemical data as effective alternatives to high resolution direct measurement techniques in estimating DIC flux among large basins. Several phases were necessary to satisfy this inquiry. Geologic maps and hydrologic data were assembled to delineate basin boundaries and represent the area of carbonate rock exposed within each basin. Climate data in the form of temperature and precipitation measurements were collected and used to calculate evapotranspiration (ET) and the final volume of water available for dissolution (P-ET) over the carbonate rock area. Secondary hydrochemical and discharge data were used in the calculation of DIC flux for each basin studied. Geologic and climate data were used in normalization of DIC flux calculations by time and volume of water free to participate in carbonate rock dissolution. The resulting normalized DIC flux values were compared to those of previous investigations employing similar techniques, and a statistical correlation was established with support from empirical evidence. The products of this study are summarized hereafter.

#### **1. What is the magnitude of the inorganic carbon flux for the Ohio River basin?**

The inorganic carbon flux for the Ohio River basin for Water Year 2014 (October 1, 2013, through September 30, 2014) normalized by time and volume of water available was estimated at  $3.36 \times 10^8 \text{ g C km}^{-3} \text{ day}^{-1}$ .



**2. Are the variables of area of carbonate rock outcrop, depth of P-ET, and duration of exposure (time) suitable considerations in normalization of DIC flux for large drainage basins?**

The proposed normalization factors appear to be effective when applied to drainage basins that display even modest percentages (in this study, over about 8%) of exposed carbonate rock relative to total basin area. The basins that displayed minimal percentages of exposed carbonates (<1%) exhibited normalized flux values that were significantly unlike those of the rest of the data set and these were considered outliers. Alkaline waters characterize the Wabash, Great Miami, Scioto, and Kanawha rivers despite the minimal presence, and in some cases absence, of exposed carbonate rocks. Other sources of alkalinity are present in these rivers, implying that the geologic and climatic data used herein may not capture effectively the major controls on DIC flux for these basins. Other considerations such as land use, soil type, sub-surfaced carbonates, biological activity, and silicate weathering may become increasingly important in such environments. As such, the method is not appropriate for use in basins where the percent of carbonate outcrop area is <1% and should be excluded from future analysis. When the Wabash, Great Miami, Scioto, and Kanawha river basins were excluded from the dataset used in regression analysis, a strong agreement existed. Sub-basins where carbonate rocks made up  $\geq 7.9\%$  of the total drainage area during WY 2014 yielded a regression coefficient that indicated a strongly positive correlation ( $R^2 = 0.97$ ,  $p = <0.001$ ). These findings suggest that model error may increase with decreasing area of carbonate rock present in a basin. Thus, the use of geologic and climate data to predict DIC flux appears to be successful among basins where carbonate rocks represent as little as 7.9% of the total basin area, but is not effective where carbonate rocks make up less than 1%. The

true threshold for model success relative to exposed carbonates could be even less, since none of the basins involved in the study contained percentages of carbonate rock between 1% and ~8%.

**3. Does the use of secondary water chemistry data appear to be as effective in determining carbon flux as similar methods employing high resolution measurements?**

A general difficulty associated with the use of existing hydrochemical data from treatment facilities is resolution. Many of the facilities do not maintain regular sampling programs. In most instances, bi-monthly or quarterly sampling represented the highest resolution chemistry data available for the rivers evaluated. The coarseness of such data may result in DIC flux estimates that over- or under-estimate the actual flux. Data gaps due to equipment failure or environmental conditions in coarse resolution hydrochemical data are also problematic. The use of low resolution water chemistry data where other sources of hydrochemical data are absent may explain variable percent agreements of normalized flux among basins evaluated in this study compared to the Green and Barren basins (Osterhoudt, 2014; Salley, 2016).

To account for the irregular frequency and data gaps, measurements were aggregated to represent daily conditions. This becomes a somewhat subjective process as the investigator must assign a limited number of sample values to an entire water year of discharge data to calculate DIC flux. For example, if sampling was conducted on a bi-monthly basis, the same input values for pH, temperature, and alkalinity must be used for every day of the two-month period. This results in generalization and a loss of the variation occurring over time scales less than two months. However, this is of less concern, as discharge has been shown to vary more considerably, whereas variables such

as pH, temperature, and alkalinity are relatively consistent throughout time and are largely controlled by discharge (Groves and Meiman, 2005), such that variation occurring over shorter timescales is not substantially dampened by use of aggregated water chemistry data. Furthermore, normalized flux values for the Kentucky River produced from high resolution monitoring data, and those calculated using coarse resolution data that was aggregated to match daily discharge measurements, showed very close agreement (98%) in flux values. This lends additional support to the use of secondary hydrochemical data in investigations at larger scales.

As discussed, comparison of time-volume normalized flux estimates generated from high resolution measurements versus lower resolution scales employed by water treatment facilities was not possible. This was a consequence of the fact that DIC flux values estimated from high resolution data logger measurements reported by Osterhoudt (2014) were normalized by time and area of exposed carbonate rock. A sub-set of data for the Green River was restricted to the period of study for Osterhoudt (2014) (October 21, 2012, to January 27, 2013) and normalized by time and area of carbonate rock yielding moderate (46% agreement).

The difference in flux values calculated for the Green River through use of existing hydrochemical data versus the flux calculated from high resolution data by Osterhoudt (2014) may expose the potential limitations associated with the method. The moderate agreement among normalized flux values for the Green River should be interpreted with caution. One consideration associated with this observance involves the location at which hydrochemical measurements were taken. The data used for this study were obtained very near to the outlet of the Green River with the Ohio at Livermore, KY.

By contrast, the hydrochemical measurements of the Green River taken by Osterhoudt (2014) were obtained several kilometers upstream at Munfordville, KY. The chemical signatures of the water near the outlet of the Green River capture alkalinity contributed from the carbonate geology downstream of Munfordville and may provide a more holistic estimate of total DIC flux for the Green River. However, it should also be noted that the area of exposed carbonates is correspondingly larger for the basin upstream of Livermore, KY, compared to the area of carbonates contributing alkalinity upstream of Munfordville, KY. Normalized flux values represent the ratio of total DIC flux to exposed carbonates and time. Therefore, if time is held constant, increases in total DIC flux based on monitoring location should be accounted for in the normalization process. Accordingly, differences in monitoring points and area of exposed carbonates prove inadequate in justifying the difference in time-area normalized flux. Variation in precipitation, contributing to enhanced carbonate dissolution for the period of interest during 2012-2013 compared to the same period evaluated in 2013-2014, is likely of greater consequence in the observed difference in time-area normalized flux.

At present, the degree of confidence in using secondary hydrochemical data in lieu of high resolution measurements to predict DIC flux remains uncertain. Although comparisons of fine versus coarse resolution within the same basin and year yielded normalized flux values in very close agreement, the “fine” resolution data represent only daily measurement frequency and are less comprehensive than more frequent measurements taken via data loggers, which can be on the scale of minutes or even seconds. Similarly, although time-area normalized flux values for the Green River for the period October 21 to January 27 differed between 2012-2013 and 2013-2014 and were

only in moderate agreement, water availability is not accounted for and this may alter the agreement. It is recommended that high resolution hydrochemical data be collected for the Green River (or other major sub-basins) representing an entire hydrologic year. This would allow DIC flux to be normalized by time and volume of water available for carbonate rock dissolution. This value could then be directly compared against time-volume normalized flux estimates generated from publicly available hydrochemical data to evaluate the true usefulness of secondary data in making estimates of DIC flux.

## 6.2 Discussion

This evaluation of the time-volume normalization technique has identified some fundamental limitations associated with implementing this technique over large scales. Most significant are the following requirements: 1) a large area of exposed carbonate minerals in basin ( $\geq 8\%$  of total surface area), and 2) all variables used in the normalization parameters must represent positive values.

There appears to be a threshold controlling the effectiveness of the model in predicting DIC flux using time-volume normalization parameters that is directly related to the carbonate surface area in the basin. All the drainage basins assessed in the study exported significant quantities of DIC, including the basins with little or no surface carbonates. The basins evaluated by this study can be assigned to one of three categories, which are characterized by the distribution of surface carbonates: 1) those in which carbonate rocks dominate surface geology, 2) those that display minimal areas of exposed carbonates, and 3) those that exhibit zero exposed carbonates. The first category is represented by the Ohio, Tennessee, Cumberland, Green, Kentucky, Licking, Monongahela, and Allegheny drainages, where carbonate rocks compose substantial

areas of the surface geology ( $\geq 7.9\%$ ). The second category contains the Wabash, Great Miami, and Scioto drainages where carbonates are present in limited areas ( $< 1\%$ ). The Kanawha River is assigned to the third category, as it contains no mapped surface carbonates (0%). DIC was observed to vary considerably between these categories. In general, the basins exhibiting appreciable areas of surface carbonates yielded DIC flux values in good agreement ( $R^2 \geq 0.90$ ). However, when basins with limited area of surface carbonates were included with the basins where carbonates dominate surface geology, the similarities in DIC flux were decoupled ( $R^2 \leq 0.15$ ). These basins include the Wabash, Great Miami, and Scioto drainages.

Positive values for carbonate rock area and depth of water available for dissolution during the period of interest are critical to the success of the model in predicting DIC flux. If either carbonate rock area or depth of P-ET equal zero, it is not possible to normalize existing flux, as dividing by zero renders an undefined quantity. It follows that under these circumstances it is not possible to establish a mathematical relationship to enable future predictions of flux based on correlation of DIC flux to geologic and climatic data. This was evidenced during examination of the DIC flux coming from the Kanawha basin, where a total absence of exposed carbonates resulted in the inability to normalize the DIC exported from the basin. Similar constraints may become apparent as the method is applied over shorter periods where water lost to evapotranspiration exceeds rainfall, rendering zero water available for the dissolution of carbonate rocks that would otherwise contribute alkalinity to streams. Over longer periods an assumption is made that the change in water storage over extended periods is equal to zero. This assumption may not hold true over shorter time periods.

Both area of carbonate rock and water availability are important controls on the drawdown of atmospheric carbon by carbonate mineral weathering, and the extent to which each influences DIC flux is mutually dependent. For example, under circumstances where more water is lost to evapotranspiration processes than is contributed by rainfall, no water is available for the dissolution of carbonate rocks. Thus, even if large areas of carbonate rocks are exposed within a basin, the absence of water availability results in a scenario where no carbon is removed from the atmosphere through interactions of acidified water with carbonate minerals. Likewise, under conditions where rainfall exceeds ET, there may be no atmospheric carbon flux if there are no exposed carbonate minerals over the area where the precipitation occurred. Therefore, DIC flux cannot be approximated from existing geologic and climate data in basins where any one of the normalization parameters equals zero, using the proposed technique.

While other sources of alkalinity exist in river systems, a fundamental assumption associated with this research is that carbonate species dominate in natural waters (Drever, 1988). A secondary assumption is that the primary mechanism by which carbonates contribute alkalinity to surface waters occurs through interactions of chemically aggressive waters from rainfall and channel storage with surface carbonates that are in contact with these solutions. For basins where surface carbonates are diffuse, this assumption may prove to be invalid. Other factors, such as the contribution of alkalinity from baseflow, may be more influential in controlling the chemical signature of surface waters among basins where exposed carbonate geology is minimal. Interactions of groundwater in the phreatic zone with carbonate bedrock is one mechanism by which

baseflow to stream channels may impart carbonate alkalinity to surface waters. Further investigation is needed to compare the hydrochemical signatures of groundwater to those observed for surface streams among said basins.

DIC flux can be described in terms of the proposed primary (time, area of carbonates, P-ET depth) and secondary (soil type, land use, weathering of silicates, island basalts, and unconsolidated carbonates, etc.) variables affecting DIC flux ( $y$ ), given as:

$$(y = x + \mu) \quad (22)$$

where  $x$  represents time-volume normalization parameters and  $\mu$  represents the myriad other variables that may influence DIC flux from a given basin. In basins where the percentage of carbonate rock area and value of P-ET are high, the value of  $x$  is large and  $y$  is small by comparison. Under these conditions, the normalization parameters of time, carbonate rock area, and P-ET are effective in generating reliable estimates of DIC flux. Alternatively, among basins where the percentage of carbonate rock area and value of P-ET is low, the value of  $x$  is small relative to  $y$ . Here, the normalization parameters are unable to capture accurately the nature of the primary influences that control the DIC flux in a basin and are not recommended for use in making direct estimation of flux.

A significant challenge associated with the normalization procedure used for this study is represented by DIC contributions from rocks that are not included on maps of carbonate outcrops. Some examples include: 1) calcium-rich loess deposits, 2) calcium and magnesium-rich lacustrine facies, 3) thin surface carbonates, 4) grain replacement in non-carbonate rocks by carbonate minerals found in calcite cements, 5) contributions of alkalinity from carbonates in the subsurface, and 6) calcite grains in stream bedload. The existence of calcium and carbonate sources of DIC beyond the mapped carbonate



bedrock given by the Weary and Doctor (2014) is an especially important consideration for DIC flux of the Wabash, Great Miami, Scioto, and Kanawha river basins. The sparse distribution of exposed carbonate bedrocks relative to substantial DIC flux issuing from said basins results in over-estimation of the normalized flux value. As such, it is recommended that maps of bedrock and Quaternary geology be used to supplement maps of carbonate geology in regions where exposed carbonate bedrock does not represent the surface geology. Although assigning area to calcite cements and bedload grains is not a feasible task, inclusion of Quaternary and bedrock carbonates would designate area to bedrock and unconsolidated sediments that are high in sources of alkalinity. By incorporating area occupied by these other sources with the area taken from maps of bedrock geology, the value of the normalized flux would likely be reduced. This would bring the normalized flux values for the basins in discussion in closer agreement with the flux from basins draining regions where extensive karst development dominates surface geology.

Differential weathering patterns, and contributions to DIC flux, among various rock types are also important factors that may complicate the accuracy of the proposed model. These variables affect thermodynamic and kinetic reaction drivers. For example, among carbonates, the solubility product of calcite is not equivalent to dolomite or calcite cements that may replace grains of a host mineral, such as sandstone. The presence of impure and interbedded carbonates presents further difficulty, as weathering rates and solubility are highly variable among such stratigraphic units. Furthermore, caution should be exercised in assigning the source of DIC in rivers. Other rock types, in addition to carbonates, have been extensively studied for their ability to function as a sink of

atmospheric C. Weathering of silicate minerals over vast areas is believed to contribute substantially to the C sink (Garziona, 2008; Li and Elderfield, 2013). More inclusive models used to estimate the C flux between the atmosphere and terrestrial reservoirs would be well served to expand considerations beyond solely examining the influence of carbonate-mineral weathering of DIC flux.

Of interest is the comparatively large DIC flux sourced from the Wabash, Great Miami, Scioto, and Kanawha river basins. Despite the elevated DIC flux observed in this region, exposed carbonate rocks represent very little of the surface geology. This suggests that other sources of alkalinity must be present in the system. Natural waters carry the chemical signature of the geologic materials with which they interact, and it is appropriate to consider geologic contributors of alkalinity aside from mapped surface carbonates. The research design of this project relied on maps of surface geology; however, it is worthy of consideration that, in many cases, massive areas of carbonate bedrock underlay mapped surface deposits and supply alkalinity to rivers through baseflow. The DIC contribution from sub-surface carbonates is undoubtedly reflected in the chemical signature of the water, yet the area representing these deposits is not included in carbonate outcrop area used in flux normalization for this investigation. A special case of this is observed among the Wabash, Great Miami, and Scioto basins, where glacial sediments form a thick covering over carbonate bedrocks (Ray, 1965, 1974; Thompson et al., 2016). Normalized flux values among the Wabash, Great Miami, and Scioto drainages exceeded that of all other basins, including the Ohio basin, by two orders of magnitude. Possible explanations for these observations represent an array of

topics including thermodynamic, kinetic, geologic, biologic, climate-driven feedback systems, weathering of silicates, soil type, and land-use practices.

DIC flux for the Kanawha River cannot be normalized per the parameters defined in this model since no exposed carbonates were present to act as a source of the observed DIC flux from the drainage basin. To evaluate if unmapped sources of DIC flux from carbonate minerals exist in the Kanawha basin, several approaches were applied. The first was to examine state geologic maps of West Virginia, where the Kanawha basin is located, and compare it to the Weary and Doctor (2014) U.S. karst map to determine if any areas of carbonates were not included in the more generalized atlas. The Federal Energy Regulatory Committee (FERC, 2016) conducted field geologic surveys as part of the environmental impact statement for the proposed Atlantic Coast Pipeline and indicated over twenty square miles of surface carbonates in Virginia that were not identified on the map produced by Weary and Doctor (2014). It was thought that perhaps a similar circumstance might exist for regions of the Kanawha Basin. A more detailed state geologic map was acquired from the West Virginia Geology and Economic Survey (WVGES, 1968). Comparison of the state-level geologic map to the U.S. karst map failed to identify any areas of surface carbonate rocks that were not included on the map by Weary and Doctor (2014). The second attempt to account for the observed DIC flux issuing from the Kanawha basin involved examination of the physiographic provinces encompassed by the Kanawha basin to determine whether the basin extended into the Valley and Ridge Province of the Appalachian Mountains, where limestone units could be exposed among folded rocks. Figure 6.1 demonstrates that the Kanawha basin is located entirely within Appalachian plateaus, which are predominantly composed of

clastic rocks (USGS, 2016k). As a final check, the geologic maps were revisited, this time for examination of the geologic groups present within the various units in the Kanawha basin. The Conemaugh, Dunkard, Monongahela, and Pottsville groups are present in the geologic units of the Kanawha River basin (Figure 6.2). The Conemaugh Group contains cyclic sequences of red and gray shale, siltstone, and sandstone, with thin limestones and coals. The Conemaugh Group includes the Ames and Brush Creek Limestones. The Dunkard Group represents sequences of sandstone, siltstone, red and gray shale, limestone, and coal, and also includes Washington Formation limestones. The Monongahela Group represents cyclic sequences of sandstone, siltstone, red and gray shale, limestone, and coal, but no major limestone formations. The Pottsville Group is predominantly composed of sandstones, with thin shales and coals, and an absence of limestones. Considering the geologic units present within the Kanawha basin, it appears that the Dunkard and Conemaugh groups are best-suited as potential contributors of the DIC flux observed in the Kanawha River basin.

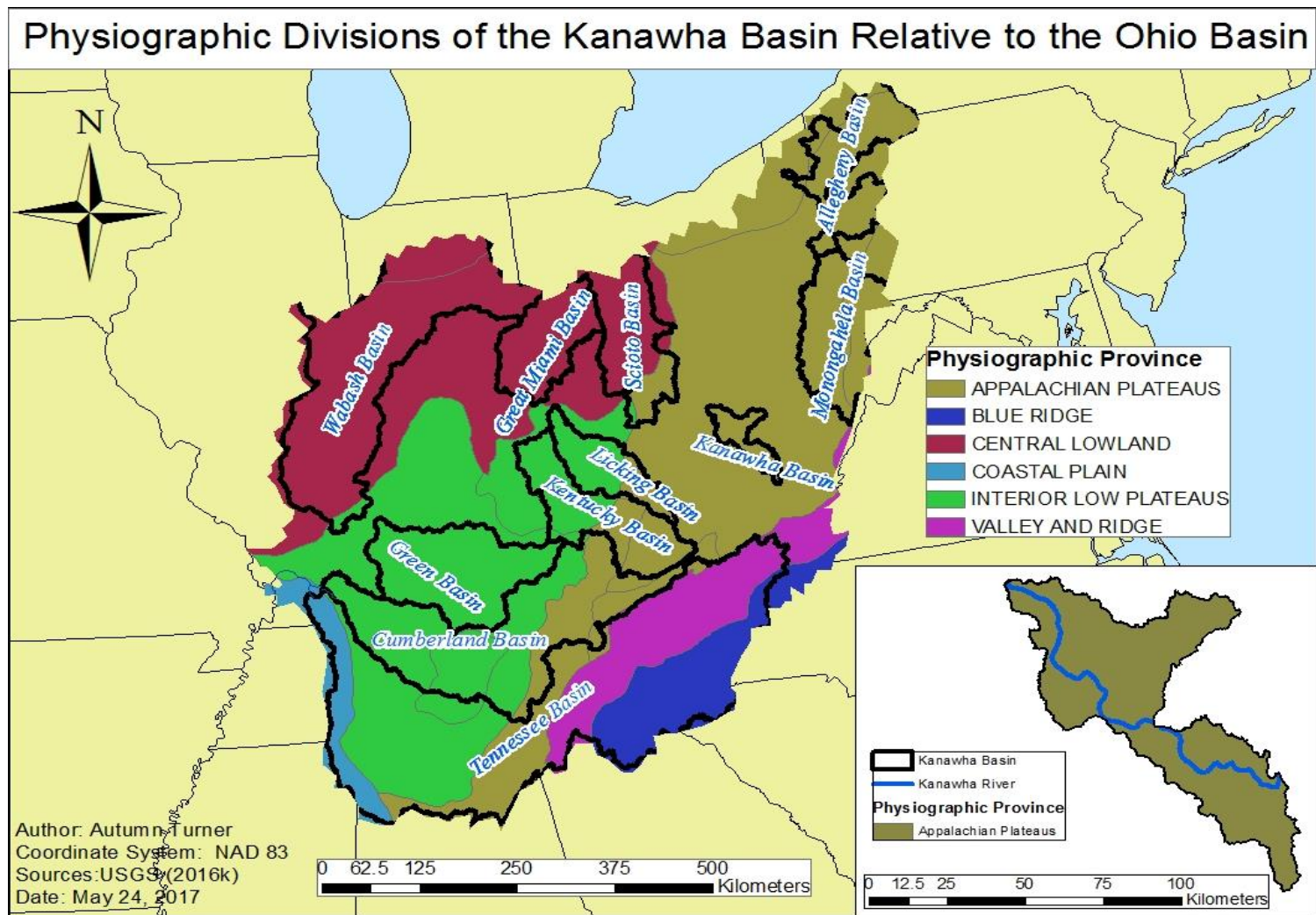


Figure 6.1. Physiographic provinces of the Ohio River basin. Inset: the Kanawha Basin is entirely within the Appalachian Plateaus physiographic province. Source: Created by the author from (USGS, 2016k) data.

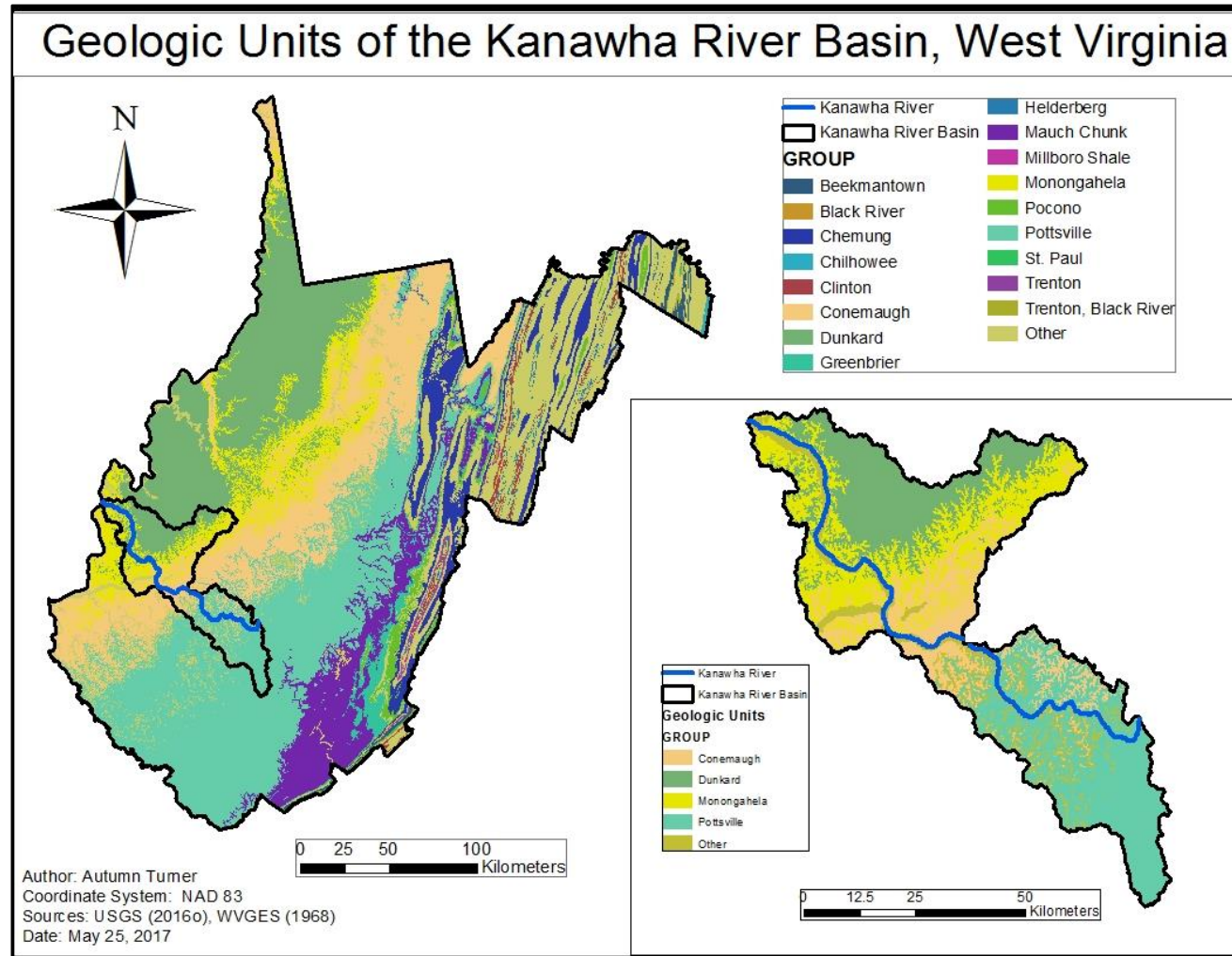


Figure 6.2. Groups represented by the geologic units of West Virginia. Inset: the Kanawha River Basin contains the Conemaugh, Dunkard, Monongahela, and Pottsville groups.

Source: Created by the author from USGS (2016o) and WVGES (1968) data.

### 6.3 Future Work

From the onset, this work has aimed to evaluate whether the described parameters of time, carbonate outcrop area, and depth of P-ET were sufficient considerations for producing acceptable approximations of DIC flux. The example drawn from the formerly glaciated basins presents the complexity that incorporation of unconsolidated material and subsurface carbonate area may be necessary among river systems where alkalinity is high but surface carbonate deposits are not well-represented. Identifying the need to include additional geologic data is an important step in understanding the model's limits as presently described. It also highlights opportunities by which the applied methodology can be refined to produce estimates in closer agreement. Subsequent evaluations may choose to account for areas of sub-surface carbonates to improve the accuracy of estimates produced using this model. In basins where carbonate rocks are present to a lesser degree, considerations such as carbonate mineral type and purity, weathering of silicates, vegetation, microbial activity, organic acids, soil type, land-use practices, and climate-driven feedback systems may necessitate a broader approach to fully understand the C sink from terrestrial weathering processes.

The scope of this project was concerned with the possibility of estimating atmospheric carbon flux from carbonate mineral weathering as a function of time, area of carbonate rock outcrop, and the amount of water available for mineral dissolution. In reality, carbonate mineral weathering is a function of numerous processes that collectively influence the amount of DIC exported from a drainage basin. This work is a first pass at attempting to decipher which processes exert the greatest influence on carbonate weathering and how knowledge of these might be used to predict DIC flux

without the use of hydrochemical data. The limitations identified in using this technique, particularly among basins that exhibit sparse or non-existent areas of carbonate rocks on the surface, highlight the potential for continued work.

Future efforts to refine this work may evaluate the influence of other sources of alkalinity and determine whether inclusion of these variables would render an improved representation of the DIC flux for large drainage basins. More complete characterizations of carbonate geology are needed to better account for the area of carbonates that contributes to the DIC measured in streams. The accuracy of the model in predicting DIC flux from large basins would likely be improved by inclusion of carbonates represented by Quaternary and bedrock geology. This allows for better accounting of areas that are not classified as surface carbonates, but which act as a source of carbonate alkalinity to rivers. Incorporation of areas covered by unconsolidated sediments rich in calcium and known to contain abundant calcite concretions should expand the normalization parameters to include additional areas of geological materials that influence alkalinity and, therefore, DIC flux from a basin. Likewise, the massive areas of carbonate bedrock, such as those buried by glacial deposits in the northern region of the Ohio Basin, are also sources of alkalinity. This area should be reflected in the refined normalization parameters of the model. The nature of carbonate rocks present in a basin should be considered as well, including solubility properties and weathering rates associated with different minerals types. An array of opportunities exists for attempts to account for the myriad variables that influence weathering rates that control the DIC flux observed from river basins, and these deserve inclusion in on-going studies. Testing of the procedure over shorter intervals is suggested to evaluate the influence of changes in water storage



observable over abbreviated temporal scales that are dampened over longer periods. Additional study is recommended to better assess the strength of the relationship between DIC flux and the exposure time and volume of water available for dissolution. In continued efforts to validate this method, DIC flux should be estimated for other large basins using the described methods and compared to the estimates of the Ohio Basin and its major tributaries presented herein and to those given by Osterhoudt (2014) and Salley (2016) for the Green and Barren river basins.

#### 6.4 Conclusion

In conclusion, the purpose of this investigation was to evaluate a method for estimating the atmospheric carbon sink due to carbonate rock dissolution as a function of time, carbonate rock area, and water availability. While numerous processes contribute to the DIC flux patterns observed among river basins, it is important to recall that the objective of this work was to determine whether DIC flux could be approximated from a set of prevailing variables, such that other considerations were minor in comparison and would not require inclusion in the model. To attempt to account for every influence on carbonate mineral weathering would undermine the goal of arriving at a set of primary controls that contribute the majority of the observed DIC removed from large river basins. The investigation concluded that time, area of carbonate rock, and the amount of water available for dissolution are a good representation of the major influences on DIC exported from river basins where large areas of carbonate bedrock is exposed at the surface. However, these parameters fail to capture the primary controls on DIC flux from carbonate weathering in basins that lack substantial carbonate outcrops. As implemented, the method appears to have some limitations among basins where DIC flux is contributed

from sources aside from mapped surface carbonate rocks (e.g., loess and lacustrine deposits, calcite concretions and nodules, sub-surface carbonates, biological inputs). This deficiency is predicted to be amended by inclusion of additional carbonate area represented by carbonate bedrock and calcium-rich Quaternary deposits. There are also inherent constraints on the use of this technique. For instance, the procedure is not suitable for use during periods where ET exceeds rainfall, leaving no balance of water available for carbonate dissolution, or in basins that are completely devoid of carbonate minerals.

Based on these findings, it appears DIC flux can be reliably estimated from geologic and climate data for large river basins where carbonate rocks contribute the primary source of alkalinity without the direct use of hydrochemical data. The strong correlation between DIC flux and time-volume normalization parameters among the basins that contain substantial amounts of exposed carbonates gives positive cause to continue exploring and refining this technique. The strength of the relationship ( $R^2=0.97$ ,  $p < 0.001$ ) suggests that, for basins with abundant surface carbonates, the primary variables influencing DIC flux are captured by the model. On the contrary, in basins that lack large areas of surface carbonates, time, area, and water availability fail to capture the major events contributing to DIC flux. The observance of elevated DIC flux for the Wabash, Great Miami, and Scioto rivers, which lack significant amounts of carbonates in the respective drainages, suggests that additional factors contribute to this alkalinity that are not accounted for in the current version of the model. Recognition of this threshold has improved knowledge of the sensitivity of the model to geologic environments that are not well-characterized by karst terrain, but which may possess other forms of carbonate

minerals. Identifying the need to expand the geologic aspects of the normalization procedure, particularly in regard to accounting for true areas of carbonate rocks contributing alkalinity, reveals how the model might be improved so that it is less limited by geologic considerations.

When applied to basins where carbonate outcrops dominate surface geology, these methods circumvent the need to collect hydrochemical data to make estimates of DIC flux from carbonate mineral weathering. By eliminating the labor-intensive work associated with hydrochemical sampling regimes, this procedure drastically increases the efficiency and lowers the cost of estimating an important component of carbon flux between the atmospheric, terrestrial, and, ultimately, oceanic carbon reservoirs. The importance of continuing exploration along these lines is reinforced by the fact that surface carbonates constitute approximately 20 percent of the Earth's surface, and the amount of carbon drawdown from the atmosphere through this process may be vast. The ability to estimate DIC flux for large, potentially global scales, promotes the capacity for more informed decision-making as society seeks to understand and control carbon-driven climate change and the associated feedback mechanisms that pose challenges to human and environmental health.

## REFERENCES

- Abell, R.A., Olson, D.M., Dinerstein, E., Hurley, P.T., Diggs, T., Eichbaum, W., Walters, S., Wettengel, W., Allnut, T., Loucks, C.J., Hedao, P. (2000). *Freshwater Ecoregions of North America: A Conservation Assessment*. Washington, D.C.: Island Press.
- Amiotte Suchet, P., Probst, J.L. (1995). A global model for present-day atmospheric/soil CO<sub>2</sub> consumption by chemical erosion of continental rocks (GEM\_CO2). *Tellus* 47B: 273-280.
- Amiotte Suchet, P., Probst, J.L., Ludwig, W. (2003). Worldwide distribution of continental rock lithology: Implications for the atmospheric/soil CO<sub>2</sub> uptake by continental weathering and alkalinity river transport to the oceans. *Global Biogeochemical Cycles* 17(2): 7.1-7.13.
- AWWA (American Water Works Association). (2006a). *Standard Methods for the Examination of Water and Wastewater: 2550 Temperature*. Washington, D.C.: American Public Health Association, American Water Works Association, Water Environment Foundation. Online at: <http://www.standardmethods.org/store/ProductView.cfm?ProductID=64> (Accessed February 15, 2016).
- AWWA (American Water Works Association). (2006b). *Standard Methods for the Examination of Water and Wastewater: 2340 Hardness*. Washington, D.C.: American Public Health Association, American Water Works Association, Water Environment Foundation. Online at: <http://www.standardmethods.org/store/ProductView.cfm?ProductID=58> (Accessed February 15, 2016).
- AWWA (American Water Works Association). (2006c). *Standard Methods for the Examination of Water and Wastewater: 2320 Alkalinity*. Washington, D.C.: American Public Health Association, American Water Works Association, Water Environment Foundation. Online at: <http://www.standardmethods.org/store/ProductView.cfm?ProductID=56> (Accessed February 15, 2016).
- Berner, R.A. (1992). Weathering, plants and the long-term carbon cycle. *Geochimica et Cosmochimica Acta* 56(8): 3225-3231.
- Berner, R.A., Lasago, A.C., Garrels, R.M. (1983). The carbonate-silicate geochemical cycle and its effect on atmospheric carbon dioxide over the past 100 million years. *American Journal of Science* 283: 641-683.

- Boden, T.A., Marland, G. Andres, R.J. (2010). *Global, regional and national fossil-fuel CO<sub>2</sub> emissions*. Oak Ridge, TN: Oak Ridge National Laboratory, U.S. Department of Energy, Carbon Dioxide Information Analysis Center. doi 10.3334/CDIAC/00001\_V2010.
- Bodine, T.S. (2016). *Reservoir study and facies analysis of the Big Clifty Sandstone in south central Kentucky*. M.S. Geoscience thesis, Department of Geography and Geology, Western Kentucky University, Bowling Green, KY. Online at: <http://digitalcommons.wku.edu/theses/1610/> (Accessed March 3, 2017).
- Butler, K.H. (2016). *The role of diagenesis in reservoir development of the Big Clifty (Jackson) Sandstone in south-central Kentucky*. M.S. Geoscience thesis, Department of Geography and Geology, Western Kentucky University, Bowling Green, KY. Online at: <http://digitalcommons.wku.edu/theses/1642/> (Accessed March 3, 2017).
- Butler, M.P., Davis, K.J., Denning, A.S., Kawa, S.R. (2010). Using continental observations in global atmospheric inversions of CO<sub>2</sub>: North American carbon sources and sinks. *Tellus* 62B: 550-572.
- Call, E.R. (1882). The loess of North America. *The American Naturalist* 16(5): 369-381.
- Cao, J., Yang, H., Kang, Z. (2011). Preliminary global estimation of carbon sink flux by carbonate rock corrosion: A case study of the Pearl River Basin. *Chinese Science Bulletin* 56(35): 3766-3773.
- Cao, J. Yuan, D., Groves, C., Huang, F., Yang, H., Lu, Q. (2012). Carbon fluxes and sinks: the consumption of atmospheric and soil CO<sub>2</sub> by carbonate rock dissolution. *Acta Geologica Sinica* 86(4): 963-972.
- Cheng, Z., Daoxian, Y., Jianhua, C. (2005). Analysis of the environmental sensitivities of a typical dynamic epikarst system at the Nongla monitoring site, Guangxi, China. *Environmental Geology* 47: 615-619.
- Cole, J.J., Prairie, Y.T., Caraco, N.F., McDowell, W.H., Tranvik, L.J., Striegl, R.G., Duarte, C.M., Kortelainen, P., Dowing, J.A., Middleburg, J.J., Melack, J. (2007). Plumbing the global carbon cycle: Integrating inland waters into the terrestrial carbon budget. *Ecosystems* 10(1): 172-185.
- Cook, W.M., Montgomery, C.W. (1914). The loess soils of southwestern Ohio. Wooster, OH: Ohio Agricultural Experiment Station Circular No. 146. Available online at: <http://kb.osu.edu/dspace/handle/1811/59833>.

- Cox, P.M., Betts, R.A., Jones, C.D., Spall, S.A. (2000). Acceleration of global warming due to carbon-cycle feedbacks in a coupled climate model. *Nature* 408(9): 184-187.
- Debye, P., Hückel, E. (1923) Zur Theorie der Electrolyte. *Physikalische Zeitschrift* 9 (11): 185-206.
- Drever, J.I. (1988). *The Geochemistry of Natural Waters* (2<sup>nd</sup> edn). Englewood Cliffs, NJ.: Prentice Hall.
- Drever, J.I., Stillings, L.L. (1997). The role of organic acids in mineral weathering. *Colloids and Surfaces A: Physicochemical and Engineering Aspects* 120(1-3): 167-181.
- Drever J.I., Vance G.F. (1994). Role of soil organic acids in mineral weathering processes. In Lewan, M.D., Pittman, E.D. (Eds.) *The Role of Organic Acids in Geological Processes*. New York, NY: Springer-Verlag, 138-161.
- Dreybrodt, W. (1988). *Processes in Karst Systems: Physics, Chemistry and Geology*. Heidelberg, Germany: Springer.
- Edmond, J.M. (1992). Himalayan tectonics, weathering processes, and the strontium isotope record in marine limestones. *Science* 28(2088): 1594-1597.
- Einsele, G., Yan, J., Hinderer, M. (2001). Atmospheric carbon burial in modern lake basins and its significance for the global carbon budget. *Global and Planetary Change* 30(3): 167-195.
- England, A.H., Duffin, A.M., Schwartz, C.P., Uejio, J.S., Prendergast, D., Saykally, R.J. (2011). On the hydration and hydrolysis of carbon dioxide. *Chemical Physics Letters* 514(1): 187-195.
- Falkowski, P., Scholes, R.J., Boyle, E., Canadell, J., Canfield, D., Elser, J., Gruber, N., Hibbard, K., Hogberg, P., Linder, S., Mackenzie, F.T., Moore III, B., Pederson, T., Rosenthal, Y., Seitzinger, S., Smetacek, V., Steffen, W. (2000). The global carbon cycle: A test of our knowledge of Earth as a system. *Science* 290(5490): 291-296.
- Fan, S., Gloor, M., Mahlman, J. Pacala, S., Sarmiento, J., Takahashi, T., Tans, P.P. (1998). A large terrestrial carbon sink in North American implied by atmospheric and oceanic carbon dioxide data and models. *Science* 282: 442-446.
- FERC (Federal Energy Regulatory Commission) (2016). *Mountain Valley Project and Equitrans Expansion Project*. Washington, D.C.: FERC. Available online at: <https://www.ferc.gov/industries/gas/enviro/eis/2016/09-16-16-eis/DEIS.pdf>

- Finlay, J.C. (2003). Controls of streamwater dissolved inorganic carbon dynamics in a forested watershed. *Biogeochemistry* 62: 231-252.
- Freeze, R.A., Cherry, J.A. (1979). *Groundwater*. Englewood Cliffs, NJ.: Prentice-Hall.
- Gabet, E.J., Edelman, R., Langner, H. (2006). Hydrological controls on chemical weathering rates at the soil-bedrock interface. *Geology* 34(12): 1065-1068.
- Garziona, C.N. (2008). Surface uplift of Tibet and Cenozoic global cooling. *Geology* 36(12): 1003-1004.
- Groves, C., Meiman, J. (2001). *Inorganic carbon flux and aquifer evolution in the south central Kentucky karst*. Reston, VA: US Geological Survey Karst Interest Group Proceedings, Water-Resources Investigations Report 01-4011: 99-105.
- Groves, C., Meiman, J. (2005). Weathering, geomorphic work, and karst landscape evolution in the Cave City groundwater basin, Mammoth Cave, Kentucky. *Geomorphology* 67(1-2): 115-126.
- Groves, C., Meiman, J., Despain, J., Liu, Z., Yuan, D. (2002). Karst Aquifers as Atmospheric Carbon Sinks: An Evolving Global Network of Research Sites. Reston, VA: US Geological Survey Water Resources Investigations Report 02-4174: 32-39.
- Hach Inc. (2012). *pH USEPA Electrode Method, Method 8156*. Loveland, CO: Hach Inc. Online at: <http://www.hach.com/asset-get.download-en.jsa?code=56935> (Accessed November 16, 2014).
- Harned, H.S., Owen, B.B. (1958). *The Physical Chemistry of Electrolytic Solutions* (3<sup>rd</sup> edn.). New York, NY: Rheinhold.
- Hartmann, J., Jansen, N. Dürr, H.H., Kempe, S., Köhler, P. (2009). Global CO<sub>2</sub>-consumption by chemical weathering: What is the contribution of highly active weathering regions? *Global and Planetary Change* 69(4): 185-194.
- Haryono, E. (2011). *Atmospheric carbon dioxide sequestration through karst denudation processes: Preliminary estimation from Gunung Sewu karst*. Paper presented at the Asian Trans-Disciplinary Karst Conference 2011, Yogyakarta, Indonesia, November 17-19, 203-207.

- Hayes, D.J. Turner, D.P., Stinson, G., Mcguire, A.D., Wei, Y., West, T.O., Heath, L.S., Dejong, B., Mcconkey, B.G., Birdsey, R.A., Kurz, W.A., Jacobson, A.R., Huntzinger, D.N., Pan, Y., Post, W.M., Cook, R.B. (2012). Reconciling estimates of the contemporary North American carbon balance among terrestrial biosphere models, atmospheric inversions, and a new approach for estimating net ecosystem exchange from inventory-based data. *Global Change Biology* 18: 1282-1299.
- He, S.Y., Kang, Z.Q., Li, Q.Y., Wang, L.L. (2013). The utilization of real-time high resolution monitoring techniques in karst carbon sequestration: A case study of the station in Banzhai subterranean stream catchment. *Advances in Climate Change Research* 3(1): 54-58.
- Hoffert, M.I., Caldeira, K., Jain, A.K., Haites, E.F, Harvey, L.D., Potter, S.D., Schlesinger, M.E., Schneider, S.H., Watts, R.G., Wigley, T.M., Wuebbles, D.J. (1998). Energy implications for future stabilization of atmospheric CO<sub>2</sub> content. *Nature* 395: 881-884.
- Huang, W.H., Keller, W.D. (1970). Dissolution of rock forming silicate minerals in organic acids: Simulated first-stage weathering of fresh mineral surfaces. *American Mineralogist* 55(11-1), 2076.
- Hunt, C.B. (1967). *Physiography of the United States*. San Francisco, CA: W.H. Freeman.
- IAWC (Illinois American Water Company). (2016). *Ohio River at Cairo, Illinois Water Year 2014 hydrochemical monitoring*. Chicago, IL: Unpublished dataset.
- IPCC (Intergovernmental Panel on Climate Change). (2014). Synthesis Report Summary for Policymakers. In Pachauri, R.K., Meyer, L.A. (eds.). *Report of the Intergovernmental Panel on Climate Change*. Geneva: Switzerland: IPCC.
- Jiang, Z., Yuan, D. (1999). CO<sub>2</sub> source-sink in karst processes in karst areas of China. *Episodes* 22(1): 33-35.
- Jones, D.L. (1998). Organic acids in the rhizosphere – a critical review. *Plant and Soil* 205(1): 25-44
- KAWC (Kentucky American Water Company). (2016). *Kentucky River at Pool 3 Water Year 2014 hydrochemical monitoring*. Lexington, KY: KAWC, Unpublished dataset.



- Kay, G.F., Leighton, M.M. (1933). Eldoran Epoch of the Pleistocene Period. *Bulletin of the Geological Society of America* (XLIV): 669-674.
- KDOW (Kentucky Division of Water). (2016a). *Green River at Livermore, KY Water Year 2014 hydrochemical monitoring*. Frankfort, KY: KDOW, Unpublished dataset.
- KDOW (Kentucky Division of Water). (2016b). *Kentucky River at Lockport, KY Water Year 2014 hydrochemical monitoring*. Frankfort, KY: KDOW, Unpublished dataset.
- KDOW (Kentucky Division of Water). (2016c). *Tennessee River at Hwy 60 near Paducah, KY Water Year 2014 hydrochemical monitoring*. Frankfort, KY: KDOW, Unpublished dataset.
- Keeling, C.D., Piper, S.C., Bacastow, R.B., Wahlen, M., Whorf, T.P., Heimann, M., Meijer, H.A. (2005). *Exchanges of atmospheric CO<sub>2</sub>- and <sup>13</sup>CO<sub>2</sub>- with the terrestrial biosphere and oceans from 1978 to 2000. I. Global aspects*. San Diego, CA: Scripps Institution of Oceanography, SIO Reference Series, 01-06.
- Khadka, M.B., Martin, J.B., Jin, J. (2014). Transport of dissolved carbon and CO<sub>2</sub> degassing from a river system in a mixed silicate and carbonate catchment. *Journal of Hydrology* 513: 391-402.
- King, A.W., Dilling, L., Zimmerman, G.P., Fairman, D.M., Houghton, R.A., Marland, G., Rose, A.Z., Wilbanks, T.J. (2007). What is the carbon cycle and why care? In King, A.W. Dilling, L., Zimmerman, G.P., Fairman, D.M., Houghton, R.A., Marland, G., Rose, A.Z., Wilbanks, T.J. (eds.) *The First State of the Carbon Cycle Report (SOCCR): The North American Carbon Budget and Implications for the Global Carbon Cycle*. Asheville, NC: National Oceanic and Atmospheric Administration, National Climatic Data Center. A report by the US Climate Change Science Program and the Subcommittee on Global Change Research, 15-20.
- Kleinbaum, D., Kupper, L., Nizam, A., Rosenberg, E. (2013). *Applied Regression Analysis and Other Multivariable Methods*. Boston, MA: Cengage.
- Kottek, M., Grieser, J., Beck, C., Rudolf, B., Rubel, F. (2006). World map of the Köppen-Geiger climate classification updated. *Meteorologische Zeitschrift* 15(3), 259-263.

- Lal, R. (2004). Soil carbon sequestration impacts on global climate change and food security. *Science* 304: 1623-1627.
- Lambers, H., Martinoia, E., Renton, M. (2015). Plant adaptations to severely phosphorus-impooverished soils. *Current Opinion in Plant Biology* 25: 23-31.
- Langelier, W.F. (1936). The analytical control of anti-corrosion water treatment. *Journal of the American Water Works Association* 28: 1500.
- Larson, T.E., Buswell, A.M. (1942). Calcium carbonate saturation index and alkalinity interpretations. *Journal of the American Water Works Association* 34(11): 1667-1679.
- Le Quéré, C., Raupach, M.R., Canadell, J.G., Marland, G., Bopp, L., Ciais, P., Conway, T.J., Doney, S.C., Feely, R.A., Foster, P., Friedlingstein, P., Gurney, K., Houghton, R.A., House, J.I., Huntingford, C., Levy, P.E., Lomas, M.R., Majkut, J., Metzl, N., Ometto, J.P. Peters, G.P., Prentice, I.C., Randerson, J.T., Running, S.W., Sarmiento, J.L., Schuster, U., Sitch, S., Takahashi, T., Viovy, N., Van der Werf, G.R., Woodwatd, F.I. (2009). Trends in the sources and sinks of carbon dioxide. *Nature Geoscience* 2: 831-836.
- Li, G., Elderfield, H. (2013). Evolution of carbon cycle over the past 100 million years. *Geochimica et Cosmochimica Acta* 103: 11-25.
- Li, J., Fang, X. (1999). Uplift of the Tibetan Plateau and environmental changes. *Chinese Science Bulletin* 44(23): 2117-2124.
- Li, W., Yu, L., He, Q., Wu, Y., Yuan, D., Cao, J. (2005). Effects of microbes and their carbonic anhydrase on  $\text{Ca}^{2+}$  and  $\text{Mg}^{2+}$  migration in column-built leached soil-limestone karst systems. *Applied Soil Ecology* 29(3): 274-281.
- Liu, Z., Dreybrodt, W. (1997). Dissolution kinetics of calcium carbonate mineral in  $\text{H}_2\text{O}-\text{CO}_2$  solutions in turbulent flow: The role of the diffusion boundary layer and the slow reaction  $\text{H}_2\text{O} + \text{CO}_2 \leftrightarrow \text{H}^+ + \text{HCO}_3^-$ . *Geochimica et Cosmochimica Acta* 61(14): 2879-2889.
- Liu, Z., Zhao, J. (2000). Contribution of carbonate rock weathering to the atmospheric  $\text{CO}_2$  sink. *Environmental Geology* 39: 1053-1058.
- Liu, Z., Dreybrodt, W., Wang, H. (2008). A possible important  $\text{CO}_2$  sink by the global water cycle. *Chinese Science Bulletin* 53(3): 402-407.

- Ludwig, W., Amiotte Suchet, P., Probst, J.L. (1998). Atmospheric CO<sub>2</sub> consumption by continental erosion: Present-day controls and implications for the last glacial maximum. *Global and Planetary Change* 16: 107-120.
- Lüttge, A. (2005). Etch pit coalescence, surface area, and overall mineral dissolution rates. *American Mineralogist* 90(11-12): 1776-1783.
- Martin, J.B., Brown, A., Ezell, J. (2013). Do carbonate karst terrains affect the global carbon cycle? *Acta Carsologica* 42(2-3): 187-196.
- Mason, J.A., Bettis, A.E., Roberts, H.M., Muhs, D.R., Joeckel, R.M. (2006). AMQUA Pre-meeting Field Trip 1: Last glacial loess sedimentary system of eastern Nebraska and western Iowa. In Mandel, R., (ed.) *Guidebook of the 18<sup>th</sup> Biennial Meeting of the American Quaternary Association*. Lawrence., KS: Kansas Geological Survey Technical Series 21, 1-19.
- Morse, J.W., Arvidson, S.A. (2002). The dissolution kinetics of major sedimentary carbonate minerals. *Earth-Science Reviews* 58: 51-84.
- Myneni, R.B., Dong, J., Tucker, C.J., Kaufmann, R.K., Kauppi, P.E., Liski, J., Zhou, L., Alexeyev, V., Hughes, M.K. (2001). A large carbon sink in the woody biomass of Northern forests. *Proceedings of the National Academy of Sciences* 98(26): 14784-14789.
- NASA (National Aeronautics and Space Administration Land Processes Distributed Active Archive Center). (2016). *ASTER Level 1 Precision Terrain Corrected Registered At-Sensor Radiance. Version 3*. Sioux Falls, SD: NASA EOSDIS Land Processes DAAC, USGS Earth Resources Observation and Science (EROS) Center. Online at: <https://gdex.cr.usgs.gov/gdex/> (Accessed January 13, 2017).
- NOAA (National Oceanic and Atmospheric Administration). (2016). *U.S. Annual Climatological Summaries Lineage*. Asheville, NC: NOAA, National Centers for Environmental Information. Online at: <https://gis.ncdc.noaa.gov/geoportal/catalog/search/resource/details.page?id=gov.noaa.ncdc:C00040> (Accessed March 4, 2016).
- Orr, J.C., Fabry, V.J., Aumont, O., Bopp, L., Doney, S.C., Feely, R.A., Yool, A. (2005). Anthropogenic ocean acidification over the twenty-first century and its impact on calcifying organisms. *Nature* 437: 685-687.

- Osterhoudt, L.L. (2014). *Impacts of Carbonate Mineral Weathering on the Hydrochemistry of the Upper Green River Basin, Kentucky*. M.S. Geoscience thesis, Department of Geography and Geology, Western Kentucky University, Bowling Green, KY. Online at: < <http://digitalcommons.wku.edu/theses/1337/> >. (Accessed October 10, 2015).
- Pacala, S., Birdsey, R.A., Bridgham, S.D., Conant, R.T., Davis, K., Hales, B., Houghton, R.A., Jenkins, J.C., Johnston, M., Marland, G., Paustian, K. (2007). *The North American carbon budget and implications for the global carbon cycle*. In King, A.W. Dilling, L., Zimmerman, G.P., Fairman, D.M., Houghton, R.A., Marland, G., Rose, A.Z., Wilbanks, T.J. (eds.) *The First State of the Carbon Cycle Report (SOCCR): The North American Carbon Budget and Implications for the Global Carbon Cycle*. Asheville, NC: National Oceanic and Atmospheric Administration, National Climatic Data Center. A report by the US Climate Change Science Program and the Subcommittee on Global Change Research, 29-36.
- Pidwirny, M.J. (2006). "The Carbon Cycle". *Fundamentals of Physical Geography* (2nd Edn). Okanagan, B.C.: University of British Columbia Press. Online at: <http://www.physicalgeography.net/fundamentals/9r.htm> (Accessed March 14, 2016).
- Plummer, L.N., Wigley, T.M.L., Parkhurst, D.L. (1978). The kinetics of calcite dissolution in CO<sub>2</sub>–water systems at 5 degrees to 60 degrees C and 0.0 to 1.0 atm CO<sub>2</sub>. *American Journal of Science* 278: 179-216.
- Post, W.M., Peng, T.H., Emanuel, W.R., King, A.W. (1990). The Global Carbon Cycle. *American Scientist* 78: 310-326.
- Ray, L.L. (1965). *Quaternary Geology of the Owensboro Quadrangle Indiana and Kentucky*. Reston, VA: United States Geological Survey Professional Paper 488.
- Ray, L.L. (1974). *Geomorphology and Quaternary Geology of the Glaciated Ohio River Valley—A Reconnaissance Study*. Reston, VA: United States Geological Survey Professional Paper 826.
- Reedy, M.M. (1981). Crystal growth of calcite from calcium bicarbonate solution under constant P<sub>CO2</sub> and 25°C: a test of a calcite dissolution model. *Geochimica et Cosmochimica Acta* 45: 1281-1289.

- Revelle, R., Suess, H. (1957). Carbon dioxide exchange between atmosphere and ocean and the question of an increase of atmospheric CO<sub>2</sub> during the past decades. *Tellus IX*(1): 18-27.
- Richey, J.E. (2003). Pathways of atmospheric CO<sub>2</sub> through fluvial systems. In Field, C.B., Raupach, M. (eds.). *Scientific Committee on Problems of the Environment (SCOPE)/United Nations Environment Program (UNEP) – The Global Carbon Cycle: Integrating Humans, Climate and the Natural World: 62*. Washington, D.C.: Island Press, 329-340.
- Sabine, C.L, Feely, R.A., Gruber, N., Key, R.M. Lee, K., Bullister, J.L., Wanninkhof, R., Wong, C.S., Wallace, D.W.R., Tilbrook, B., Millero, F.J., Peng, T., Kozyr, A., Ono, T., Rios, A.F. (2004). The oceanic sink for atmospheric carbon. *Science* 305(5682): 367-371.
- Salley, D.C. (2016). *Advancing methods to measure the atmospheric CO<sub>2</sub> sink from carbonate rock weathering*. M.S. Geoscience thesis, Department of Geography and Geology, Western Kentucky University, Bowling Green, KY. Online at: <http://digitalcommons.wku.edu/theses/1603/> (Accessed October 10, 2015).
- Sarmiento, J.L., Sundquist, E.T. (1992). Revised budget for the oceanic uptake of anthropogenic carbon dioxide. *Nature* 356: 589-593.
- Sellinger, C.E. (1996). Computer program for estimating evapotranspiration using the Thornthwaite method. Ann Arbor, MI: National Ocean and Atmospheric Administration (NOAA) Technical Memorandum ERL FLERL-101. Online at: [http://ftp.glerl.noaa.gov/ftp/publications/tech\\_reports/glerl-101/tm-101.pdf](http://ftp.glerl.noaa.gov/ftp/publications/tech_reports/glerl-101/tm-101.pdf) (Accessed March 4, 2016.)
- Shrock, R.R., Malott, C.A. (1929). Structural features of the West Franklin Formation of Southwestern Indiana. *American Association of Petroleum Geologists Bulletin* 13(10): 1301-1315.
- Siegenthaler, U., Sarmiento, J.L. (1993). Atmospheric carbon dioxide and the ocean. *Nature* 365(9): 119-125.
- Sigman, D.M., Boyle, E.A. (2000). Glacial/interglacial variations in atmospheric carbon dioxide. *Nature* 407: 859-869.

- Silva, L.C.R. (2017). Carbon sequestration beyond tree longevity. *Science* 355(6330): 1141.
- Solomon, S., Plattner, G.K., Knutti, R., Friedlingstein, P. (2009). Irreversible climate change to due carbon dioxide emissions. *Proceedings of the National Academy for Sciences Journal* 106(6): 1704-1709.
- Stumm, M., Morgan, J.J. (1981). *Aquatic Chemistry: An Introduction Emphasizing Chemical Equilibria in Natural Waters*. New York, NY: John Wiley.
- Sundquist, E.T. (1993). The global carbon dioxide budget. *Science* 259(5097): 934-941.
- Sweeting, M. (1972). *Karst Landforms*. London, U.K.: Macmillan Press.
- Tan, K.H. (1986). Degradation of Soil Minerals by Organic Acids. *SSSA Special Publication, Interactions of Soil Minerals with Natural Organics and Microbes* 17: 1-27.
- Tans, P.P., Keeling, R. (2017). *Trends in Atmospheric Carbon Dioxide*. Silver Springs, MD: NOAA/ESRL (National Oceanic & Atmospheric Administration/Earth System Research Laboratory), Mauna Loa, HI: Scripps Institution of Oceanography. Online at: <http://www.esrl.noaa.gov/gmd/ccgg/trends/> (Accessed July 10, 2017).
- Tans, P.P., Fung, I.Y., Takahashi, T. (1990). Observational constrains on the global atmospheric CO<sub>2</sub> budget. *Science* 247(4949): 1431-1438.
- Taylor, L.L., Banwart, S.A., Valdes, P.J., Leake, J.R., Beerling, D.J. (2012). Evaluating the effects of terrestrial exosystems, climat and carbon dioxide on weathering over geological time: a global-scale process-based approach. *Philosophical Transactions of the Royal Society B: Biological Sciences* 367(1588): 565-582.
- Taymo, M.E., Ruddiman, W.F. (1992). Tectonic forcing of late Cenozoic climate. *Nature* 359(6391): 117-122.
- Thorley, R.M.S, Taylor, L.L., Banwart, S.A., Leake, J.R., Beerling, D.J. (2015). The role of forest trees and their mycorrhizal fungi in carbonate rock weathering and its significance for global carbon cycling. *Plant, Cell and Environment* 38: 1947-1961.

- Thompson, T.A., Sowder, K.H., Johnson, M.R. (2016). *Generalized stratigraphic column of Indiana bedrock*. Bloomington, IN: Indiana Geological Survey.
- Thornbury, W.D. (1940). Weathered zones and glacial chronology in southern Indiana. *The Journal of Geology* 48(5): 449-475.
- Thornbury, W.D. (1950). *Glacial sluiceways and lacustrine plains of southern Indiana*. Bloomington, IN: Indiana Department of Conservation, Division of Geology Professional Bulletin No. 4.
- Thornthwaite, C.W., Mather, J.R. (1955). *The Water Balance*. Centerton, NJ: Laboratory of Climatology Publication 8.
- Thornthwaite, C.W., Mather, J.R. (1957). Instruction and tables for computing potential evapotranspiration and the water balance. *Drexel Institute of Technology, Laboratory of Climatology, Publications in Climatology* 10(3): 311.
- USACE (United States Army Corps of Engineers). (2016a). *Streamflow discharge for the Cumberland River at Lake Barkley, KY Water Year 2014*. Washington, D.C.: USACE, Unpublished dataset.
- USACE (United States Army Corps of Engineers). (2016b). *Streamflow discharge for the Tennessee River at Kentucky Dam, KY Water Year 2014*. Washington, D.C.: USACE, Unpublished dataset.
- USDA (United States Department of Agriculture). (2016a). *National Hydrography Dataset. Stream networks dataset*. Washington D.C.: USDA, Natural Resources Conservation Service. Online at <http://datagateway.nrcs.usda.gov/> (Accessed October 3, 2016).
- USDA (United States Department of Agriculture). (2016b). *National scale geology dataset*. Washington D.C.: USDA, Natural Resources Conservation Service. Online at <http://datagateway.nrcs.usda.gov/> (Accessed October 3, 2016).
- USGS (United States Geological Survey). (2016a). *National Hydrography Dataset. Watershed boundary dataset*. Reston, VA: USGS, National Water Information System Web Interface. Online at: <http://nhd.usgs.gov/> (Accessed April 3, 2016).

- USGS (United States Geological Survey). (2016b). *Water Resources of the United States. Boundary Descriptions and Names of Regions, Subregions, Accounting Units and Cataloging Units. Region 05 Ohio Basin*. Reston, VA: USGS, Water Resources. Online at: [https://water.usgs.gov/GIS/huc\\_name.html](https://water.usgs.gov/GIS/huc_name.html) (Accessed January 14, 2017).
- USGS (United States Geological Survey). (2016c). *Hydrochemical data for the Allegheny River at Oakmont, PA Water Year 2014*. Reston, VA: USGS, Ohio River Sanitation Company (ORSANCO) Water Quality Portal (WQP). Online at: <https://www.waterqualitydata.us/portal/> (Accessed December 5, 2016).
- USGS (United States Geological Survey). (2016d). *Hydrochemical data for the Cumberland River at Pinckneyville, KY Water Year 2014*. Reston, VA: USGS, Ohio River Sanitation Company (ORSANCO) Water Quality Portal (WQP). Online at: <https://www.waterqualitydata.us/portal/> (Accessed December 7, 2016).
- USGS (United States Geological Survey). (2016e). *Hydrochemical data for the Great Miami River at Elizabethtown, OH Water Year 2014*. Reston, VA: USGS, Ohio River Sanitation Company (ORSANCO) Water Quality Portal (WQP). Online at: <https://www.waterqualitydata.us/portal/> (Accessed December 6, 2016).
- USGS (United States Geological Survey). (2016f). *Hydrochemical data for the Kanawha River at Winfield, WV Water Year 2014*. Reston, VA: USGS, Ohio River Sanitation Company (ORSANCO) Water Quality Portal (WQP). Online at: <https://www.waterqualitydata.us/portal/> (Accessed December 6, 2016).
- USGS (United States Geological Survey). (2016g). *Hydrochemical data for the Licking River at Covington, KY Water Year 2014*. Reston, VA: USGS, Ohio River Sanitation Company (ORSANCO) Water Quality Portal (WQP). Online at: <https://www.waterqualitydata.us/portal/> (Accessed December 7, 2016).
- USGS (United States Geological Survey). (2016h). *Hydrochemical data for the Monongahela River at Elizabeth, PA Water Year 2014*. Reston, VA: USGS, Ohio River Sanitation Company (ORSANCO) Water Quality Portal (WQP). Online at: <https://www.waterqualitydata.us/portal/> (Accessed December 5, 2016).
- USGS (United States Geological Survey). (2016i). *Hydrochemical data for the Scioto River at Lucasville, OH Water Year 2014*. US EPA Storage and Retrieval (STORET) database via USGS, Water Quality Portal (WQP). Online at <https://www.waterqualitydata.us/portal/> (Accessed December 6, 2016).



- USGS (United States Geological Survey). (2016j). *Hydrochemical data for the Wabash River at New Harmony, IN Water Year 2014*. Reston, VA: USGS, Ohio River Sanitation Company (ORSANCO) Water Quality Portal (WQP). Online at: <https://www.waterqualitydata.us/portal/> (Accessed December 6, 2016).
- USGS (United States Geological Survey). (2016k). *Physiographic divisions of the conterminous U.S.* Reston, VA: USGS, Water Resources National Spatial Data Infrastructure. Online at: <https://water.usgs.gov/GIS/metadata/usgswrd/XML/physio.xml#stdorder> (Accessed on May 24, 2017).
- USGS (United States Geological Survey). (2016l). *Streamflow discharge for the Allegheny River at Natrona, PA Water Year 2014*. Reston, VA: USGS, National Water Information System Web Interface. Online at: <https://maps.waterdata.usgs.gov/mpper/index.html> (Accessed September 30, 2016).
- USGS (United States Geological Survey). (2016m). *Streamflow discharge for the Great Miami River at Hamilton, OH Water Year 2014*. Reston, VA: USGS, National Water Information System Web Interface. Online at: <https://maps.waterdata.usgs.gov/mapper/index.html> (Accessed September 30, 2016).
- USGS (United States Geological Survey). (2016n). *Streamflow discharge for the Green River at Spottsville, KY Water Year 2014*. Reston, VA: USGS, National Water Information System Web Interface. Online at: <https://maps.waterdata.usgs.gov/mapper/index.html> (Accessed September 30, 2016).
- USGS (United States Geological Survey). (2016o). *Streamflow discharge for the Kanawha River at Charleston, WV Water Year 2014*. Reston, VA: USGS, National Water Information System Web Interface. Online at: <https://maps.waterdata.usgs.gov/mapper/index.html> (Accessed September 30, 2016).
- USGS (United States Geological Survey). (2016p). *Streamflow discharge for the Kentucky River at Lockport, KY Water Year 2014*. Reston, VA: USGS, National Water Information System Web Interface. Online at: <https://maps.waterdata.usgs.gov/mapper/index.html> (Accessed September 30, 2016).

- USGS (United States Geological Survey). (2016q). *Streamflow discharge for the Licking River at McKinnneysburg, KY Water Year 2014*. Reston, VA: USGS, National Water Information System. Online at: <https://maps.waterdata.usgs.gov/mapper/index.html> (Accessed September 31, 2016).
- USGS (United States Geological Survey). (2016r). *Streamflow discharge for the Monongahela River at Elizabeth, PA Water Year 2014*. Reston, VA: USGS, National Water Information System. Online at: <https://maps.waterdata.usgs.gov/mapper/index.html> (Accessed September 31, 2016).
- USGS (United States Geological Survey). (2016s). *Streamflow discharge for the Ohio River at Olmsted, IL Water Year 2014*. Reston, VA: USGS, National Water Information System. Online at: <https://maps.waterdata.usgs.gov/mapper/index.html> (Accessed September 30, 2016).
- USGS (United States Geological Survey). (2016t). *Streamflow discharge for the Scioto River at Piketon, OH Water Year 2014*. Reston, VA: USGS, National Water Information System. Online at: <https://maps.waterdata.usgs.gov/mapper/index.html> (Accessed September 31, 2016).
- USGS (United States Geological Survey). (2016u). *Streamflow discharge for the Wabash River at New Harmony, IN Water Year 2014*. Reston, VA: USGS, National Water Information System. Online at: <https://maps.waterdata.usgs.gov/mapper/index.html> (Accessed September 31, 2016).
- UTIA (University of Tennessee Institute of Agriculture). (2016). *Tennessee Climatological Service: Climate Data for Tennessee*. Knoxville, TN: UTIA. Online at: [https://ag.tennessee.edu/climate/Pages/climate\\_dataTN.aspx](https://ag.tennessee.edu/climate/Pages/climate_dataTN.aspx) (Accessed April 4, 2016).
- Veni, G., DuChene, H. Crawford, N.C., Groves, C.G., Huppert, G.N., Kastning, E.H., Olson, R., Wheeler, B.J. (2001). *Living With Karst: A Fragile Foundation*. American Geological Institute Environmental Awareness Series Volume 4. Online at: < <https://www.agiweb.org/environment/publications/karst.pdf>>. (Accessed May 18, 2017).

- Walter, K.M., Zimov, S.A., Chanton, J.P. Verbyla, D., Chapin II, F.S. (2006). Methane bubbling from Siberian thaw lakes as a positive feedback to climate warming. *Nature* 443(7107): 71-75.
- Weary, D.J., Doctor, D.H. (2014). *Karst in the United States: A Digital Map Compilation and Database*. Reston, VA: United States Geological Survey Open-File Report 2014-1156. Online at: <http://pubs.usgs.gov/of/2014/1156/> (Accessed April 1, 2016).
- White, A.F., Peterson, M.L. (1990). Sources and fractionation processes influencing the isotopic distribution of H, O and C in the Long Valley hydrothermal system, California, USA. *Applied Geochemistry* 5(5-6): 571-585.
- White, D., Johnstron, K., Miller, M. (2005). The Ohio River Basin. In Benke, A.C., Cushing, C.E. (eds.) *Rivers of North America*. Amsterdam, Netherlands: Elsevier, 375-409.
- White, W.B. (1988). *Geomorphology and Hydrology of Karst Terrains*. New York, NY: Oxford University Press.
- White, W.B. (2013). Carbon fluxes in karst aquifers: Sources, sinks, and the effect of storm flow. *Acta Carsologica* 42(2-3): 177-186.
- Whitney, J.D. (1877). The Chinese loess puzzle. *The American Naturalist* 11(12): 705-718.
- WVGES (West Virginia Geological and Economic Survey). (1968). *Geologic map of West Virginia*. Morgantown, WV: West Virginia GIS Technical Center. Online at: <http://wvgis.wvu.edu/data/dataset.php?action=search&ID=43> (Accessed on May 25, 2016).
- Yadav, S.K., Chakrapani, G.J., Gupta, M.K. (2008). An experimental study of dissolution kinetics of calcite, dolomite, leucogranite and gneiss in buffered solutions at temperature 25 and 5°C. *Environmental Ecology* 53: 1683-1694.
- Yang, H., Xing, Y., Xie, P., Ni, L., Rong, K. (2008). Carbon source/sink function of a subtropical, eutrophic lake determined from an overall mass balance and a gas exchange and carbon burial balance. *Environmental Pollution* 151(3): 559-568.
- Yuan, D. (1997). The carbon cycle in karst. *Zeitschrift Fur Geomorphologie* 108: 91-102.

Zhang, C. (2011). Carbonate rock dissolution rates in different land uses and their carbon sink effect. *Chinese Science Bulletin* 56(35): 3759-3765.